Journal of Ankara Medical School

ISSN 1300-5464

Vol 23, No 2, 2001

Journal of Ankara Medical School

Vol 23, No: 2, 2001

CONTENTS

Journal of Ankara Medical School

All the authors stated in the published paper are kindly requested to be a subscriber to the Journal. Subscription price for the teaching staff members is 20.000.000 TL; 50% reductions for research fellows, practioners, etc.; 75% reductions for students, Subscription for the foreign countries: 17$ or 40DM.

Ek bası (Reprint) ücretlidir. Reprint ücreti makalenin sayfa adedi ve reprint adedine göre yazarlara makale kabul yazısı ile bildirilir.

For Subscription :

Ankara Üniversitesi Tıp Fakültesi Vakfı - ANKARA

Editorial Office :

A.Ü. Tıp Fakültesi Yayın Komisyonu Başkanlığı Sıhhiye - ANKARA

ISSN 1300 - 5464

Design & Preparation: ANTIP A.Ş. 0 (312) 310 63 05 - 362 30 30/7005 Hakan Ellidokuzoğlu

Constraint: *BARAN Ofset* 0 (312) 336 68 74

Journal of Ankara Medical School

Published Quarterly by
ANKARA UNIVERSITY MEDICAL SCHOOL

INTRUCTIONS TO AUTHORS:

Journal of Ankara Medical School publishes original articles of research on clinical and basic sciences and concise case reports.

The language of the Journal is English.

All material should be addressed to the Editor, (Ankara Ünivversitesi Tıp Fakültesi Yayın Komisyonluğu Başkanlığı, 06100-Ankara, Turkey), in three copies and a floppy disk, ideally **Microsoft Word 6.0 or 2.0**. An introductory letter identifying the authors (s), their telephone and fax numbers and their address (s) should accompany the manuscript.

Journal accepts the contributions with the understanding that neither the article nor any part of its essential results has been published or submitted for publication elsewhere prior to its appearance in this Journal. Work already presented in a congress or published as an abstract within the context of congress or scientific meetings may be accepted for publication provided that this fact is mentioned.

All materials including text, figures, tables, references and glossy prints of figures should not exceed ten pages. The upperlimit for case presentation is three pages.

Title of the Paper: Must not exceed 80 spaces. If title exceeds 80 letter space a "running title" fewer than 40 letter spaces should be prepared in order to be placed on top of odd numbered pages.

The names (s) of author(s), including first name (s) must be written below the title. The academic degree(s) of author(s) can be stated as a foot-note with an asterix placed on surname(s) of the author(s). The name and address of Correspondent author should be stated.

Summary in a foreign language: An abstract not more then 200 words must be written in English.

Key Words not more than five should be added below the summary in alphabethical order.

Form: Article submitted must be double-spaced typewritten on standard size paper (21x30 cm). margins 3 cm to the left and 2 cm to the right should be left.

Illustrations: Photographs, graphics, and all other illustrations must be numbered according to consecutive appearence order. Graphics and figures should be made on glossy paper, preferably with china ink. Photogarphs should be made on glossy paper, black and white, with sufficient contrast. A small legend must accompany each figure numbered letters.

The legends must be written on a separate sheet of paper, in the order of appearance within the article.

Figures and photographs must be presented in an envelope. Title of the article and author(s) must be written at the back of the samples with a light pencil.

The place where the illustrations are desired to appear within the text should be indicated by numbering it on left margin.

Tables: The tables must be typewritten double-spaced on a separate sheet of paper numbered with Arabic numerals. The contents of the table must be clearly expressed with a short title.

The results of the work must be stated either by table or by explanation within the text. Duplication of the above should be avoided.

The desired place for the tables should be indicated on the left margin of the written text.

References: Must be numbered in parenthesis on the same level the manuscript line. In papers representing a research work only those references which deal with the research should be mentioned. References should not exceed 25 in research and 10 in case reports. References should be arranged sequentially as they appear in the text. Example references are given below:

- **Gozal D, Tiser A, Shupak A, et al. Necrotizing fasciitis. Arch Surg 1986; 121: 233-5.**
- **Moon RE, Gorman DF. Treatment of the decompression disorders. In: Bennett BP, Eliot DH, eds. The Physiology and Medicine of Diving. 4th ed. Philadelphia: W.B. Saunders, 1993: 454-80.**

Reprints are available at prices determined by article length and quantity.

JOURNAL OF ANKARA MEDICAL SCHOOL Vol 23, No 2, 2001 85-90

EFFECT OF ADRENOCORTICOTROPIC HORMONE ON THE ULTRASTRUCTURE OF SINUSOIDAL ENDOTHELIAL CELLS IN THE RAT LIVER

Belgin CAN*

SUMMARY

In this study the effects of ACTH on the ultrastructure of rat liver sinusoidal endothelium cells were evaluated by transmission electron microscopy(TEM). Thirty male (experimental group=20, control group=10) Wistar Type rats were used. After a single dose of (10units/100g) subcutaneous ACTH injection the rats were sacrificed and liver tissue samples were taken. After preparing with conventional tissue techniques for TEM the specimens were examined and photographed. When compared with the controls, the sinusoids appeared distended and sinusoidal endothelium was damaged, fragmented and desquamated. Sinusoids were plugged with aggregated red blood cells. Kupffer cells were swollen and contained phagocytic inclusions and increased number of microbodies.

As a conclusion these findings were probably due to the effects of free fatty acids caused by lipid mobilization induced by ACTH.

Key Words: *ACTH, Liver, Sinusoidal Endothelium, Ultrastructure*

ÖZET

SIÇAN KARACİĞER SİNUZOİD ENDOTELİNİN İNCE YAPISI ÜZERİNE ADRENOKORTİKOTROPİK HORMONUN ETKİLERİ

Bu çalışmada ACTH nın karaciğer sinuzoid endotel hücrelerinin ince yapısı üzerine olan etkileri geçirmeli elektron mikroskobunda incelendi.

Wistar tipi otuz tane erkek sıçan (deney grubu=20, kontrol grubu=10) kullanıldı. Tek doz (10ünite/100g) subkutan yolla ACTH enjeksiyonundan sonra sıçanlar sakrifiye edildi ve karaciğer doku örnekleri alındı. Geçirmeli elektron mikroskobu için uygun tekniklerle hazırlandıktan sonra örnekler incelendi ve fotoğraflandı.

Kontrollerle karşılaştırıldığı zaman, sinusoidlerin genişlediği sinuzoid endotelinin hasar gördüğü, parçalandığı ve döküldüğü görüldü. Kırmızı kan hücreleri sinuzoidlerin lümeninde tıkaç yapıyordu. Kupffer hücreleri şişkindi ve fagosite ettikleri inklüzyonları ve artmış sayıda mikrocisimi içeriyordu.

Sonuç olarak bu bulgular muhtemelen ACTH ile indüklenen lipid hareketinin yol açtığı serbest yağ asitlerinin etkisine bağlı olarak ortaya çıkmaktadır.

Anahtar Kelimeler: *ACTH, İnce Yapı, Karaciğer, Sinusoid Endoteli.*

Several detailed correlative and morphological description using light microscopy, transmission electron microscopy and scanning electron microscopy were performed to evalaluate the cellular damage to sinusoidal morphology and endothelial structure of experimental animals which had received steroids and chemical mediators (1,2,3,4). ACTH (adrenocorticotropic hor-

*Assoc.Prof., Department of Histology & Embryology Ankara University Faculty of Medicine

Received: Nov 29,2000 Accepted: March 26,2001

mone) administiration was followed by lipid mobilization and marked elevation of plasma free fatty acids and resulted in a disturbance of the hepatocytes ultrastructure and various degree of endothelial injury (1,3,4). In this study some of the alterations in subcellular endothelial structure of sinusoids of rats which had received ACTH has been examined.

MATERIALS AND METHODS

Thirty male Wistar rats , 4-6 months old and weighing 200-250 g were used. The experimental group (n:20) was injected single dose (10units/100g) ACTH subcutaneously and the control group (n:10) was injected physiological saline (0.9%) simultaneously. Two hours after ACTH administration the animals were sacrificed by ether anesthesia, dissected and the livers were immediately removed and fixed in 2.5% glutaraldehyde in a phosphate buffer (pH 7.2) for 24 hours. The livers were then postfixed in 1% osmium tetroxide. The materials were dehydrated in graded alcohols and embedded in Araldite CY 212. 1µm semi-thin sections were stained with toluidine blue-Azur II and examined under a Zeiss Axioskop photomicroscope. Ultrathin sections (50nm) were cut on a LKB Ultatome III, stained with uranyl acetate and lead citrate and examined on a Jeol 100 transmission electron microscope.

RESULTS

In control group liver parenchymal cells (hepatocytes) were arranged as cords or plates between sinusoidal spaces. Hepatic cells nuclei were spherical or ovoid with a regular surface. Each nucleus was vesicular with prominent scattered chromatin granules and bearing one or more nucleoli. Two main types of cells were present in the sinusoidal lining of the liver. Endothelial cells had elongated darkly staining nucleus and greatly attenuated cytoplasm. Phagocytic cells of Kupffer had a larger, paler nucleus and more extensive cytoplasm (Figure 1)

In the ACTH treated rat livers sinusoids appeared distended and sinusoidal endothelium was damaged, fragmented and desquamated

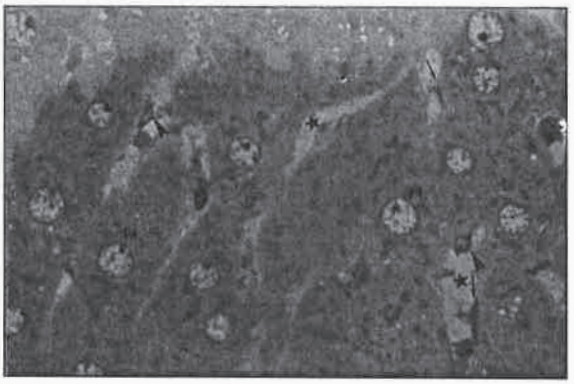

Figure 1: Light micrograph of control group liver . Sinusoidal spaces (stars) are between the cords of parenchymal cells (Hepatocytes=H). Endothelial cell nuclei (arrows), Kupffer cell (arrow heads). Toluidin blue-Azur II X 250.

(Figure 2-6). Some of the liver sinusoids were observed plugged with aggregated red blood cells (erytrocytes) (Figure 2A-B). Cytoplasmic blebs protruding into the sinusoidal lumen were noted (Figure 3). Marked cytoplasmic vacuolation, mitochondrial swelling(Figure 3,4,5) and unusually clear cytoplasm were seen in the endothelium of the majority of sinusoids (Figure 4). The cell containing fat droplets located in the space of Disse might be the fat-storing cells or myofibroblast like cells which transforming type from this cell (Figure 4-5). Sinusoidal space frequently contained cellular debris of disrupted endothelium (Figure 5). Most of the Kupffer cells were swollen and contained phagocytic inclusions and increased number of microbodies. Ruptures of cell membrane were also noticed (Figure 6).

DISCUSSION

In this study all the control group livers exhibited normal findings indifferent from routine examinations (5,6,7). Liver sinusoidal endothelial cells differ in fine structure from endothelial cells lining larger blood vessels and from other capillary endothelia in that they lack a distinct basement membrane and also contain open pores, or fenestrae, in thin cytoplasmic projections which constitute the sinusoidal wall. This distinctive morphology supports the protective role played by liver endothelium, the cells forming a general

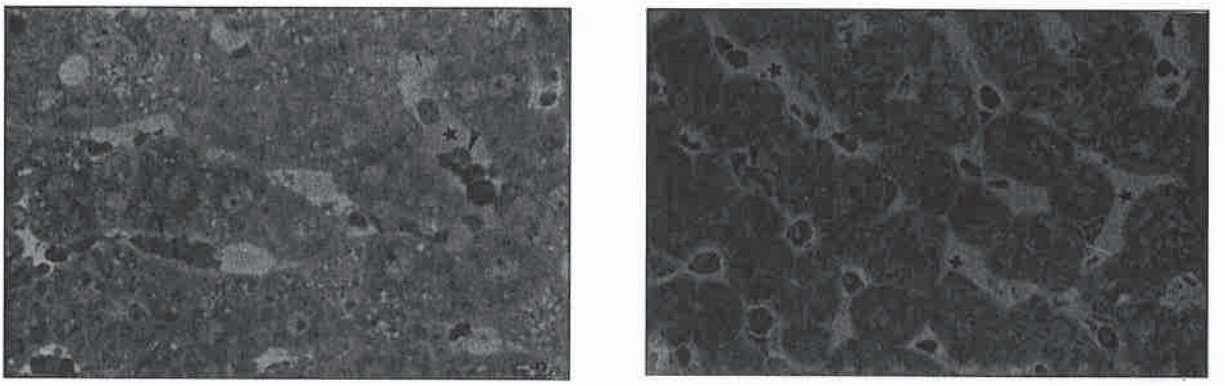

Figure 2 a-b: Light micrograph of ACTH treated liver. Distended sinusoids (stars) are seen. Erytrocyte plugging is prominent in most of the sinusoids (arrow head). Endothelial cell (thick arrow), Kupffer cell (thin arrow). Toluidin blue-Azur II X 250.

barrier against pathogenic agents and serving as a selective sieve for substances passing from the blood to parenchymal and fat-storing cells, and vice versa. Sinusoidal endothelial cells, furthermore, significantly participate in the metabolic and clearance functions of the liver (8). They have been shown to be involved in the endocytosis and metabolism of a wide range of macromolecules, including glycoproteins, lipoproteins, extracellular matrix components, and inert colloids, establishing endothelial cells as a vital link in the complex network of cellular interactions and cooperation in the liver (8). Each non-parenchymal cell and parenchymal cell of the liver interacts with all others and with the extracellular matrix. Therefore, the functional ability of each cell is constantly being modified by the metabolic activity of the others (9).

The mechanism of corticotropin (ACTH) action in the livers of rats following multiple injections of ACTH was studied and found that the effect of this hormone to albino rats resulted in a disturbance of the hepatocyte ultrastructure (10). Single administration of ACTH led to stimulation of synthesis of satured and monoenic fatty acids in liver tissue. It has been reported that the tropic hormone activated glyceroneogenesis contributing to an increase in concentration of both

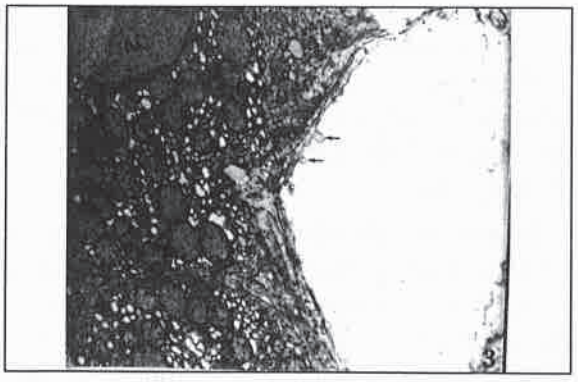

Figure 3: Electron micrograph of ACTH treated liver. Cytoplasmic blebs protruding into the sinusoidal lumen (arrows). Nucleus of hepatocyt (N). Miyofibroblast-like cell is seen (star). Uranil acetate-lead citrate X 9000.

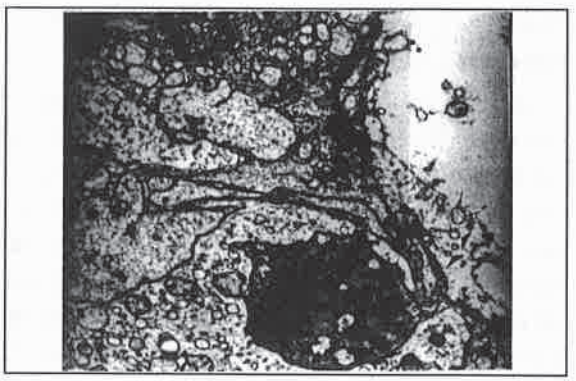

Figure 4: Electron micrograph of ACTH- treated liver. Cytoplasmic vacuolation (arrow head) and mitochondrial swelling (arrows) in the cytoplasm of endothelium. The cell containing fat droplets similar to fat-storing cells (star). Uranil acetate-lead citrate X 9000.

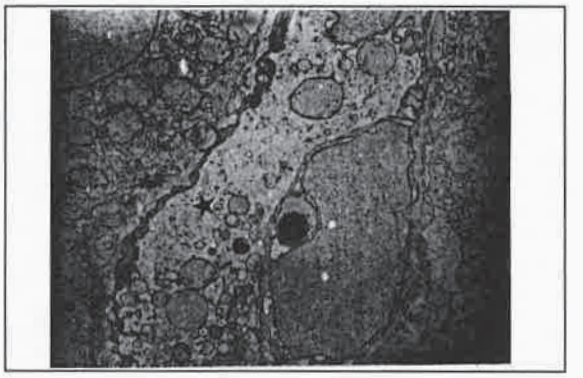

Figure 5: Electron micrograph of ACTH treated liver. Severely damaged endothelium become detached and disturbed cytoplasmic structures were observed in sinusoidal space (star). Fat droplet (arrow head) containing cell located in the space of Disse maybe fat-storing cell or transforming type of this cell. Uranil acetate-lead citrate X 9000.

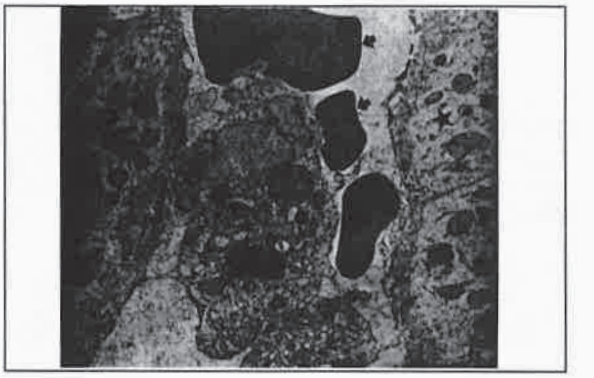

Figure 6: Electron micrograph of ACTH treated liver. Erythrocytes cytoplasm (arrow), Kupffer cell containing phagocytic inclusions (I) and rupture of all the membranes (arrow head). Hepatocytes (star). Uranil acetate-lead citrate X 9000.

alpha-glycerophosphate and long–chain fatty acids in hepatocytes(11). Endothelial cells filter the fluids, exchanged between the sinusoid and the space of Disse through fenestra. The structure of endothelial cell membrane changes ultrastructurally in special conditions that is disease and experiments with various factors such as pressure, alcohol, seratonin and nicotin (12). These changes mainly affect the passage of lipoproteins which contain cholesterol and vitamin A among other components (12).

In cultured liver endothelial cells, physiological scavenger function and catabolicevent in the turnover of connective tissue protein and transport mechanism through the endocytic pathway was described (13). Another observations of endothelial cell pockets , tight junctional complexes and membrane filled ghost sacs were recorded from perfused monkeys adrenal. However the argument existed that ghosts were artifactural and their role as steroid hormone releasing structures remains an open question. These structural features were considered for the potential of gating and sorting of metabolites and release of glucocorticoids in response to ACTH stimulated stresss events (14). Depending on the effects of glucocorticoids on cultured human endothelial cells a study was performed and indicated that glucocorticoids can alter the morphology and biochemistry of cultured endothelial cells and may have implications for the effects of steroids in the treatment of trombocytopenic states and vascular disorders in man (2,3)

Fat storing cells located in the space of Disse with long, contractile processes probably influence sinusoidal blood flow. These cells contain a large part of the body's depot of vitamin A. Strongly reduced levels of vitamin A occur in alcoholic liver developing fibrosis. Vitamin A deficiency transforms fat-storing cells into miyofibroblast-like cells with enhanced extracellular matrix (12,15).

In another study after cold ischemic storage of rat liver morphological changes were observed by transmission electron microscopy. There were two types of endothelial cell damage in the hepatic sinusoids. One was disruption of the endothelial linings, and the other detachment of endothelial cells into the sinusoidal space accompanied by fat-storing cell abnormalities (16).

Cellular and matrix changes in drug abuser liver sinusoids had been also analysed (17). In

addicts, hepatic vascular pole changes were a constant finding, accompanied by interhepatocyte space disjunction and perisinusoidal collagenization. Morphometric assessment confirmed a significant increase of sinusoidal wall surface, endothelial cell body and processes and Ito cell process surface was significantly different. This cellular hypertrophy may represent hyperactivation of the sinusoidal cell functional capacity, triggering the fibrogenesis in the space of Disse (17).

Kupffer cells are activated by lipopolysaccharide and endotoxins. As a result of activation these cells secrete oxygen radicals and become cytotoxic against tumor cells. Toxic secretory products can cause necrosis of the liver parenchyma and degeneration of sinusoidal endothelium (12).

In conclusion in this study dilatation of sinusoids and damaged endothelial cells were seen after ACTH treated rats. Kupffer cells were swollen and contained phagocytic inclusions and increased number of microbodies. These findings were probably due to effects of free fatty acids caused by lipid mobilization induced by ACTH. These cellular changes were similar to those seen previous findings and may account for some of the different systemic and metabolic alterations seen in ACTH induced animals.

REFERENCES

1-Maca RD, Hoak JC. Endothelial injury and platelet aggregation associated with acute lipid mobilization. Lab Invest 1974;30: 589-95.

2-Maca RD, Fry GL, Hakes AD. Effects of glucocorticoids on the interaction of lymphoblastoid cells with human endothelial cells in vitro. Cancer Res 1978; 38: 2224-8.

3-Maca RD, Fry GL, Hoak JC. The effects of glucocorticoids on cultured human endothelial cells. Br J Haematol 1978; 38: 501-9.

4-Rodriguez-Acosta A, Pulido-Mendez M, Finol HJ, Giron ME, Aguilar I. Liver ultrastructural pathology in mice envenomed with Uracoan rattlesnake (Crotalus vegrandis) venom. J Submicrosc Cytol Pathol 1999; 31:433-9.

5- Leeson TS, Leeson CR, Paparo: The Digestive System. Text /Atlas of Histology. Philadelphia: W.B. Saunders , 1988:475-96.

6-Fawcett DW: The Liver and Gallbladder: Bloom and Fawcett A Textbook of Histology. New York Chapman&Hall, 1994: 652-77.

7-Gartner LP, Hiatt JL: Digestive System III-Glands. Color Textbook of Histology. Philadelphia: W.B. Saunders, 1997: 346-55.

8-De Leeuw AM, Brouwer A, Knook DL. Sinosoidal endothelial cells of the liver : fine structure and function relation to age. J Electron Microsc Tech 1990; 14:218-36.

9-Le Bail B, Bioulac-Sage P, Senuita R, Quinton A, Saric J, Balabaud C. Fine structure of hepatic sinusoids and sinusoidal cells in disease. J Electron Microsc Tech 1990; 14:257-82.

10-Germaniuk IaL, Minchenko AG, Kozyritskii VG. Ultrastuctural changes in the livers of rats following multiple injections of corticotropin and sodium ribonucleinate. Tsitol Genet 1976; 10:409-12.

11-Pitsin DG, Titov VN, Vasileva-Dimova MP, Sanfirova VM. Effect of adrenocorticotropic hormone on the biosynthesis of glycerolipid components in the rat liver. Vopr Med Khim 1985; 31:53-60.

12-Wisse E, Braet F, Luo D, De Zanger R, Jans D, Crabbe E, Vermoesen A. Structure and function of sinusoidal lining cells in the liver. Toxicol Pathol 1996; 24:100-11.

13-Hellevik T, Martinez I, Olsen R, Toh BH, Webster P, Smedsrod B. Transport of residual endocytosed products into terminal lysosomes occurs slowly in rat liver endothelial cells. Hepatology 1998; 28:1378-89.

14-Apkarian RP, L'Hernault NL. Correlative light, transmission, and high resolution (SE-I) scanning electron microscopy studies of

adrenocortical vascular morphology. Scanning Microsc 1990; 4:125-32.

15-Tanuma Y, Ito T. Electron microscope study on the hepatic sinusoidal wall and fat-storing cells in the bat. Arch Histol Jpn 1978;41:1-39.

16-Ohno A, Mochida S, Arai M, Hirata K, Fujiwara K. Fat-storing cell abnormalities associated with endothelial cell damage after cold ischemic storage of rat liver in UW solution. Dig Dis Sci 1994; 39:861-5.

17-Trigueiro de Araujo MS, Gerard F, Chossegros P, Guerret S, Barlet P, Adeleine P, Grimaud JA. Cellular and matrix changes in drug abuser liver sinusoids: a semiquantitative and morphometric ultrastructural study. Virchows Arch A Pathol Anat Histopathol 1993; 422:145-52.

JOURNAL OF ANKARA MEDICAL SCHOOL Vol 23, No 2, 2001 91-94

ULTRASTRUCTURAL CHANGES IN THE ADRENAL CORTEX UNDER THE STRESS OF FASTING

Bizden SABUNCUOĞLU*

SUMMARY

In this study, the ultrastructural changes in adrenal cortex of rats were investigated under the stress of fasting. For this purpose, 15 male albino rats were used. Three of them were selected as control group. The others were parted in three groups. The experimental animals were kept fasted for 24 hours, 48 hours and 72 hours. After the animals were sacrified, the adrenal glands were removed and prepared for examining by transmission electron microscope.The most striking difference compared with to the controls, was the increased number of lipid droplets present in the cells of zona fasciculata and zona reticularis of the experimental animals. The lipid accumulation was in accordance with the time of fasting period. Increased microvilli and lysosomes of the cells, wided intercellular spaces and abundant macrophages were observed in both zona fasciculata and zona reticularis. In the animals which were kept fasted for 72 hours, the cells of zona fasciculata had irregular myelin like figures. In conclusion, fasting caused to several degenerative changes in the adrenal cortex.

Key words: *Adrenal Gland, Fasting, Ultrastructure*

ÖZET

AÇLIK STRESİ ALTINDA ADRENAL KORTEKSTE İNCE YAPI DEĞİŞİKLİKLERİ

Bu çalışmada, açlık durumunda sıçanların adrenal korteksindeki ince yapı değişiklikleri araştırıldı. Bu amaçla, 15 erkek albino sıçan kullanıldı. Bunların 3'ü kontrol grubu olarak seçildi. Geri kalanlar 3 gruba ayrıldı. Deney grubunun hayvanları 24, 48 ve 72 saat aç bırakıldı. Hayvanlar kurban edildikten sonra adrenal bezleri çıkarıldı ve geçirmeli elektron mikroskobuyla değerlendirilmek için hazırlandı. Kontrol grubuyla karşılaştırıldığında en belirgin farklılık, deney grubu hayvanlarında zona fasikülata ve zona retikülaris hücrelerinde artmış sayıda lipid damlacıklarının bulunmasıydı. Lipid birikimi açlık süresiyle uyumluydu. Hücrelerde artmış mikrovillus ve lizozomlar, genişlemiş hücrelerarası alan ve bol makrofaj hem zona fasikülata hem de zona retikülariste gözlendi.Yetmiş iki saat aç bırakılan hayvanlarda, zona fasikülata hücrelerinde düzensiz miyelin benzeri görünümler vardı. Sonuçta açlık, adrenal kortekste bir çok dejeneratif değişikliğe neden oldu.

Anahtar kelimeler: *Adrenal Bez, Açlık, İnce Yapı*

Life threatening events such as fasting effect various organs. It is known that fasting may cause various side effects on endocrine functions (1). It has been reported that fasting leads to metabolic change (2).The effects of fasting on the metabolism and the various organs are important. Hypothalamic-pituitary-adrenal axis responses during the fasting period. Maintenance of adequate levels of response of the hypothalamic-pituitary-adrenal axis during chronic stress is important for survival. Fasting is a stressor, as evidence by elevated levels of plasma and adrenal

*Department of Histology-Embryology, Ankara University Faculty of Medicine

Received: Jan 23,2001 Accepted: March 26,2001

corticosteroids. Dietary manipulation may produce functional changes (3). Fasting results in hyperadrenocorticism (4). Hyperadrenocorticism may play a role in activating cellular mechanism that retard aging (5,6). Hyperadrenocorticism causes to increased corticostreoid synthesis. Adrenal glucocorticoids, as being important in fuel mobilization and homeostasis during fasting. In the adrenal cortex, some ultrastructural changes appeare due to increased synthesis (7).

In this study, the ultrastructural changes in adrenal cortex of rats were investigated under the stress of fasting.

MATERIALS AND METHODS

In this study, 15 male albino rats were used. The main weight of the rats was 200gr. Three of the rats were selected as the control group. The rats of the control group were fedded normally. The remaining rats were parted in three groups. The experimental rats were kept fasted for 24 hours as the first group, 48 hours as the second group and 72 hours as the third group. The animals were sacrified under ether anesthesia. The removed adrenal glands were fixed in 2.5% glutaraldehyde in a phosphate buffer (PH:7.2) for 24 hours and postfixed in 1% osmium tetroxide. The materials were dehydrated in graded alcohol, embedded in Araldite CY 212, sectioned with a LKB Ultratome 3, stained with uranil acetate and lead citrate and examined in Jeol 100 transmission electron microscope.

RESULTS

The adrenocortical cells of the control group didn't show any structural abnormality. Some lipid droplets and abundant mithocondria with tubular cristae were observed in these cells (Fig.1).

The most striking difference compared with to the controls, was the increased number of lipid droplets present in the cells of zona fasciculata and zona reticularis of the experimental animals (Fig 2,3 and 4). The lipid accumulation was in accordance with the time of fasting period. Increased microvilli and lysosomes of the cells, wided intercellular spaces and abundant macrophages were observed in both zona fasciculata and zona reticularis (Fig 4, 5 and 6). All findings increased due to fasting period. In the rats of the third group which were kept fasted for 72 hours, the cells of zona fasciculata had irregular boundary of lipid droplets and irregular myelin like figures (Fig 7). Myelin like figures were also seen in the intercellular spaces and macrophage. In some of the macrophages, granular endoplasmic reticulum cisternae were wided and contained moderate density material. Also these cells had large golgi vesicles. (Fig 6, 8). These findings were due to the increased activity.

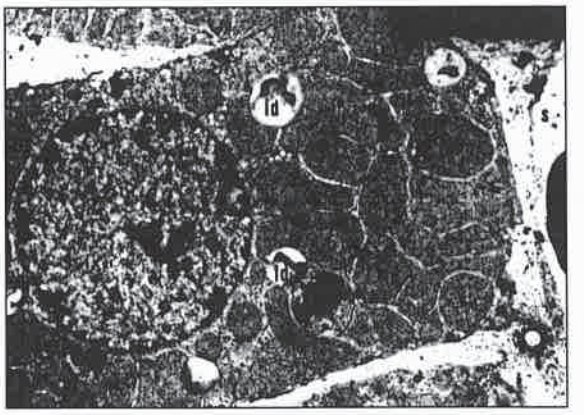

Figure 1: A cell in the zona fasciculata of the control group contains abundant mithocondria with tubular cristae (m) and some lipid droplets (ld). s:sinuzoid x 4800

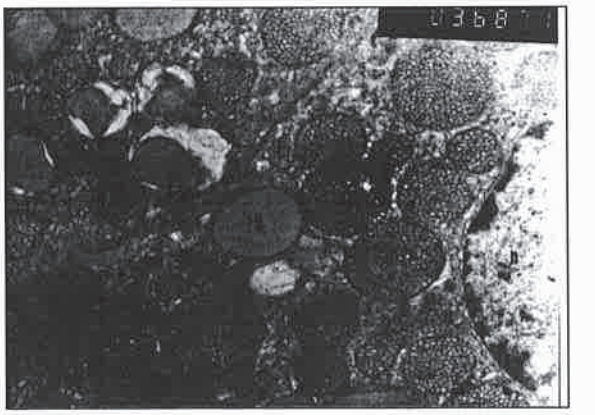

Figure 2: In the experimental group fasted for 72 hours, the cells of zona fasciculata are seen. m:mithocondrion, ld:lipid droplet, n:nucleus x10000

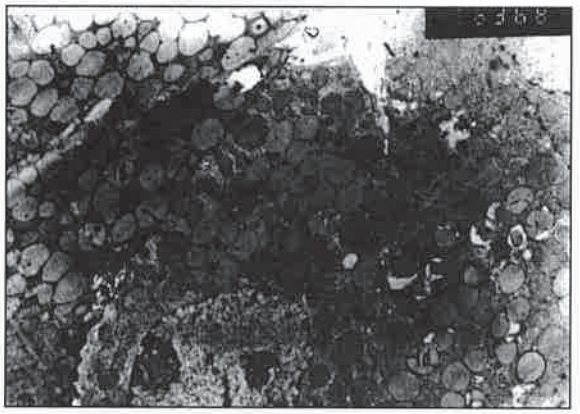

Figure 3: In the experimental group fasted for 72 hours, the cells of zona fasciculata are seen. Abundance of lipid droplets (ld) are prominent. m:mithocondria, n:nucleus x3600

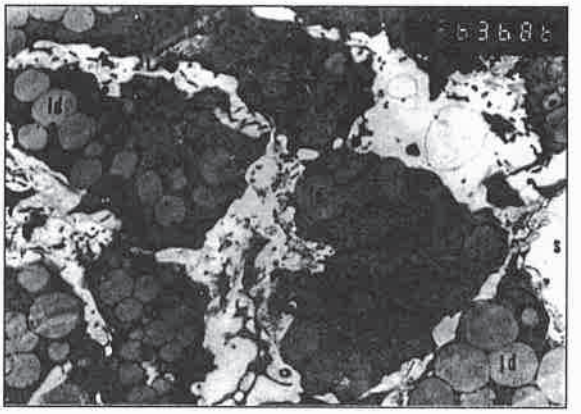

Figure 4: Cells in the zona reticularis of the group fasted for 72 hours. Lipid droplets (ld) are abundant and showing various size. Wided intercellular spaces are prominent. s:sinusoid x3600

DISCUSSION

Life threatening events such as fasting effect adrenal cortex. With the effect of adrenocorticotropic hormone (ACTH) which increases during the stress of fasting there becomes a rise in the synthesis and secretion of corticosteroids from the adrenal cortex. The glucocorticoid synthesis and release phenomena is associated with stress stimulated release of ACTH via the hypotalamic-pituitary axis (7,8). However some authors suggest that chronic food restriction induced hyperadrenocorticism is not due to an activated hypothalamo-pituitary unit. Their results indicate that enhanced adrenocortical responsiveness to ACTH plays a major role in the hyperadrenocortical state of chronically food restriction (6).

The excess ACTH causes to enlargement of adrenal glands and hypertrophy of adrenal cortex, resulting in overproduction of glucocorticoid hormones. Especially zona fasciculata and zona reticularis of adrenal cortex is affected by ACTH (7).

In this study, the stress of fasting caused to several changes in the adrenocortical cells especially in the zona fasciculata and zona reticularis as increased lipid accumulation and abundant

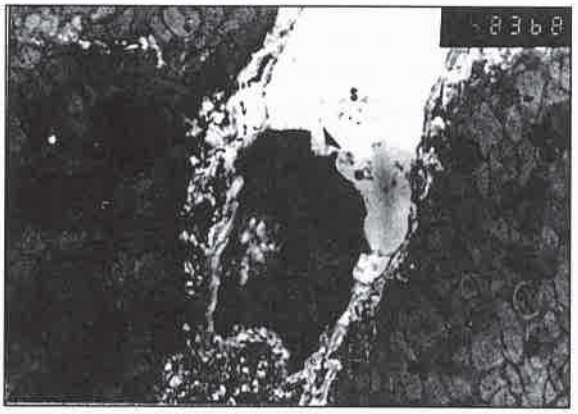

Figure 5: Cells in the zona fasciculata of the group fasted for 72 hours have abundant lysosomes (l) and microvilli (*). s:sinusoid, arrow head:endothelial cell x4800

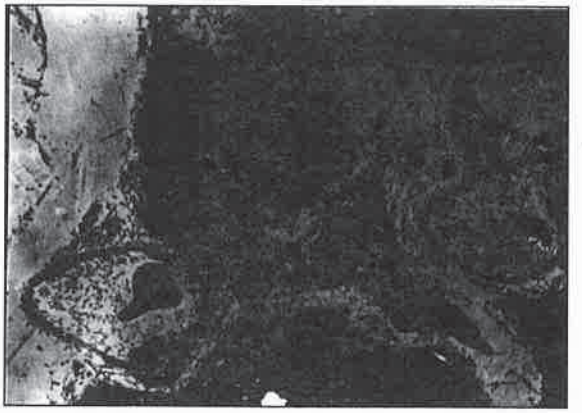

Figure 6: Zona reticularis of the group fasted for 72 hours. Macrophages (arrows) are seen. s:sinusoids x2900

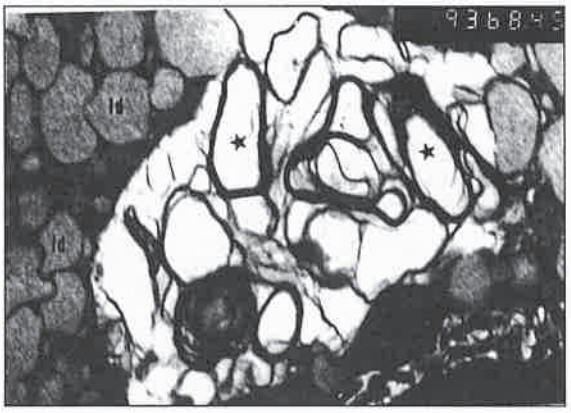

Figure 7: A cell in the zona fasciculata of the group fasted for 72 hours shows irregularly shaped lipid droplets (ld) and myelin like figures (*) x19000

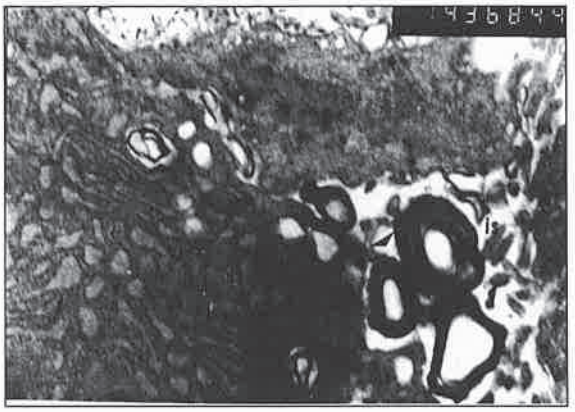

Figure 8: Zona fasciculata of the group fasted for 72 hours. Myelin like figures (arrow heads) are seen in the intercellular space (is) and a macrophage (M). The macrophage contains large golgi vesicles (arrows) x19000

lysosomes. Also wided intercellular spaces and abundant macrophages were observed. Alterations of adrenal cortex in rats may be releated to increased glucocorticoid synthesis, secretion and adrenocortical dysfunction caused by hypoglycemic stress in accordance with observed in previous experiment (9,10).

REFERENCES

1.Wright ML, Proctor KL, Alves CD. Hormonal profiles correlated with season, cold and starvation in Rana Catesbeiana (bullfrog) tadpoles. Comp Biochem Physiol C Pharmacol Toxicol Endocrinol 1999; 124 (1): 109-16

2. Dallman MF, Akana SF, et al. Starvation: early signals, sensors, and sequelae. Endocrinology 1999; 140 (9): 4015-23

3. Buchan AM, Pederson RA, Koop I, et al. Morphological and functional alterations to a

sub-group of regulatory peptides in human pancreas and intestine after jejuna-ileal bypass. Int J Obes Relat Metab Disord 1993; 17 (2): 109-13

4. Klebanov S, Diais S, et al. Hyperadrenocorticism, attenuated imflammation and the life-prolonging action of food restriction in mice. J Gerontol A Biol Sci Med Sci 1995; 50 (2): 79-82

5. Aquilera G. Regulation of pituitary ACTH secretion during chronic stress. Neuroendocrinol 1994; 15 (4): 321-50

6. Han ES, Evans TR, Nelson JF. Adrenocortical responsiveness to adrenocorticotropic hormone is enhanced in chronically food restricted rats. J Nutr 1998; 128(9): 1415-20

7. Rhodin JAG. The ultrastructure of the adrenal cortex of the rat under normal and experimental condition. J Ultras Res 1971; 34: 23-71.

8. Apkarian RP, Hernault NL. Correlative light, transmission and high resolution scanning electron microscopy studies of rhesus adrenocortical vascular morphology. Scanning Microsc 1990; 4(1): 125-132

9. Mazzocchi G, Malendowiez LK, et al. Pancreatic polypeptide enhances plasma glucocortlcoid concentration in rats: possible role in hypoglycemic stress. Life Sci 1995; 56(8): 595-600.

10. Aquilera G. Regulation of pituitary ACTH secretion during chronic stress. Front Neuroendocrinol 1994; 15(4): 321-350

JOURNAL OF ANKARA MEDICAL SCHOOL Vol 23, No 2, 2001 95-102

THREE-DIMENSIONAL CT ANGIOGRAPHY

Suat Fitoz* ✣ Çetin Atasoy* ✣ Cemil Yağcı** ✣ Serdar Akyar***

SUMMARY

The aim of this study was to determine the role of the volume-rendering technique in three-dimensional CT angiography and compare this method with maximum-intensity projection and surface-shaded displays.

Twenty-eight patients underwent CT angiography. Axial source images were transformed into three-dimensional images using maximum-intensity projection, surface-shaded display and volume-rendering techniques on separate workstations. Two radiologists compared the three-dimensional images obtained with each of the methods.

Anatomical detail was better depicted with the volume-rendering technique, which utilizes all raw data. This technique also enabled a conception of depth and could discern superimposed vascular structures. Mural calcifications prevented assessment of luminal patency in maximum intensity projection images, which select only the pixels with the highest opacities. Other disadvantages of maximum intensity projections included superimposition of vessels and lack of depth information. With the surface-shaded method, inappropriate threshold levels and high filter values resulted in under- or overestimation of the degree of stenosis.

In conclusion, as a result of minimal loss of data and inclusion of all density information, volume rendering demonstrated clear-cut superiority over maximum-intensity projection and surface-shaded display methods.

Key words: *CT Angiography, Maximum-İntensity Projection, Surface-Shaded Display, Three-Dimensional İmaging, Volume Rendering.*

ÖZET

ÜÇ BOYUTLU BT ANJİOGRAFİ

Volüm rendering (VR) tekniğinin üç boyutlu BT anjiyografideki rolü ve maximum intensity projection (MIP) ve surface shaded display (SSD) tekniklerine olan üstünlüğü araştırıldı.

BT anjiyografi protokolü ile incelenen, vasküler sistem anomali ya da patolojisi bulunan 28 olgu çalışmaya dahil edildi. BT inceleme sonrası aksiyal görüntüler bilgisayar ağına transfer edilerek uygun yazılım programları ile vasküler yapıların standart açılarla MIP, SSD ve VR teknikleri ile üç boyutlu görüntüleri oluşturuldu. İki radyolog tarafından tekniklerin birbirlerine üstünlükleri araştırıldı.

VR tekniğinde ham görüntülerdeki bilgilerin tümünün kullanılması anatomik detayı daha net ortaya koydu. Derinlik bilgisi taşıdığından VR ile süperpoze vasküler yapılar net olarak değerlendirilebildi. MIP tekniğinde incelenen kesimdeki en yüksek piksel değerleri yansıtıldığından kalsifiye vasküler yapılarda luminal patens net olarak değerlendirilemedi. Yine MIP tekniğinde vasküler yapılarda süperpozisyon ve derinlik bilgisi olmayışı önemli bir dezavantaj olarak izlendi. SSD tekniği vasküler yapıyı izole şekilde tüm seyri boyunca net olarak ortaya koydu. SSD'nin uygun eşik değeri ve filtrenin ayarlanamadığı olgularda özellikle stenozlarda yanılgı nedeni olabileceği gözlendi.

Sonuçta VR tekniği ilgili voksellerdeki bilgilerin tümünün üç boyutlu görüntüye aktarılması ve minimal veri kaybı ile MIP ve SSD'ye göre üstün bir teknik olarak göze çarptı.

Anahtar kelimeler: *BT Anjiyografi, Maximum İntensity Projection, Surface-Shaded Display, Üç-Boyutlu Görüntüleme, Volüm Rendering*

*Specialist in Ankara University, School of Medicine, Department of Radiology

**Associate Professor in Ankara University, School of Medicine, Department of Radiology

***Professor in Ankara University, School of Medicine, Department of Radiology

Received: March 23,2001 Accepted: May 01,2001

The development of the spiral CT has enabled volumetric scanning and three-dimensional imaging (1). Three-dimensional imaging allows a better appraisal of the extent of craniocaudal lesions and eliminates the need for angiography in selected patients with selected vascular disease. Maximum intensity projection (MIP) and surface-shaded display (SSD) are well-known three-dimensional imaging techniques. Volume rendering (VR) is a relatively new method that requires a faster, high-capacity software program (1). In this study, we compared this latest method of three-dimensional imaging with the earlier-developed techniques.

Materials and methods: The study group included 28 patients with congenital or acquired vascular lesions. These included: renal artery stenosis (6 patients), pulmonary embolism (3 patients), coarctation of the aorta (1 patient), aberrant right subclavian artery (2 patients), double aortic arch (1 patient), portal vein aneurysm (1 patient), splenic artery aneurysm (1 patient), intralobar pulmonary sequestration (1 patient), aortic aneurysm (3 patients), aortic dissection (2 patients), superior vena cava thrombosis (1 patient), atherosclerotic aorta (1 patient), bilateral carotid artery stenosis (1 patient), Takayasu arteritis and subclavian artery occlusion (1 patient) and ureteropelvic stenoses due to vascular compression (3 patients). CT examinations were performed using a helical scanner (HiSpeed CT/i, General Electric Medical Systems, Wisconsin, USA). All vascular structures except for central veins were opacified using 80-150ml non-ionic contrast media delivered at a rate of 3-5ml/s via an automated injector after the determination of delay time using a 20ml test dose. Patients were scanned during a single breath-hold period with 1-5mm section thickness, 1-1.7 pitch, 120-140 kV and 200-280 mA. Slice thickness was 1mm in carotid artery examinations, 3mm in CT angiography of the renal artery, portal vein, pulmonary thromboembolism and pulmonary sequestration, and 5mm for examinations of long arterial segments in patients with aortic dissection, atherosclerotic disease and aortic aneurysm. The table feed varied inversely with the selected slice thickness: the pitch was 1.7 for a slice thickness of 1mm, 1.5 for a slice thickness of 3mm, and 1 for a slice thickness of 5mm. Helical data was reconstructed with a 30-70% overlap and transformed into three-dimensional images using the MIP, SSD and VR methods. With SSD, threshold levels were selected on an individual basis according to the degree of intravascular opacification. With VR, three-dimensional images were produced using the semitransparent method, allowing visualization of the vessel wall. Three-dimensional images with 15 degree increments in the x and y axes were printed for hand-copy analysis of each method. Images were assessed for origin of vascular branches, course of vascular structures, relationship of vessels with adjacent organs, luminal patency, stenosis and plaques. Two radiologists interpreted the images and compared the three techniques. In patients with renal artery stenoses, the three-dimensional images were correlated with digital subtraction angiography images.

Results: Pulmonary arteries were better assessed with VR owing to the depth information provided by this technique. Although a higher number of vessels were visualized with MIP, superimposition prevented a thorough evaluation of pulmonary vascularity (Fig 1). Because MIP selected those pixels with the highest attenuation numbers, vascular calcifications caused inaccurate assessment of luminal patency and degree of stenosis. While superimposition of contrast-enhancing parenchymal organs over the vessels of interest was a major disadvantage of MIP, VR allowed for differential visualization of organs and vascular structures by differential color mapping (Figs 2-4). Inappropriate levels of threshold and filtration caused errors in the grading of stenosis with SSD; however, the luminal patency was better assessed than with MIP and VR (Fig 5).

VR was successful in showing small-calibre vessels and the relationship of vascular structures and neighboring organs and tissues (Fig 6). With MIP, obliquely oriented vessels showed artifactual mural irregularities that were not observed with VR (Fig 7).

Figure 1. Pulmonary embolism. Vascular map produced with VR **(a)** and MIP **(b)** techniques. Inferior view. VR provides depth impression, while the superimposition of vascular structures degrades the image quality with MIP.

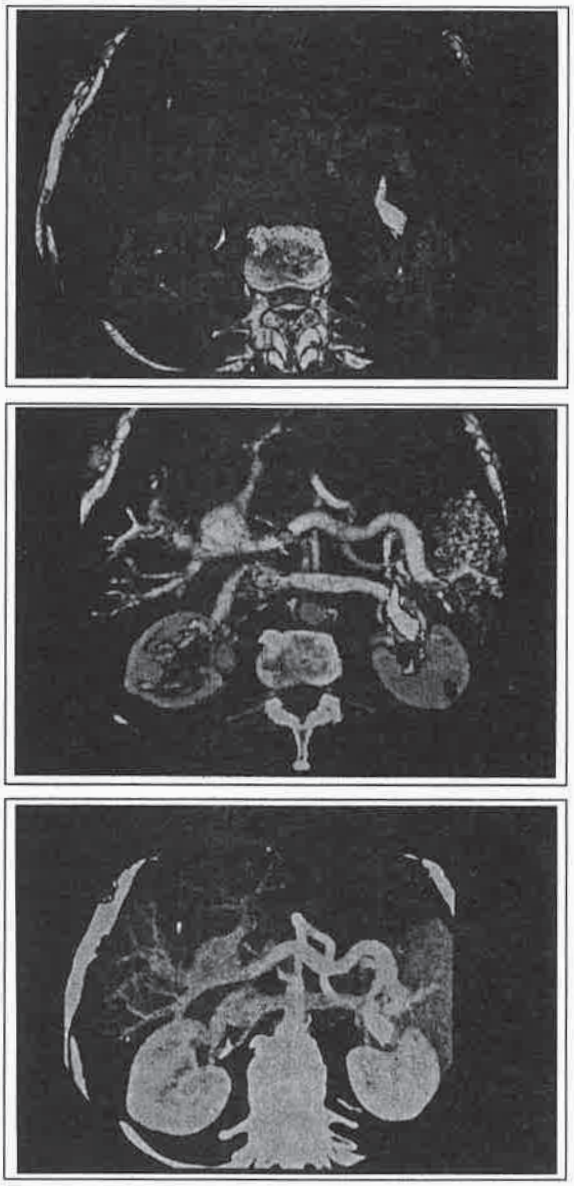

Figure 2. Portal vein aneurysm. Depth information on VR **(a)** and SSD **(b)** images is not provided by the MIP image **(c)**.

Discussion: Advancement in spiral technology has allowed for evaluation of vessel diseases using CT. Recently, academic and clinical interest has focused on three-dimensional imaging using VR (1). The technique is appealing mostly for its ability to provide all necessary information regarding the region of interest. Axial scan data is reconstructed into volume elements called 'voxels' in a three-dimensional matrix. The data con-

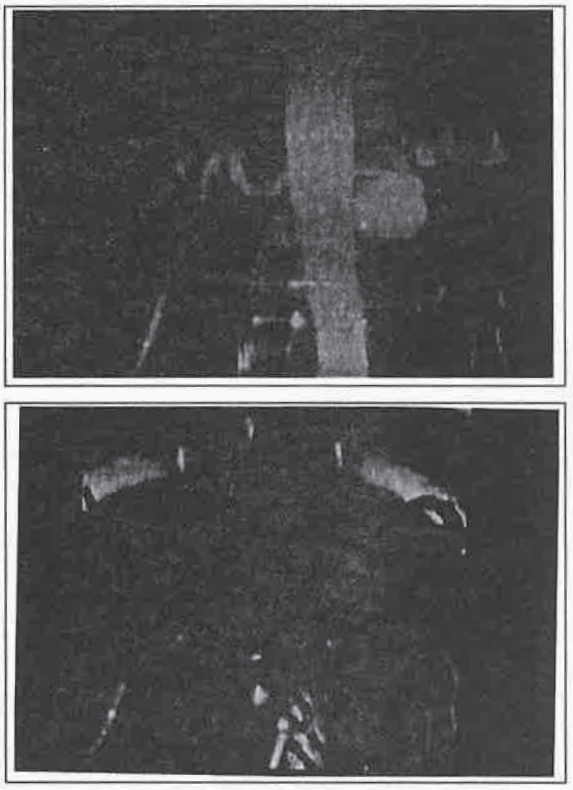

Figure 3. Splenic artery aneurysm. Proximal splenic artery cannot be assessed on MIP image **(a)** but is shown by VR **(b)**.

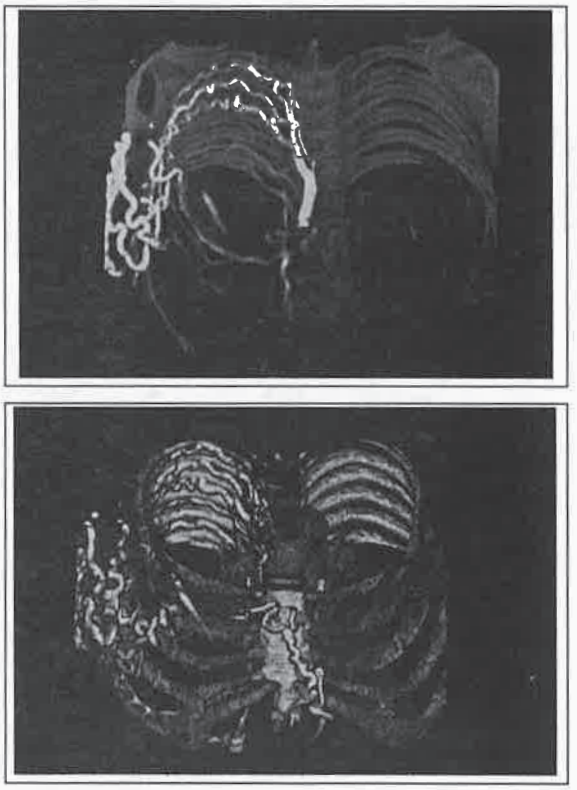

Figure 4. Superior vena cava thrombosis in patient with Behçet's disease. Because of their relatively low density values, some of the chest wall collaterals are not visible in the MIP image **(a)**. VR, which codes a full range of density differences, can show all the collateral veins along with a depth impression **(b)**.

tained within the voxels is processed into three-dimensional images by several different techniques in order to render either surface or internal details (1).

SSD is a relatively older technique that incorporates only about 10% of all CT data into three-dimensional images that simply reflect the surface detail of the structures within the scanned volume (1). The most commonly employed surface-rendering method is simple thresholding, which only processes voxels within an operator-specified density range (1,2). Surface contours are generated by polygonal coding of density values in the surfaces of the structures of interest (1). However, some of the voxels may be misclassified due to partial volume effects (2). With virtual illumination of every polygon, a surface-shaded image of the object is produced that also has depth information (1,2). SSD is a fast technique that renders depth impression well and can image objects separately (1,2). However, this technique has three main limitations (2,3). Firstly, inappropriate thresholding causes errors in the grading of stenoses. Unduly high threshold levels make stenoses appear more severe, while lower threshold levels result in underestimation of stenoses (3). In one of our patients, renal artery stenosis was overestimated as total occlusion due to high threshold levels. The second drawback of SSD is stair-step artifact, which is related to the thickness of the section used in scanning (3). The third limitation of the technique results from image degradation caused by density or contrast differences along the z axis (3). This occurred in one of our patients, in

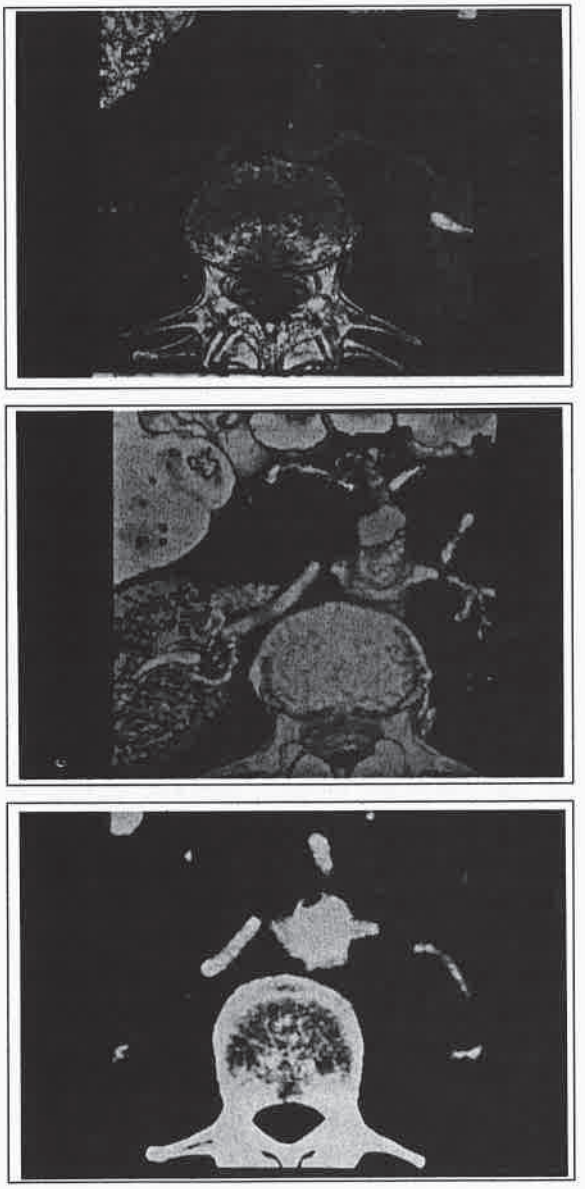

Figure 5. CT angiography in bilateral renal artery stenoses. VR **(a)**, SSD **(b)**, and MIP **(c)** images, inferior oblique view. Due to inappropriate levels of threshold and filtration, the right renal artery appears occluded in the SSD image, while the MIP and VR images dislocate the patent lumen.

whom uniform enhancement of the aorta could not be attained.

MIP is probably the most popular rendering technique employed in CT angiography (4). Since they are threshold independent, MIP images conserve attenuation data (2,5). Thin slabs allow for imaging of small vascular structures and visualisation of renal artery stenoses (2,6). Simply, in MIP, the highest density voxels along the line of vision are selected and form the image (1,7). One important disadvantage of the technique results from superimposition, which makes evaluation of complex anatomical structures difficult (3). This drawback may be potentially overcome by selecting thinner slabs and time-consuming interactive manipulations to highlight the specific structure of interest. MIP images are devoid of depth impression (2). Since the voxels with the highest density values are selected, vessel calcifications int-

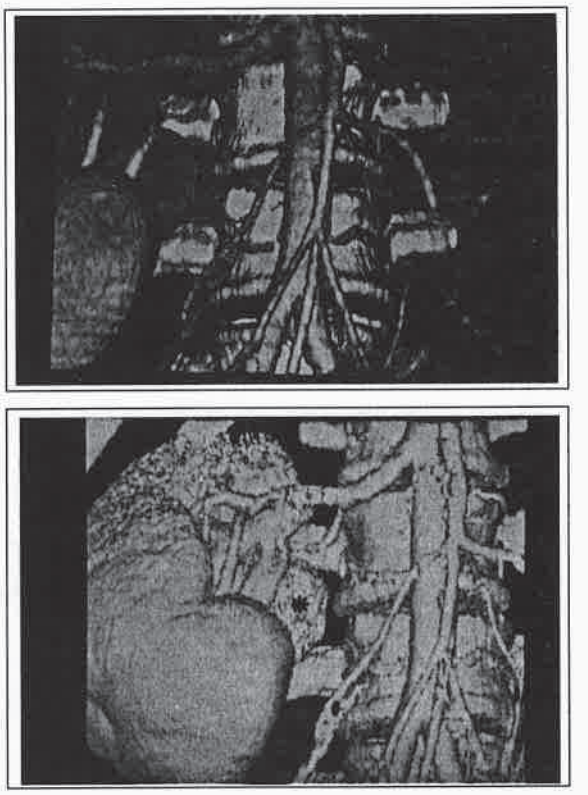

Figure 6. Ureteropelvic stenosis with suspected vascular copmression. VR image shows the vascular branches superimposed on the renal pelvis **(a)**. In the SSD image, the vessels cannot be distinguished from the specified pelvis renalis **(b)** (asterisk: pelvis renalis).

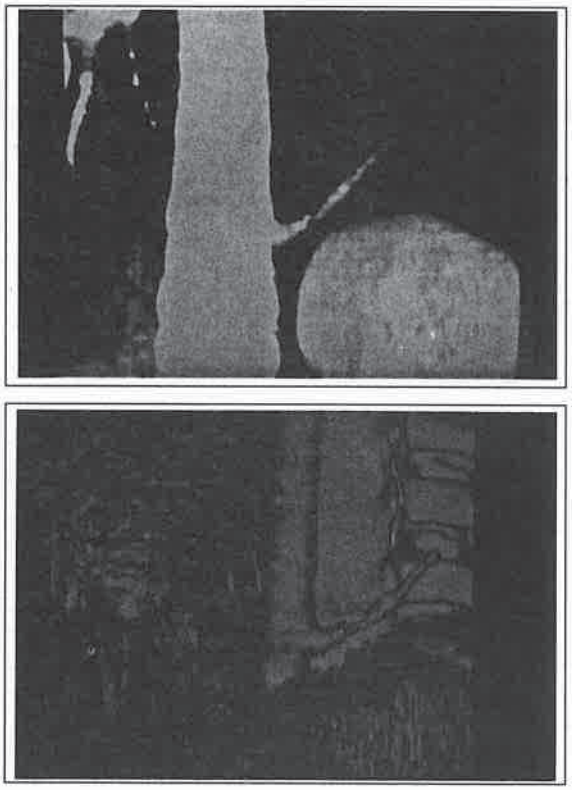

Figure 7. Pulmonary sequestration. Due to its oblique course, the feeding artery originating from the aorta appears irregular on the MIP image **(a)**. The artifactual contour irregularity disappears in the VR image **(b)**.

roduce confusion in vascular examinations, as was the case in several of our patients. For the same reason, pulmonary emboli that are not contiguous with the vessel wall may escape detection when thick slabs are used (2,6). When one of our patients underwent MIP, the test dose of contrast media used to determine delay time collected in the renal pelvis and obscured the renal arterial branch crossing the renal pelvis. Another disadvantage of MIP comes from the string-beaded appearance of the small vascular structures that run obliquely within the plane of the scan (1,2,8). This hampered the visualisation of the feeding artery in a patient with pulmonary sequestration in our series.

A combined use of MIP and SSD techniques in patients with aortic coarctation can noninvasively visualise stenoses with a success rate comparable to angiography and may be used in pre- and postoperative assessment. Becker et al found no significant difference between MIP and angiography in the measurement of coarctation and poststenotic dilatation. These authors also employed three-dimensional imaging of collateral vessels using SSD (9).

VR is a recently introduced technique that has overcome many of the limitations of SSD and MIP imaging (1,2). Aided by advanced computer software, this technique utilises all scan data present in the axial raw images (1,2,10). Using various algorithms, either the surface or the internal details of structures can be imaged (1). In VR, the operator can manipulate a variety of parameters including opacity, brightness, peak attenuation value, far or near shading, and kinetic-stereo depth curves, as well as window width and level (1,2). The technique is very effective in the assessment of vessels perpendicular to the axial plane, the degree and length of stenoses, and the relationship of vessels to other anatomic structures. Conventional angiography-like images can be generated using VR (11,12,13). In addition to evaluation of renal artery stenoses, vascular variations in potential kidney donors can be reliably shown, thereby reducing the need for conventional angiography and intravenous urography (14,15). Today, VR has supplanted MIP in the three-dimensional imaging of vascular anatomy (16). While the overall success of VR in vessel stenoses is high, the technique has limitations in the imaging of vessels coursing the axial plane (17). Thus, VR is more accurate in imaging the aorta and carotid arteries than in imaging renal arteries (18,19). Pulmonary sequestration feeding arteries can be shown successfully, and venography-like images can be obtained in patients with superior vena cava syndrome (2). VR has an important advantage over MIP in imaging the splanchnic vascular bed because VR can show the major branches of the aorta, including the celiac truncus and superior mesenteric artery, along with depth information. VR can also show the portal venous structures, including the superior mesenteric vein, at the

same time, providing another advantage over MIP, which cannot resolve superimposed structures and convey depth information (12). Reported accuracy rates in detecting thoracic and abdominal aorta aneurysms and renal artery stenoses are almost the same with VR as with conventional angiography (1). Very minute vessels are not sacrificed with VR (20), and the three-dimensional imaging allows for better assessment of pulmonary vessels, pulmonary arteriovenous malformations, marginated thrombi and postoperative orientation of vessels (21).

To conclude, VR is the most commonly employed three-dimensional imaging modality. Recent advances in software technology have expanded the use of this technique considerably. Color coding of different attenuation values and rendering of depth impression are the major advantages of VR.

REFERENCES

1. Calhoun PS, Kuszyk BS, Heath DG, Carley JC, Fishman EK. Three dimensional volume rendering of spiral CT data: theory and method. Radiographics 1999; 19:745-764.
2. Remy J, Remy-Jardin M, Fribourg M. Multiplanar and three-dimensional reconstruction techniques in CT: impact on chest disease. Eur Radiol 1998; 8:335-351.
3. Takahashi M, Ashtari M, Papp Z, et al. CT angiography of carotid bifurcation: artifacts and pitfalls in shaded-surface display. AJR 1997; 168:813-817.
4. Heath DG, Soyer PA, Kuszyk BS et al. Three-dimensional spiral CT during arterial portography: comparison of three rendering techniques. Radiographics 1995; 15:1001-1011.
5. Prokop M, Oh Shin H, Schanz A, Schaefer-Prokop CM. Use of maximum intensity projections in CT angiography: a basic review. Radiographics 1997; 17:433-451.
6. Prokop M. CT angiography of the abdominal arteries. Abdom Imaging 1998; 23:462-469.
7. Schreiner S, Paschal CB, Galloway RL. Comparison of projection algorithms used for the construction maximum intensity projection images. J Comput Assist Tomogr 1996; 20:56-57.
8. Remy-Jardin M, Remy J, Cauvain O, Petyt L, Wanebroucq J, Beregi JP. Diagnosis of central pulmonary embolism with helical CT: role of two-dimensional multiplanar reformations. AJR 1995; 165:1131-1138.
9. Becker C, Soppa C, Fink U, et al. Spiral CT angiography and 3D reconstruction in patients with aortic coarctation. Eur Radiol 1997; 7:1473-7.
10. Kuszyk BS, Heath DG, Ney DR, Bluemke DA, Urban BA, Chambers TP, Fishman EK. CT angiography with volume rendering: imaging findings. AJR 1995; 165:445-448.
11. Johnson PT, Heath DG, Kuszyk BS, Fishman EK. CT angiography: thoracic vascular imaging with interactive volume rendering technique. J Comput Assit Tomogr 1997; 21:110-114.
12. Johnson PT, Heath DG, Kuszyk BS, Fishman EK. CT angiography with volume rendering: advantages and applications in splanchnic vascular imaging. Radiology 1996; 200:564-568.
13. Smith PA, Marshall FF, Urban BA, Heath DG, Fishman EK. Three-dimensional CT stereoscopic visualization of renal masses: impact on diagnosis and patient management. AJR 1995; 165:445-448.
14. Rubin GD, Alfrey EJ, Dake MD, et al. Assessment of living donors with spiral CT. Radiology 1995; 195:457-462.
15. Johnson PT, Halpern EJ, Kuszyk BS, et al. Renal artery stenosis: CT angiography-comparison of real-time volume-rendering and maximum intensity projection algorithms. Radiology 1999; 211:337-43.
16. Marro B, Valery CA, Bitard A, et al. Intracranial aneurysm on CTA: demonstration using a transparency volume-rendering technique. J Comput Assist Tomogr 200; 24:96-98.
17. Kuszyk BS, Heath DG, Johnson PT, Eng J, Fishman EK. CT angiography with volume rendering

for quantifying vascular stenoses: in vitro validation of accuracy. AJR 1999; 173:449-455.

18. Kuszyk BS, Heath DG, Johnson PT, Fishman EK. CT angiography with volume rendering: in vitro optimization and evaluation of accuracy in quantifying stenoses. AJR 1997; 168:79.
19. Marcus CD, Ladam-Marcus VJ, Bigot JL, Clement C, Baehrel B, Menanteau BP. Carotid arterial stenosis: evaluation at CT angiography with the volume-rendering technique. Radiology 1999; 211:775-80.
20. Hong KC, Freeny PC. Pancreaticoduodenal arcades and dorsal pancreatic artery: comparison of CT angiography with three-dimensional volume rendering, maximum intensity projection, and shaded-surface display. AJR 1999;172:925-31.
21. Remy J, Remy-Jardin M, Artaud D, Friborg M. Multiplanar and three-dimensional reconstruction techniques in CT: impact on chest diseases. Eur Radiol 1998; 8:335-51.

JOURNAL OF ANKARA MEDICAL SCHOOL Vol 23, No 2, 2001 103-109

MAMMOGRAPHIC PARENCHYMAL PATTERNS OF THE MALE BREAST WITH GYNECOMASTIA

Selma Tükel*

SUMMARY

Aim and background : *The mammographic findings of male patients were reviewed in order to evaluate parenchymal patterns in gynecomastia as a means for distinguishing between gynecomastia and cancer in differential diagnosis.*

Methods and materials: *Over a two-year period, 95 male patients were examined, and mammographic findings of 73 patients found to have gynecomastia were evaluated (Mean age: 34 years; age range: 12-87 years). Parenchymal patterns were classified according to criteria previously described in the radiology literature. All patients underwent ultrasonography.*

Results: *Of the 73 gynecomastia patients, 37 (48.7%) had bilateral gynecomastia, 30 (43.4%) had unilateral gynecomastia and six (7.9%) had pseudogynecomastia in one breast and gynecomastia in the other. Types of gynecomastia found were dendritic (32 patients, 46.1%), nodular (18 patients, 23.7%) and diffuse (18 patients, 23.7%). In five of the patients (6.5%) with bilateral gynecomastia, different types of gynecomastia were detected in each breast. There was no development of cancer during follow-up periods ranging from 6-27 months.*

Conclusions: *The detection of carcinoma in early stages directly influences survival. A better understanding of the mammographic parenchymal patterns of gynecomastia leads to more successful differential diagnosis between cancer and gynecomastia.*

Keywords: *Gynecomastia, Mammography, Parenchymal Patterns*

ÖZET

JİNEKOMASTİLİ OLGULARDA MAMOGRAFİK PARANKİMAL PATERNLER

Amaç: *Jinekomasti ve meme kanserinin ayırıcı tanısına katkıda bulunabilmek için, jinekomastili olguların mamografi bulguları gözden geçirildi.*

Materyal ve metod: *İki yıllık süreçte 95 erkek olgu incelendi. 73 olgu jinekomasti tanısı aldı. Radyoloji literatür bulguları ile uyumlu olarak parankim özellikleri sınıflandırıldı. Tüm olgulara ultrasonografi uygulandı.*

Sonuçlar: *73 olgunun 37'si bilateral (%48.7), 30'u unilateral (%43.4) jinekomasti iken, 6 olguda bir memede adipomasti diğer memede jinekomasti saptandı (%7.9). 32 dendritik (%46.1), 18 nodüler (%23.7), 18 diffüz (%23.7) tip jinekomasti tanımlandı. 5 olgunun herbir memesinde farklı patern mevcuttu (%6.5). 6-27 aylık takip sürecinde hiçbir olguda malignite gelişmedi.*

Tartışma: *Karsinomanın erken dönemde saptanması direkt olarak sağkalım süresini etkilemektedir. Ancak mamografik paternler iyi tanınırsa gereksiz biyopsilerden koruma ve jinekomasti ile karsinoma arasında doğru ayırıcı tanı mümkün olacaktır.*

Anahtar Kelimeler: *Jinekomasti, Mammografi, Parankimal Paternler*

**Associate professor Ankara University, Faculty of Medicine, Radiology Department*

Received: April 25,2001 Accepted: May 15,2001

Gynecomastia is the most common breast pathology found in men. Although gynecomastia is a benign disease, it may on rare occasion coexist with carcinoma. Furthermore, physical examination and mammographic findings may occasionally suggest malignancy. In our department, ultrasonography is performed on all gynecomastia patients to rule out mass lesions, except when mammographic examination reveals bilateral fatty breasts (pseudogynecomastia or adipomastia).

In some cases, ultrasonographic findings are equivocal, making differential diagnosis difficult. As a result, biopsy or surgery may be performed unnecessarily. A better awareness of parenchymal patterns in gynecomastia could aid in differential diagnosis.

Materials and methods :

Over a two-year period, 95 male patients were examined. The patients had breast tenderness, bilateral or unilateral breast enlargement, palpable lumps, pathological findings of the skin, nipple flow or nipple retraction.

Mammograms were obtained using a Senograph DMR Mammography Unit (General Electric, Paris) and Agfa "Mammoray HDR" film. Bilateral craniocaudal and mediolateral oblique views were obtained on all patients.

Ultrasonography was performed using an RT-X400 Unit (General Electric) with a 7.5MHz linear transducer and water pad. Results of mammography and ultrasonography were reviewed for all patients. In cases where gynecomastia could not be definitively diagnosed, Doppler ultrasonography, magnetic resonance imaging (MRI) or fine needle aspiration biopsy (FNAB) was performed.

Patients were diagnosed with pseudogynecomastia if fatty tissue with no soft tissue density was observed on both mammographic projections (Fig 1). No further study was performed on this group of patients.

Patients were diagnosed with gynecomastia if a triangular or roughly circular area of increased density, usually abutting the nipple, was

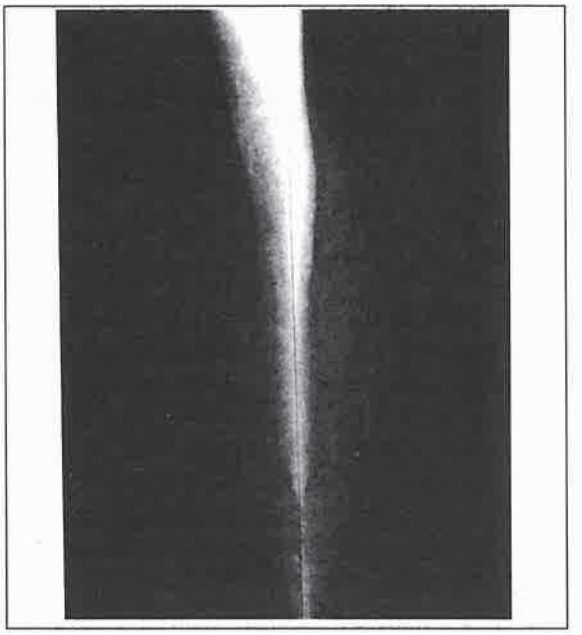

Fig. 1: Bilateral MLO mammograms of a 56-year-old man with bilateral breast enlargement diagnosed as pseudogynecomastia. There are no retroareolar density or ductal structures.

observed in the retroareolar region on mammogram. When the gynecomastia was bilateral, it was generally symmetrical on both sides.

Ultrasonography was performed in all cases to rule out mass lesions. A diagnosis of gynecomastia was made when ultrasonography revealed glandular tissue enlarged to several centimetres or to the size of a fully developed female breast. The sonographic appearance of gynecomastia is indistinguishable from that of a normal female breast. Sonographic features of the young male breast are usually that of sonographic features of juvenile mammary tissue. Sonographically, the breast in gynecomastia appears structurally normal (1).

Doppler ultrasonography and/or MRI were performed in cases where ultrasonographic findings were equivocal.

Parenchymal patterns on mammograms were identified by the following characteristics (2) :

1- Nodular patterns: varying in size, with extremely smooth contours at the subareolar region (Fig. 2 a-b)

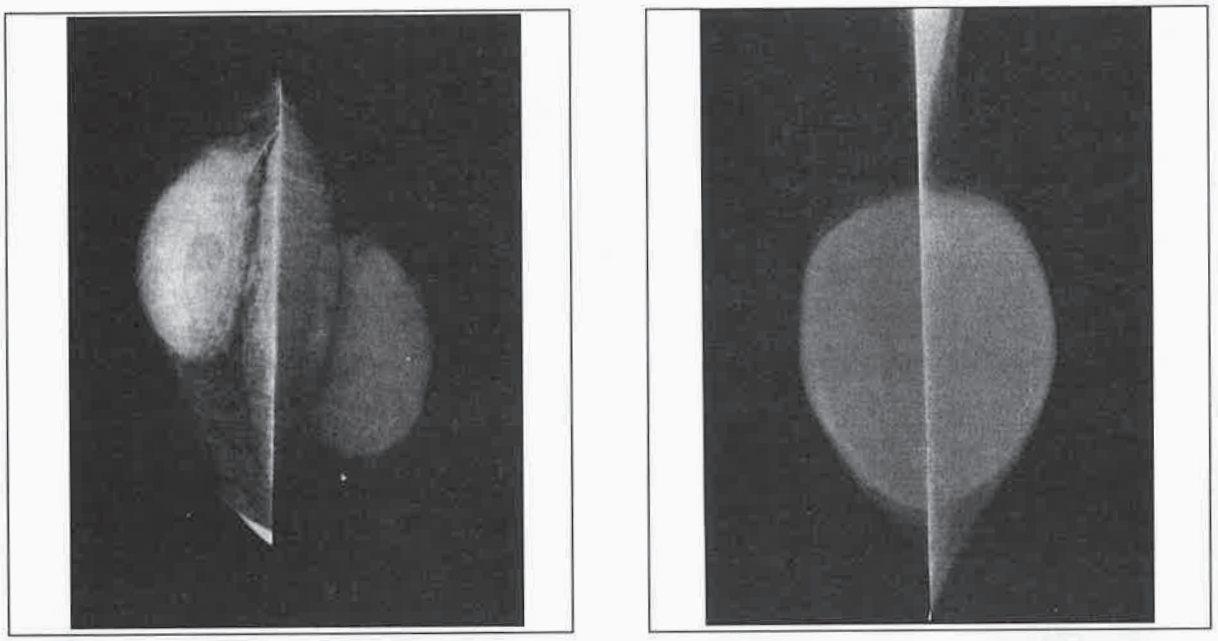

Fig. 2-a: Bilateral CC and **Fig. 2-b:** MLO mammograms. There are nodular type patterns of bilateral subareolar density with smooth contour.

2- Dendritic patterns: increased retroareolar density extending from the areola and abutting the nipple (Fig. 3 a-b-c)

3- Diffuse patterns: diffuse fibroglandular density resembling female breast pattern (Fig. 4 a-b).

Results: Out of 95 patients, 14 had fatty breasts without retroareolar density or ductal structures (pseudogynecomastia or adipomastia).There was no further examination and/or follow-up of these patients.

Primary breast cancer was diagnosed in eight patients. Of these, six were diagnosed with infiltrative ductal carcinoma (IDC), one with Paget disease and one with adenocarcinoma (with low-grade differentiation). Three of the IDC patients also had dendritic gynecomastia. (The mean age of over-50 patients with carcinomas was 70.2 years, with an age range of 52-87 years. The mean age of under-50 patients with carcinomas was 24.9 years, with an age range of 12-48 years.)

Gynecomastia was diagnosed in 73 patients. (Mean age: 34; age range: 12-87). The mammographic parenchymal patterns were identified as diffuse, nodular or dendritic (2). Of the patients in this study, 35 had dendritic, 18 diffuse, 18 nodular and five had mixed parenchymal patterns (Fig. 5).

Unilateral gynecomastia was reported in 30 patients, and bilateral gynecomastia was reported in 40 patients. In six patients presenting with complaints of enlargement in both breasts, pseudogynecomastia was detected in one breast and gynecomastia (3 dendritic, 2 nodular, 1 diffuse pattern) in the other (Fig 6 a-b).

Of the patients with bilateral gynecomastia, five had different parenchymal patterns in each breast (2 nodular/dendritic, 2 nodular/diffuse, 1 dendritic/diffuse) and 32 had the same patterns in both breasts (16 dendritic, 8 nodular, 8 diffuse type) (Table 1).

Of the patients with unilateral gynecomastia, 18 had gynecomastia of the right breast (7 dendritic, 6 diffuse, 5 nodular) and 12 had gynecomastia of the left breast (6 dendritic, 3 nodular, 3 diffuse).

Not including those with diffuse density, the diameter of retroareolar density varied between 10-90mm (Mean: 32.8mm).

Fine needle aspiration biopsy (FNAB) was per-

TABLE 1: Mammographic parenchymal patterns of gynecomastia

	Dendritic	Nodular	Diffuse	Mixed	TOTAL
Bilateral gynecomastia	16	8	8	5	37
Pseudogynecomastia+gynecomastia	3	2	1	-	6
Right gynecomastia	7	5	6	-	18
Left gynecomastia	6	3	3	-	12
TOTAL	32	18	18	5	73

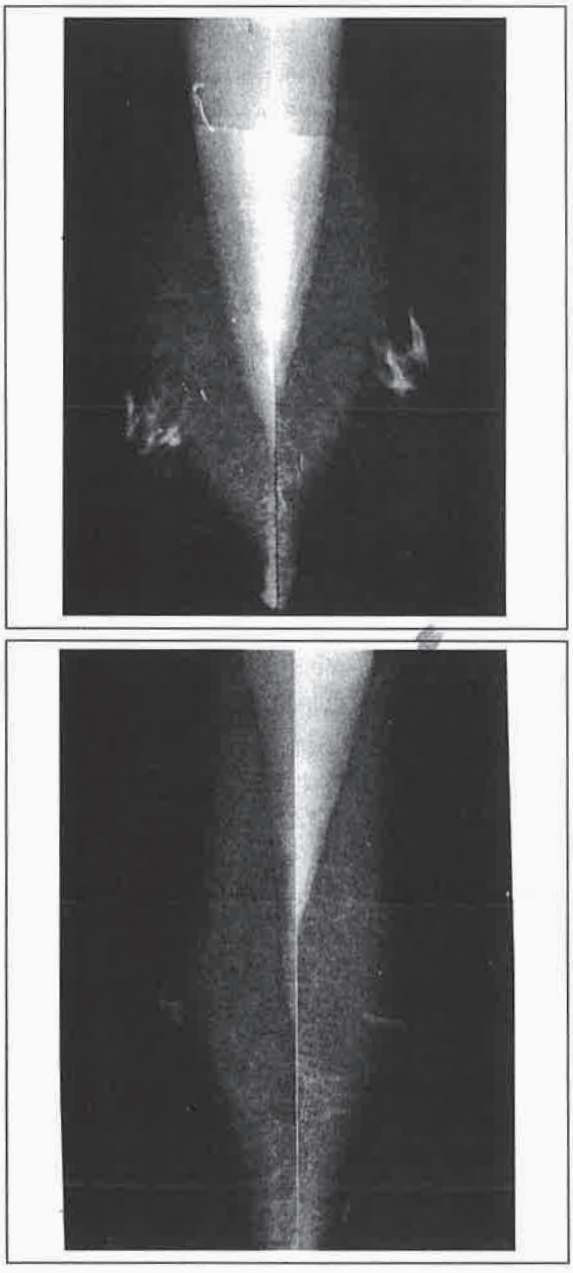

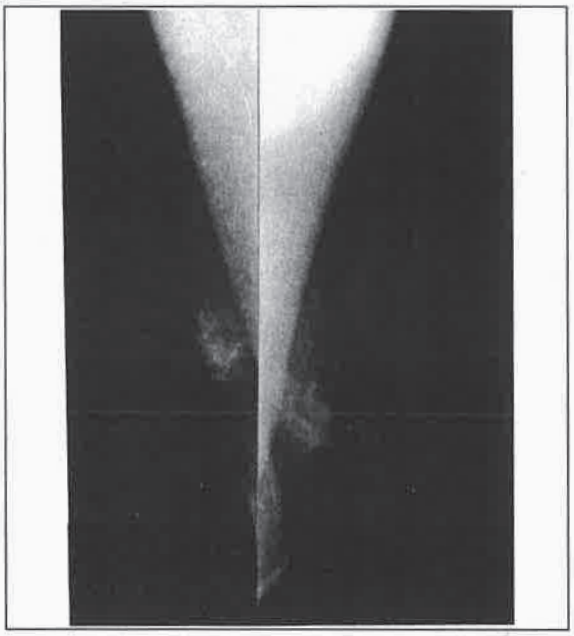

Fig. 3 a-b-c: The patients had bilateral gynecomastia and dendritic breast patterns in MLO mammograms.

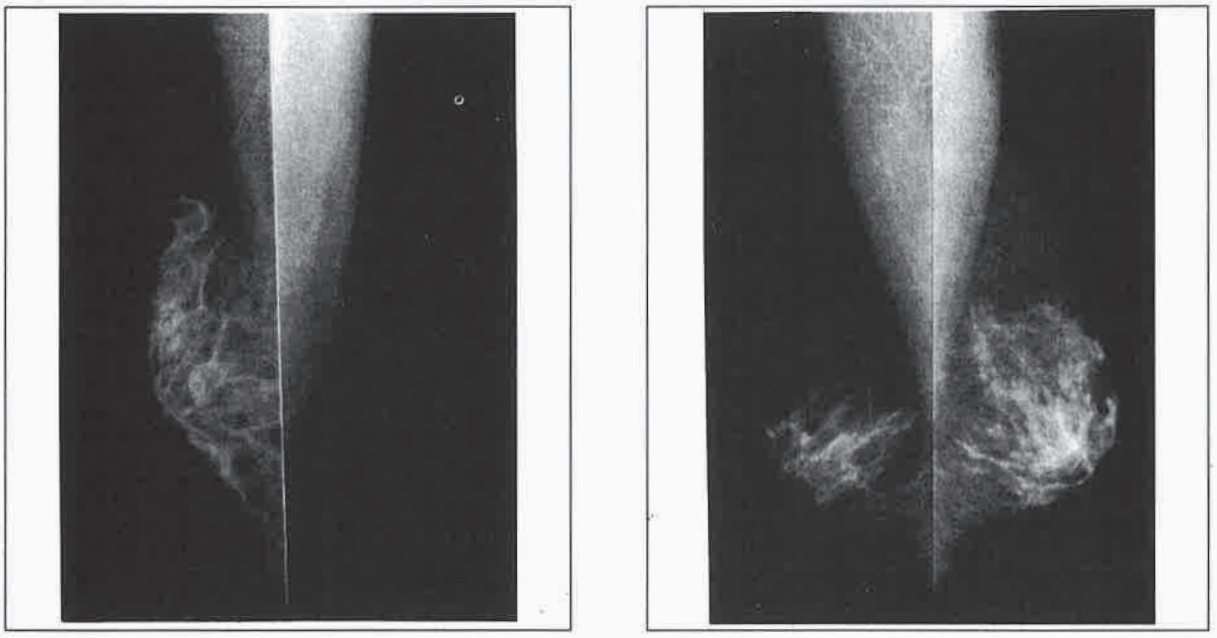

Fig. 4 a: Bilateral MLO mammograms. The right breast presents a diffuse parenchymal pattern, and pseudogynecomastia is found in the left breast.

b: Mixed-type parenchymal pattern: The left breast has diffuse and the right has dendritic patterns in MLO mammograms.

formed on five patients for whom both mammography and ultrasonography proved to be inconclusive. A mastectomy was performed on one patient whose FNAB result was reported as malign, but histopathological examination resulted in a diagnosis of gynecomastia.

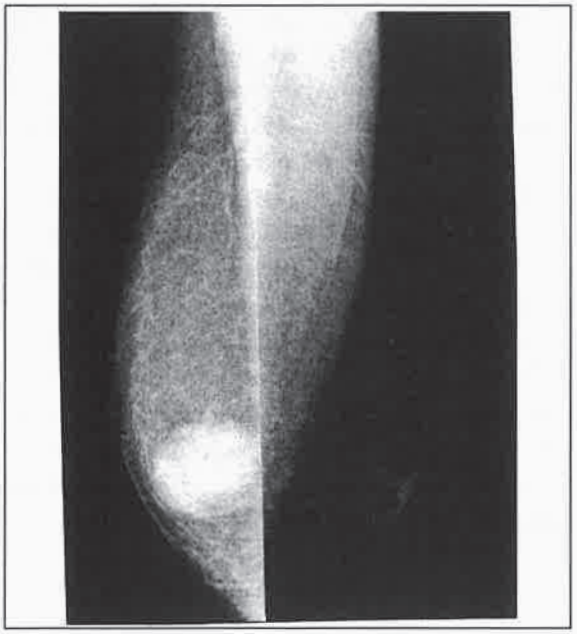

Fig. 5: MLO mammograms of a patient with mixed-type parenchymal pattern - nodular pattern in right breast, dendritic pattern in left breast.

All the patients were followed-up clinically, and, in some cases, by mammography. No carcinoma developed in any of the patients during a follow-up period of between six months and two years, three months.

Discussion: Gynecomastia can be described briefly as benign ductal and stromal proliferation, usually without any real asiner proliferation (3). Clinical features include enlargement, often bilateral, and hard, mobile, subareolar palpable lumps of an average two centimetres in diameter. On mammography, gynecomastia is typically seen as a triangular or roughly circular area of increasing density, located symmetrically in the retroareolar region and usually abutting the nipple. In contrast, male breast cancer is seen as a small, well-defined or spiculated mass eccentric to the nipple, sometimes containing microcalcifications and irregular margins (4-5).Self-reduction is recorded in many patients.

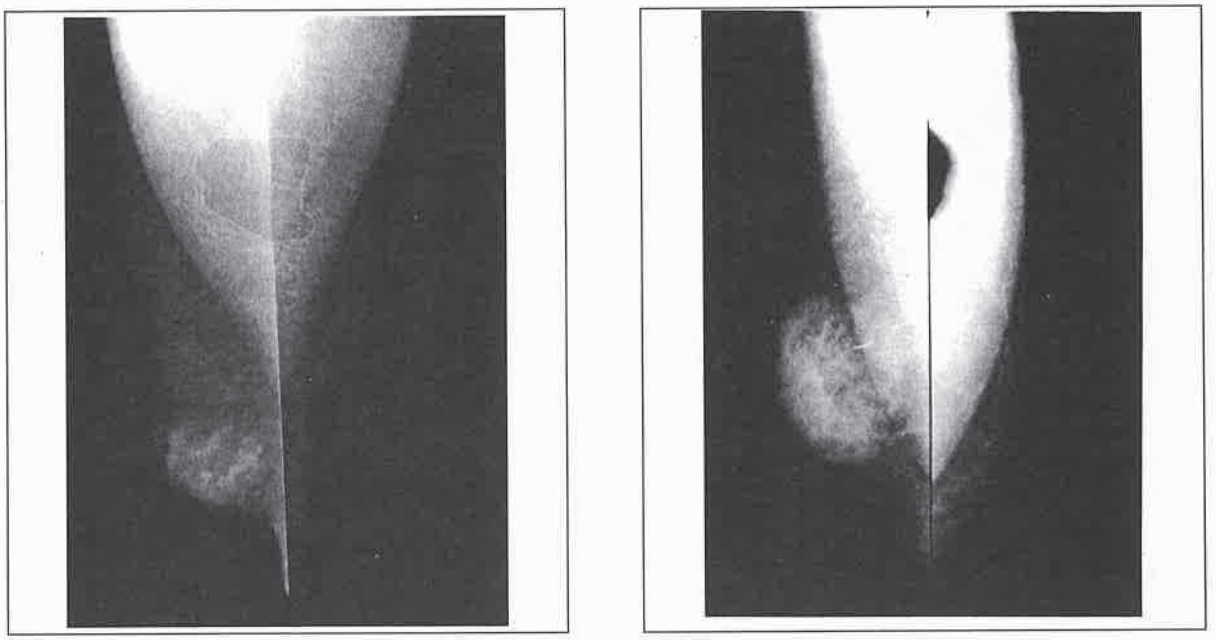

Fig. 6 a-b: Dendritic (a) and nodular (b) patterns in the right breasts of two different patients. The left breasts display only fat tissue.

Gynecomastia is reported at rates of 50-60% in adolescents (6-7), 30-40% in adults (7-8-9) and 32-65% of the male population in general (10). Many patients don't apply to a doctor or radiologist, since it is not considered clinically suspicious. Mammography of the male breast accounts for less than 1% of mammographic examinations done in breast imaging centres (11). As a result, radiological features of gynecomastia are not well known.

Gynecomastia and breast cancer are found to coexist at a rate of 0-20% (12). In this regard, it is important to keep in mind both the difficulty in differentiating certain nodular and dendritic types of gynecomastia from carcinoma as well as the coexistence of some carcinomas with gynecomastia (13). The more gynecomastia pattern features are known, the easier it will be to detect and to differentiate gynecomastia from carcinoma by mammography.

The difficulty of diagnosing breast cancer solely by mammography is already well known (14). If difficulty is experienced in defining the mammographic features of the breast pathology or if dense parenchymal patterns exist, ultrasonography is the most commonly used supporting method of diagnosis (15-16). While the rate of mammographic detection of lesions a few centimetres in diameter is 92-95% (17-18), the detection rate increases to 97% when mammography is used in conjunction with ultrasonography (17,19). For this reason, ultrasonography should be used together with mammography as a standard (5). Using the best possible existing detection methods to diagnose carcinoma in the earliest stages is important in males as well as in females, as early detection directly influences survival.

REFERENCES

1. Sohn C, Blohmer J-U, Hamper UM. Sonography of the male breast. In Breast Ultrasound, Georg Thieme Verlag, New York 1999, pp. 103.
2. Appelbaum AH, Evans GFF, Levy KR, Amirkhan RH, Schumpert TD. Mammographic appearances of male breast disease. RadioGraphics. 1999, 19:559-568.
3- Michels LG, Gold RH, Arndt RD. Radiography of gynecomastia and other disorders of male breast. Radiology. 1977, 122: 117-122.
4- Tükel S, Özcan H. Mammography in men with breast cancer: Review of the mammographic findings in five cases. Australasian Radiology. 1996, 40: 387-390.
5- Stewart RA, Howlett DC, Hearn FJ. Pictorial review: the imaging features of male breast disease. Clin. Radiol. 1997, 52: 739-744.
6- Biro FM, Lucky AW, Huster GA, Morrison JA. Hormonal studies and physical maturation in adolescent gynecomastia. Journal of Pediatry 1190, 116: 450.
7- Courtiss EH. Gynecomastia. Analysis of 159 patients and current recommendations for treatment. Plast.Reconstr.Surg. 1987, 79: 740.
8- Carlson HE. Gynecomastia. N.Engl.J.Med. 1980, 303: 795.
9- Rissanen TJ, Makarainen HP, Kallioinen MJ, Kiviniemi HO, Salmela PI. Radiography of the male breast in gynecomastia. Acta. Radiol. 1992, 33:110-114.
10- Braunstein GD. Gynecomastia. N. Engl. J. Med. 1993, 328: 490-495.
11- Chantra PK, So GJ, Wollman JS, Bassett LW. Mammography of the male breast. AJR. 1995, 164: 853-858.
12- Jackson VP, Gilmor RL. Male breast carcinoma and gynecomastia. Radiology. 1983, 149: 533-536.
13- Fodor PB. Breast cancer in a patient with gynecomastia. Plast. Reconstr. Surg. 1989, 84:976-979.
14- Kapdi CC, Parekh NJ. The male breast. Radiologic Clinics of North America. 1983, 21: 137-147.
15- Rosner D, Bilard D. What ultrasonography can tell in breast masses that mammography and physical examination cannot. Journal of Surgical Oncology. 1985, 28: 308-313.
16- Britton PD, Coulden RA. The use of dupplex doppler ultrasound in the diagnosis of breast cancer. Clinical Radiology. 1990, 42: 399-401.
17- Fodor PB. Breast cancer in a patient with gynecomastia. Plast. Reconstr. Surg. 1989, 84: 976-979.
18- Cosgrove D, Meire H, Dewbury K. Abdominal and General Ultrasound. Vol.2, pp 726. Churchill Livingstone, Longmann Group U.K. Ltd. , London, 1993.
19. Cooper RA, Gunter BA, Ramamurthy L. Mammography in men. Radiology. 1994, 191: 651-656.

VESICOURETERAL REFLUX IN CHILDREN CLINIC-RADIOLOGIC EVALUATION-FOLLOW UP

Nuray Özkaya* ✣ Fatoş Yalçınkaya* ✣ Necmiye Tümer* ✣ Mesiha Ekim*

SUMMARY

A total one-hundred sixtyfour children (123 girls – 41 boys) with vesicoureteral reflux entered this retrospective study. Clinical and laboratory features and radiologic examinations were evaluated at onset. The value of the IVP, USG and DMSA findings were compared at the diagnosis. The results of the long term follow up (6 months –12 years, 3.16 ± 2.73 years) of these patients with medical and surgical treatment were also investigated. New renal scarring developed in 2.1% of medically and 6.8% of surgically treated patients. We concluded that antireflux surgery did not prevent progression of renal scarring. Therefore, even children who have had successful surgical treatment should remain under regular nephrological supervision with particular attention to new scars, proteinuria, renal functions and blood pressure.

Key words: *Vesicoureteral Reflux, Children.*

ÖZET

ÇOCUKLARDA VEZİKO ÜRETERAL REFLÜ

Vesikoureteral reflüsü olan 164 çocuk (123 kız-41 erkek) retrospektif olarak bu çalışmaya alındı. Başvurudaki klinik, laboratuar ve radyolojik değerlendirmeler yapıldı. Tanı sırasındaki IVP, USG ve DMSA bulguları karşılaştırıldı. Bu hastaların medikal ve cerrahi tedavi sonrası izlem sonuçları (6 ay-12 yıl, 3.16±2.73 yıl) araştırıldı. Yeni skar gelişimi medikal izlenen grupta %2.1, cerrahi uygulanan grupta %6.8 bulundu. Sonuç olarak, cerrahi olarak başarılı tedavi edilen hastalarda antireflux cerrahi skar progresyonunu önleyememektedir. Bu hastalar yeni skar oluşumu, proteinuri, renal fonksiyon ve kan basıncı açısından düzenli olarak nefroloji izleminde de olmalıdırlar.

Anahtar Kelimeler: *Vesicoureteral Reflü-Çocuk.*

Reflux nephropathy (RN) is an important cause of chronic renal failure (CRF) and severe hypertension in childhood (1). Vesicoureteral reflux (VUR) is present in 29% to 50% of children with urinary tract infection and almost 30% of such patients have evidence of renal parenchymal scarring at the time of presentation (1-5). Some nephrological centers reported 10% to 20% of patients entering the dialysis and transplantation program had reflux nephropathy (2,4). The etiology, epidemiology, natural history and clinical consequences of VUR have all been well described in the last 3 decades (6-7). Yet there remains much disagreement on the management of these patients. In this retrospective study, we evaluated clinical, laboratory and radiologic examinations of the patients with VUR at the time of the diagnosis. The value of the IVP, USG and DMSA findings were compared. In addition, we evaluated the long term follow up result of a total of 248 ureters; (212 received medical and 36 received surgical treatments).

PATIENTS and METHODS

One hundred sixty four patients (123 girls, 41 boys) with VUR included in this retrospective

*Ankara University Faculty of Medicine, Department of Pediatric Nephrology, Ankara, Türkiye

Received: April 25,2001 Accepted: May 10,2001

study. These 164 patients had 248 refluxing ureters. The mean age was 4.9±3.8 years, follow up time was 6 months – 12 years (3.16±2.73 years).

VUR was diagnosed by voiding cystouretrography (VCUG) as a standardized method. Voiding cystouretrograms were graded according to the International Reflux Study in Children (IRSC). VCUG was repeated 6 to 12 months later. Excretory urograms (IVP) were performed in 137 patients at the time of diagnosis and repeated not more than one year. Renal ultrasonography was performed in 96 patients at diagnosis. Renal scars were investigated by dimercaptosuccinic acid scan(DMSA) in 130 patients at diagnosis. If the initial scan was abnormal, it was repeated 3 to 6 months later and if still abnormal, it vas repeated again. The value of the IVP, USG and DMSA findings were compared at the diagnosis of VUR. In addition, the results of the long trem therapy with medical and surgical were evaluated.

For the statistical analysis Chi-square test were used.

RESULTS

There were 123 girls (75%), 41 boys (25%) mean age was 4.9 ± 3.8 years and follow-up time was 6 months to 12 years (3.16±2.73 years). The clinical presentations are included in Table 1.

Chronic renal failure rate was 13% at presentation. Mean age of the patients with CRF was 9.2±2.8 years.

LABORATORY FEATURES

Urine examination; Proteinuria was detected 26 (16%) patients at presentation, 15 of them had renal failure. If the patients who had chronic renal failure were excluded, proteinuria rate was 7.3% at presentation. Escherichia Coli and Proteus Mirabilis were noted as the most common microorganisms seen in 63% and 14% of the patients with UTI, respectively.

Radiologic examination; VUR was diagnosed 248 ureters of 164 patients by VCUG. Eighty patients (49%) had unilateral, 84 (51%) had bilateral VUR. Initial grades of VUR are shown Table 2. High grade reflux (grade IV-V) were found approximately in one fourth of ureters at diagnosis. One hundred and fifty-five kidneys evaluated by IVP at diagnosis. Table 3 shows grades of VUR and results of initial IVP findings. One hundred and sixty-five kidneys were evaluated with DMSA and 115 kidneys were evaluated with USG at diagnosis. Table 4 shows the correlation of VUR

Table 1: Clinical presentations of the patients with VUR

		N	(%)
Urinary tract Infection	Acute Pyelonephritis	37	23
	Lower urinary tract infection	43	26
Enuresis		12	7
Hematuria		6	4
Gastrointestinal symptoms		17	2
Convulsion		2	1
From other centers *(CRF)		47 (21)*	29 (13)*

Table 2. Initial Grades of VUR

Initial Grade	Ureter (n)	%
I	32	13
II	73	29
III	76	31
IV	29	12
V	38	15

grades and normal findings on initial IVP, USG, DMSA. Twenty three percent (23%) of the patients had renal parenchymal scarring at diagnosis.

Treatment; Two hundred - twelve ureters with VUR received medical treatment, consisted of low dose continuous antibiotic prophylaxis. VUR resolved in 93 (44%) ureters in this group in 1.9±1.1 years. After 2.4±1.1 years of follow up, 119 (56%) ureters still had reflux. New renal scarring development rate was 2.1% in the medically treated group. Thirty-six ureters (14%) were treated surgically (2 ureters with grade II, 10 ureters with grade III, 24 ureters with grade IV-V). Seven ureters (19%) had ureteronephrectomy, 29 ureters (81%) had antireflux surgery. New renal scarrring rate was 6.8% in the surgically treated group. Prognosis of 248 refluxing ureters are shown in Figure 1.

DISCUSSION

The most common clinical presentation has been reported to be urinary tract infection in childhood of VUR (1-5). Our study confirms this observation and nearly half of 164 patients with VUR peresented with urinary tract infection (Table 1). Interestingly the rates of upper and lower urinary tract infection were similar at presentation. Moreover 2% of our study group were healthy children who were siblings of the patients with VUR or patients who have asymtomatic bacteriuria during routine examination.

Reflux nephropathy is an important cause of CRF. It was reported that 10 to 20% of patients entering the dialysis and transplantation program had reflux nephropathy (2-5). Reflux nefropathy is the most common cause of CRF in Turkey. We have found that reflux nefropaty is the first cause of CRF in our department of Pediatric Neprology (8). It is reported that 26% - 44% from different centers (9-11). In this study CRF rate was 13% (21 patients).

We compared initial IVP, USG, DMSA findings at the diagnosis. We found normal kidneys in 54% - 50% at IVP, 93% -98% at USG in grade I and grade II VUR respectively ($p<0.05$). In grade IV VUR normal kidneys rates were 50% at USG and 9% at IVP ($p<o.o5$). Although some authors recommended IVP if USG appears abnormal. We recommended that IVP should be performed in addition to USG in all patients with VUR in childhood at diagnosis USG could be normal but minor and negligible changes could be seen on IVP.

Table 3. VUR Grade and Results of Initial IVP Findings

	VUR GRADES				
IVP FINDINGS	I %	II %	III %	IV %	V %
Normal kidney	54	50	31	9	
Dilatation Clubbing collecting system	21	33	42	46	6
Double collecting system/bifid pelvis	4	6		9	
Parenchymal reduction/small kidney			7	16	28
Dilatation of ureter		4	17	20	
Hydronefrosis					46
Nonfunctional kidney					20
Bladder trabeculation	21	7	3		

Table 4: The correlation of VUR grades and normal kidneys on initial IVP, USG and DMSA.

	Normal kidneys		
Initial VUR grade	IVP n %	USG n %	DMSA n %
I	13/24 54	14/95 93	22/25 88
II	24/48 50	39/40 98	58/64 91
III	15/43 34	30/39 77	33/46 72
IV	2/22 9	6/12 50	5/14 36
V	0/18 0	0/9 0	1/16 6,2

In this study renal parenchymal scarring rate was 23% at diagnosis with DMSA. Medical treatment was performed to 212 (86%) of 248 ureters and VUR resolved in 93 ureters (44%). Thithy-six ureters (14%) were treated surgically. Surgery success rate was 80% in our study (Figure 1).

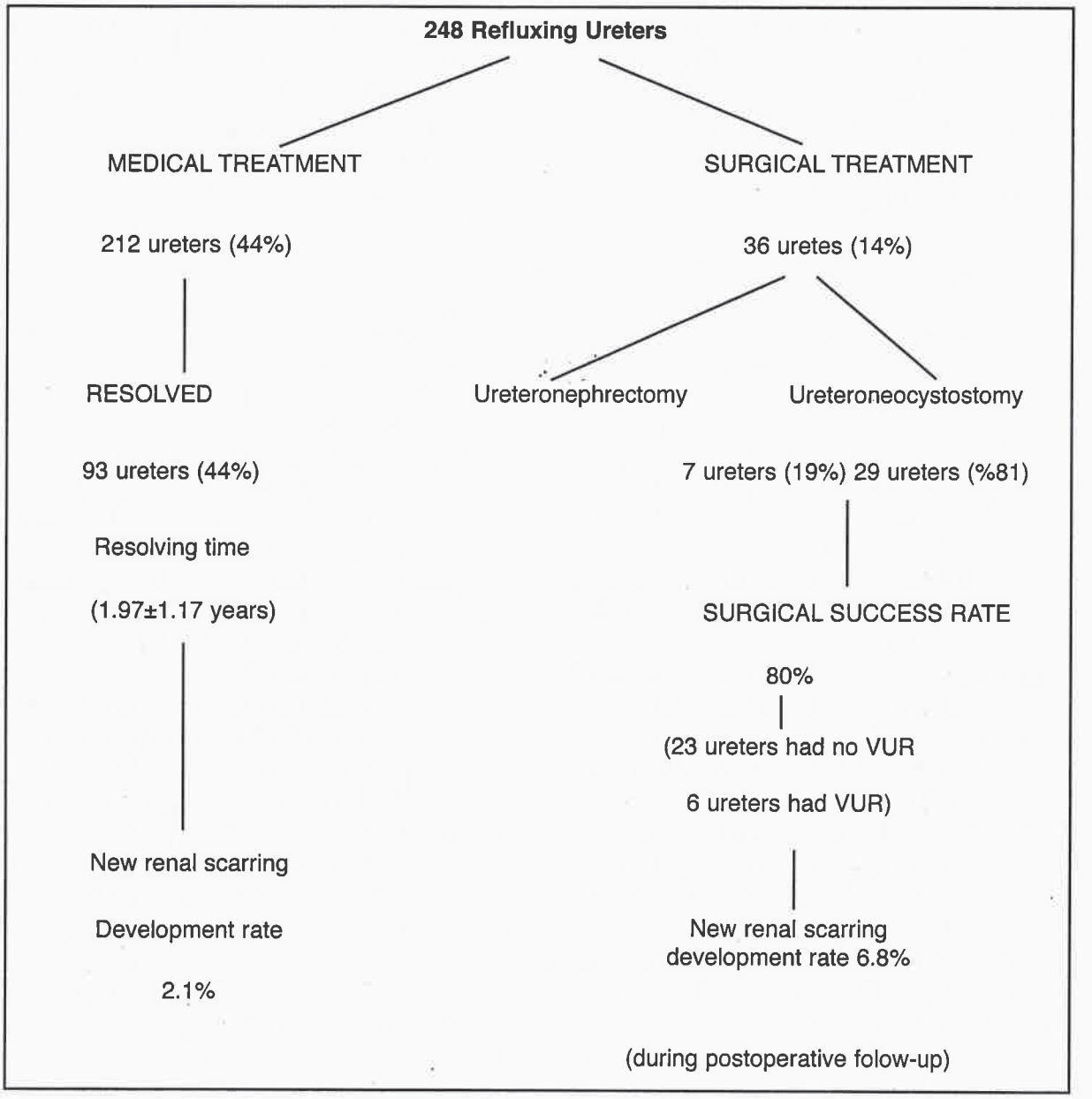

Figure 1: Prognosis of 248 refluxing ureters

New scars were investigated with DMSA in successfully treated patients both medically and surgically. New scarring development was found 2.1% and 6.8% in medically and surgically treated patients, respectively. Anti reflux surgery did not prevent the progression of parenchymal damage.

What is the correct treatment and follow up for a given child with reflux? Yet there remains much disagreement for the management. Different children with similar grades of reflux might best be served by different strategies. This differences are regional, national, economic and social. The American Urology Association recommended continious antibiotic prophylaxis as initial treatment. Surgery was recommended for children with persisitent reflux and other indications (such as age, sex, grade of VUR and renal scar) (12).

In conclusion, a number of complications can be associated with VUR in children, including recurrent urinary tract infection, renal scarring, sterile reflux nephropathy, hypertension and renal failure. All children with urinary tract infection should be evaluate after their first infection and VCUG should be performed. Treatment should be planned according to the patient characteristics. All the patient should remain under regular nephrological supervision after resolved their reflux with particular attention given to new scars, proteinuria renal functions and blood pressure for a long time.

REFERENCES

1. Jakopson SH, Nansson S, Jakobsson B. Vesicoureteric reflux: Occurence and long-term risks Acta Pediatr Suppl 1999; 431: 22-30.
2. Weiss R, Duchett J. Results of a randomized clinical trial of medical versus surgical management of infant and children with grades III and IV primary vesicoureteral reflux. J Urol. 1992; 148: 1667-1673
3. M Mellström, B. Jacobsson. Diagnosis of vesicoureteric reflux Acta Pediatr Suppl 1998; 431:3-12
4. Bailey R. Vesico-ureteric reflux and reflux nephropathy. Kidney Int. 1993; 542: 80-85
5. Greenfield S,P. Wan Vesicoureteral reflux: practical aspects of evaluation and management. Pediatr Nephrol 1996; 10: 789-794
6. Alon U. Berond M. Intravenous pyelography in children with urinary tract infection and vesicouretral reflux, Pediatrics 1989; 83: 332-335.
7. Jones K. Vesicoureteral reflux. A medical perspective on management. Pediatr Nephrol 1996; 10: 795-797.
8. Tümer N, Çakar N, Özkaya N, Yalçınkaya F, Ekim M. Etiology and outcome of continuous ambulatory peritoneal dialysis in children. Perit Dial Int 2001;21 (supll 1): 92
9. İşlek I, Sancak R, Van A, Gürses N. Etiology of chronic renal failure in children in the Back See region of Turkey. Pediatr Nephr 1996;10:815.
10. Şirin A, Emre S, Alpay H, Nayır A, Bilge I, Tanman F. Etiology of chronic renal failure in Turkish children. Pediatr Nephrol 1995;9:549-552.
11. Bircan Z, Kervancıoğlu M, Katar S, Onur A, Onur H. The etiology of renal failure in South-East anatolia. Pediatr Nephrol 2000; 14: 87-88.
12. Elder J, Peter C, Arant B. Pediatric vesicureteral reflux guidelınes panel summary report on the management of primary vesicoureteral reflux in children. J Urol 1997;157; 1846-1851.

JOURNAL OF ANKARA MEDICAL SCHOOL Vol 23, No 2, 2001 117-121

UNUSUAL RADIOGRAPHIC FEATURES OF PRIMARY PULMONARY TUBERCULOSIS IN ADULTS*

Adil Zamani** ✣ Kemal Ödev*** ✣ Abdulcelil Kalem****

SUMMARY

Study objective: *To determine the incidence of three unusual radiographic features of primary tuberculosis : (1) isolated unilateral pleural effusion in patients ≥ 40 years of age , (2) isolated hilar adenopathy, and (3) negative chest radiograph.*

Design: *The medical records and admission chest radiographs of adult patients (older than 18 years) with newly diagnosed active pulmonary tuberculosis (TB) were retrospectively assessed.*

Setting: *A university respiratory disease clinic.*

Patients and methods: *During a 12 – month period from 1995 to 1996, patients diagnosed with active pulmonary TB were included in this study. Inclusion criteria were (1) absence of prior history of TB, (2) bacteriologic and/or histopathologic evidence of TB. Admission chest radiographs were assessed independently by two observers. The radiographic findings were categorized as follows: (1)usual features of postprimary TB;(2)usual features of primary TB;(3) unusual features of primary TB.*

Results: *Of the 157 patients, 110 (70%) presented with usual radiographic features of postprimary TB, 47 (30%) with usual or unusual features of primary TB. Unusual features of primary TB were present in 9.6 % of all patients (15/157). The most frequent feature was isolated unilateral pleural effusion in 11 patients ≥ 40 years of age (7%). Two patients (1.3%) had isolated bilateral pleural effusion. Isolated hilar adenopathy was present in two patients (1.3%). No cases with negative chest radiograph were seen.*

Conclusions: *A high level of suspicion for tuberculous pleurisy must be maintained in patients ≥ 40 years of age , whose chest radiograph demonstrates isolated unilateral pleural effusion. Also,we believe that tuberculosis patients with negative chest radiograph can escape initial radiographic diagnosis. Therefore, clinicians should be aware of this unusual radiographic feature .*

Key words: *Adults, Chest Radiograph, Primary Pulmonary Tuberculosis.*

ÖZET

ERİŞKİNLERDE PRİMER AKCİĞER TÜBERKÜLOZUNUN ATİPİK RADYOLOJİK GÖRÜNÜMLERİ

Amaç: *Primer akciğer tüberkülozunun üç atipik radyolojik görünümünün insidansını belirlemek:(1)40 yaş ve üzerindeki olgularda izole tek taraflı plevral effüzyon,(2)izole hiler adenopati,(3)normal akciğer grafisi.*

Tasarım: *İlk defa aktif akciğer tüberkülozu (TB) tanısı konulan erişkin hastaların (18 yaş üstü)dosya kayıtlarının ve akciğer grafilerinin geriye dönük analizi.*

Ortam: *Üniversiteye bağlı bir Göğüs Hastalıkları Kliniği.*

Hastalar ve yöntemler: *1995-1996 yılları arasında (12 ay) aktif akciğer tüberkülozu tanısı konulan olgular çalışma kapsamına alındı.Çalışmaya alınma ölçütleri (1)daha önce geçirilmiş TB öyküsünün olmaması ve (2)TB'nin bakteriyolojik ve/veya histopatolojik olarak doğrulanması şeklinde belirlendi.Olguların ilk başvuru akciğer grafileri iki bağımsız araştırıcı tarafından değerlendirildi.Radyolojik bulgular (1) postprimer TB için tipik görünüm,(2) primer TB için tipik görünüm ve (3) primer TB için atipik görünüm şeklinde sınıflandırıldı.*

Sonuçlar: *Değerlendirilen 157 hastadan 110 (%70)'unda postprimer TB için tipik radyolojik görünüm,47 (%30)'sinde ise primer TB için tipik veya atipik görünüm vardı.Primer TB için atipik görünüm olguların %9.6'sında bulundu.(15/157);en sık saptanan radyolojik görünüm 40 yaş ve üzerindeki olgularda izole tek taraflı effüzyondu (%7).İki olguda (%1.3)izole iki taraflı plevral effüzyon ,iki olguda (%1.3) ise izole hiler adenopati vardı.Akciğer grafisi normal olan hiçbir hasta saptanmadı.*

Yorum: *Sonuç olarak,40 yaş ve üzerindeki hastaların akciğer grafilerinde izole tek taraflı plevral effüzyon saptanması halinde ayırıcı tanıda öncelikle tüberküloz plörezi dikkate alınmalıdır.Ayrıca,akciğer grafisi normal olan tüberkülozlu olgularda ilk radyolojik tanının atlanabileceği kanısındayız.Bu nedenle,klinisyenler bu atipik radyolojik görünüm ile karşılaştıklarında dikkat olmalıdırlar.*

Anahtar Kelimeler: *Erişkinler,Akciğer Grafisi, Primer Akciğer Tüberkülozu*

---

*Presented in part at the Second Congress of Thoracic Society, 6 – 10 May, 1998, Antalya

**Associate Professor, Department of Chest Diseases, Faculty of Medicine, Selçuk University, Konya

***Professor, Department of Radiology, Faculty of Medicine, Selçuk University, Konya

****Research assistant, Department of Chest Diseases, Faculty of Medicine, Selçuk University, Konya

Received: Oct 18,2000 Accepted : Feb 20,2001

The chest radiograph plays an important role in the initial detection of pulmonary tuberculosis (TB) . Although physicians are familiar with the radiographic manifestations of postprimary TB, problems in radiographic diagnosis do occur. The likelihood of misdiagnosis is greater when the adult patient has radiographic features of primary TB. During the past decades, several studies have reported the more frequency of these findings in the adult population (1, 2). It has been suggested that the decreasing exposure in childhood in developed countries , owing to careful public health measures and effects of antituberculous chemotherapy, has resulted in later initial exposure to tuberculosis and increased likelihood of susceptibility to this infection during adulthood. Hence, some authors state that the term "childhood" tuberculosis to describe primary TB should be abandoned (3, 4). At present, however, it is important to point out that this approach is not suitable for the countries (including Turkey) with high rates of tuberculous infection (5, 6).

Isolated hilar and/or mediastinal adenopathy or negative chest radiograph may be the unusual manifestations of primary TB in adults . Another finding of primary TB, isolated unilateral pleural effusion is also uncommon in patients above 40 years of age (7, 8). These unusual radiographic features may seriously delay diagnosis and treatment (2, 8).

Based on these suggestions, the present study was designed to determine retrospectively the incidence of three unusual radiograpfic features (isolated unilateral pleural effusion in patients ≥ 40 years of age, isolated hilar adenopathy and negative chest radiograph) of primary TB in new active adult patients admitted to our department during a 12 - month period.

MATERIALS AND METHODS

We reviewed hospital records and admission chest radiographs of adult patients (older than 18 years) with newly diagnosed active pulmonary tuberculosis admitted to our department over a 12 – month period from 1995 to 1996 .

Patients were included in the study if they met the following criteria : (a) absence of prior history of tuberculosis; (b) bacteriologic and/or histopathologic evidence of tuberculosis.

Data gathered from the hospital records included characteristics and admission chest radiographs of the patients. Most of the radiographs were single posteroanterior films. Additional lateral films and computed tomography (CT) scans were available in 78 and 19 patients, respectively.

Chest radiographs were assessed independently by two observers (A.Z., K.Ö.) with experience in tuberculosis who were blinded to the clinical status of the patients. A standard reporting form was completed for each radiograph. The observers reached a decision by consensus.

The radiographic features were categorized as follows (8):

1. Usual (typical) features of postprimary tuberculosis: Cavitary or non – cavitary infiltrates, unilateral or bilateral, predominantly in the apical or posterior segments of the upper lobe(s) or apical segment of the lower lobe, with occasional evidence of endobronchial spread to the lower lobe.

2. Usual (typical) features of primary tuberculosis: (a) isolated unilateral pleural effusion in patients < 40 years of age; (b) unilateral pleural effusion with ipsilateral infiltrate; (c) unilateral hilar adenopathy with ipsilateral infiltrate.

3. Unusual (atypical) features of primary tuberculosis : (a) isolated unilateral pleural effusion in patients ≥ 40 years of age ; (b) isolated bilateral pleural effusion; (c) isolated unilateral hilar adenopathy; (d) isolated bilateral hilar adenopathy; (e) negative chest radiograph .

RESULTS

Among the 164 patients , 7 were excluded from this study because they did not meet the criteria previously pointed out. One hundred fifty seven patients were enrolled in the study. Diagnosis was documented on the basis of the following criteria: (1) positive culture for acid

– fast bacilli from various specimens (sputum , gastric aspirate , bronchial washings , bronchoalveolar lavage fluid) (120 patients); (2) pleural biyopsy (34 patients); (3) lymph node biopsy (3 patients).

Of the 157 patients, 110 (70%) presented with usual (typical) radiographic features of postprimary TB .There were 68 men and 42 women with a mean age of 36.8 years (range , 18 to 71 years). The most common radiographic features were infiltrates in the upper zone(s) (99 /157). Cavitation was present in 27 patients.

Of the remaining 47 (30%) patients , 32 had usual (typical) and 15 had unusual (atypical) radiographic features of primary TB . These patients constituted the present study group. Characteristics and the source of the specimens of this group are given in Table1 and Table 2 , respectively. Table 3 shows radiographic features of these patients. Isolated unilateral pleural effusion was seen in 20.4% of all patients (32/157). Most of pleural effusions were on the right side (24/32). No pleural effusion with ipsilateral infiltrate was detected. Hilar adenopathy was detected in 8.3 % of all patients (13/157).

Usual (typical) features of primary TB were revealed in 20.4% of all patients (32/157). The mean age of these patients was 25.5 years. Isolated pleural effusion was seen in 21 patients < 40 years of age (13.4%). In 11 patients (7%) unilateral hilar adenopathy was with ipsilateral parenchymal infiltrate in various zones.

Unusual (atypical) features of primary TB were present in 9.6 % of all patients (15/157). The mean age of patients with unusual features was 56 years compared with 25.5 and 36.8 years with usual features of primary and postprimary TB, respectively. In our series , the percentage of patients ≥ 40 years of age was 33.8 % (53/157) . The most common feature was isolated unilateral pleural effusion in 11 patients ≥ 40 years of age (7%). Two patients (1.3%) had isolated bilateral pleural effusion. CT scans showed no parenchymal abnormalities. Isolated hilar adenopathy was present in two patients (1.3%) . One of them (0.6 %) was < 40 years of age and had bilateral hilar adenopathy. No cases with negative chest radiograph was detected in our series.

Table 1. Characteristics of 47 Patients

No. of patients	47
Gender (male/female)	27/20
Age (years)	
Mean	35.3
Range	18 – 68
BCG	30/47
Family history of TB	7
Diabetes mellitus	1

Table 2. Source of Specimens in 47 Patients

Source	**No. of patients (n=47)**
Pleural biopsy	34
Bronchial washing	7
Lymph node biopsy	3
Bronchoalveolar lavage fluid	3

DISCUSSION

The results of our study show that 9.6% of admission chest radiographs had unusual radiographic features of primary TB. In one study, the incidence of these findings was found to be 3 % (8). This difference may be due to the demographic characteristics of the populations and a higher prevalence of tuberculosis in our country (6).

Previous studies have reported that tuberculous pleural effusions occur in 5 – 7 % of adult patients with primary TB (1 , 7). In the present study, isolated unilateral pleural effusion was detected in 20.4% of patients. Seven percent of these patients were ≥ 40 years of age. This proportion is considerably higher than those reported by other authors (0.4 – 3.7 %) (7, 8). Two patients (1.3%) ≥ 40 years of age had isolated bilateral pleural effusion as an unusual manifes-

Table 3. Usual and Unusual Radiographic Features of Primary Tuberculosis in 47 Patients

USUAL (n=32)	UNUSUAL (n=15)
Pleural effusion	**Pleural effusion**
Isolated unilateral (< 40 yrs) : 21	Isolated unilateral(≥ 40 yrs) : 11
Right : 14	Right : 10
Left : 7	Left : 1
With ipsilateral infiltrate : 0	Isolated bilateral : 2
Hilar adenopathy	**Hilar adenopathy**
With ipsilateral infiltrate : 11	Isolated unilateral : 1
Right : 4	Isolated bilateral : 1
Left : 7	
	Negative chest radiograph 0

tation. The age cutoff selected for our patients with isolated unilateral pleural effusion was 40 years. Because, the presence of this finding is unusual after this point (8) .

In our series, we found that 8.3% of patients had hilar adenopathy. Our finding is in agreement with those findings (4 – 13 %) reported previously (1). Only two patients (1.3%) had isolated hilar adenopathy as an unusual manifestation.

In children, the diagnosis of primary TB is usually based on clinical findings, abnormal chest radiograph, a history of close contact with a tuberculous case, and a documented conversion of the PPD skin test. However, in adults, radiographic findings of primary TB, such as isolated hilar and /or mediastinal lymphadenopathy often are viewed as unusual or incompatible with tuberculosis, and tuberculin conversion may be viewed as a coincidental and unrelated phenomenon. Therefore, it is difficult to obtain the good tuberculin skin conversion data in adults . In one series, 35 % of patients either had an inadequate PPD history or never received a skin test (3, 4). In our retrospective study almost all patients had inadequate documentation of tuberculin conversion. As a result of these diagnostic difficulties , chest radiography remains the first diagnostic choice of evaluation of the patients with thorasic tuberculosis (2). In addition, computed tomography (CT) can also be helpful in the assessment of tuberculous patients with hilar and/or mediastinal adenopathy (9, 10).

Several previous studies have reported that 15 % of patients with primary TB have negative chest radiograph (2 , 4). This finding is more frequent in tuberculosis patients with endobronchial disease or AIDS (7, 11) . Interestingly, in view of the relative high prevalence of tuberculosis in our country, no cases with negative chest radiograph were seen in this study . We suggest that some of tuberculosis patients with this unusual manifestation of primary TB were missed by the clinician and radiologist. Therefore , it is important to note that the absence of radiologic finding , in an appropriate setting of symtoms (fever, malaise, and weight loss), a history of contact, and a recent PPD conversion should suggest the possibility of tuberculosis and should be pursued with the examination of sputum for acid–fast bacilli (8). Additionally, CT scan may be helpful in the patients who initially present with a negative chest radiograph (11, 12).

In conclusion, a high level of suspicion for

tuberculous pleurisy must be maintained in patients ≥ 40 years of age, whose chest radiograph demonstrates isolated unilateral pleural effusion pattern. Also, we believe that tuberculosis patients with negative chest radiograph can escape initial radiographic diagnosis. Therefore, CT scan can be recommended in the assessment of these patients .

REFERENCES

1. Miller WT , Miller WT Jr. Tuberculosis in the normal host : radiological findings. Semin Roentgenol 1993 ; 28 :109 – 118.
2. Beigelman C, Sellami D, Brauner M. CT of parenchymal and bronchial tuberculosis. Eur Radiol 2000 ; 10 : 699 – 709.
3. Choyke PL , Sostman HD , Curtis AM , Ravin CE , Chen JTT , Godwin JD , Putman CE. Adult – onset pulmonary tuberculosis . Radiology 1983 ; 148 : 357 – 362.
4. Woodring JH , Vandiviere HM , Fried AM , Dillon ML , Williams TD , Melvin IG. Update: the radiographic features of pulmonary tuberculosis. AJR 1986 ; 146 : 497 – 506.
5. Lauzardo M, Ashkin D. Phthisiology at the dawn of the new century: A review of tuberculosis and the prospects for its elimination. Chest 2000;117:1455 – 1473.
6. Bilgiç H. Tüberküloz epidemiyolojisi . Kocabaş A , editör. Tüberküloz kliniği ve kontrolü. Adana : Çukurova Üniversitesi Basımevi , 1991 ; 401 – 437.
7. Krysl J , Korzeniewska – Kosela M , Müller NL , FitzGerald JM. Radiologic features of pulmonary tuberculosis : an assessment of 188 cases . Can Assoc Radiol J 1994 ; 45 : 101 – 107.
8. Hadlock FP , Park SK , Awe RJ , Rivera M . Unusual radiographic findings in adult pulmonary tuberculosis. AJR 1980 ; 134 : 1015 – 1018.
9. Ödev K , Zamani A , Vural A , Satılmaz I , Emlik D , Paksoy Y . Akciğer tüberkülozunda radyolojik bulgular. Tanısal ve Girişimsel Radyoloji 2000 ; 6 : 63 – 69.
10. Hansell DM , Dee P. Infections of the lungs and pleura. In: Armstrong P, Wilson AG, Dee P, Hansell DM, eds. Imaging of diseases of the chest. 3rd ed. London: Mosby , 2000 : 163 – 253.
11. Lee KS , Song KS , Lim TH , Kim PN , Kim IY, Lee BH. Adult – onset pulmonary tuberculosis : findings on chest radiographs and CT scans. AJR 1993 : 160 : 753 –758.
12. Lee KS, Hwang JW, Chung MP, Kim H, Kwon OJ. Utility of CT in the evaluation of pulmonary tuberculosis in patients without AIDS. Chest 1996 ; 110: 977 – 984.

JOURNAL OF ANKARA MEDICAL SCHOOL Vol 23, No 2, 2001 123-128

PLASMA INSULIN AND C-PEPTIDE LEVELS IN NON-DIABETIC ESSENTIAL HYPERTENSIVE PATIENTS

Ahmet Temizhan* ✣ Erdal Eskioğlu ✣ İzzet Tandoğan* ✣ Ayşegül Vural*** ✣ Ömer Dönderdici****

SUMMARY

Objective: *We aimed to investigate the presence of hyperinsulinemia and its relation to obesity and other lipid metabolism disorders in essential hypertensive patients who have no diabetes mellitus or glucose intolerance.*

Design and methods: This study comprised 50 essential hypertensive and 19 normotensive patients. All patients had oral glucose tolerance tests. Plasma insulin, C-peptide, urea, creatinin, uric acid, aspartate aminotransferase, alanine aminotransferase, gamma-glutamyl transpeptidase, very low density lipoprotein cholesterol, low density lipoprotein cholesterol and total high density lipoprotein cholesterol levels were measured.

Results: Plasma C-peptide levels were found to be significantly higher in hypertensive patients (p<0,01), but the difference in plasma insulin levels between the two groups was not significant. Differences in plasma C-peptide and insulin levels were not significant when compared according to obesity and blood lipids.

Conclusions: Our results showed that both hyperinsulinemia and obesity are independently associated with hypertension. Plasma C-peptide levels are a better indicator of insulin activity than plasma insulin levels.

Key words: *Hypertension, Hyperinsulinemia, C-Peptide*

ÖZET

DİYABETİK OLMAYAN ESANSİYEL HİPERTANSİF HASTALARADA PLAZMA İNSÜLİN VE C-PEPTİD DÜZEYLERİ

Amaç: *Diyebetes mellitusu ve glükoz intoleransı olmayan esansiyel hipertansif hastalardaki hiperinsülinemiyi ve bunun obezite ve lipid metabolizma bozukluklarıyla olan ilişkisini araştırmayı amaçladık.*

Hastalar ve yöntem: *Elli esansiyel hipertansif hasta ve 19 normotensif hasta çalışmaya dahil edildi. Plazma insülin, C-peptid, üre, kreatinin, ürik asit, aspartat aminotransferaz, alanin aminotransferaz, gama-glutamil transpeptidaz, düşük dansiteli lipoprotein kolestreol, çok düşük dansiteli lipoprotein kolesterol ve total yüksek dansiteli lipoprotein kolesterol düzeyleri ölçüldü.*

Bulgular: *Plazma C-peptid düzeyleri hipertansif hastalarda istatiksel anlamlı olarak yüksek bulunurken (p<0,01) plazma insülin düzeyleri her iki grup arasında farklı değildi. Plazma insülin ve C-peptid düzeyleri kan lipidlerine ve obezite durumuna göre karşılaştırıldığında istatiksel anlamlı bir fark bulunmamıştır.*

Sonuç: *Hiperinsülinemi ve obezite birbirinden bağımsız olarak hipertansiyon ile ilişkilidir. Plazma C-peptid düzeylerinin insülin aktivitesinin daha iyi bir göstergesi olduğunu düşünmekteyiz.*

Anahtar kelimeler: *Hipertansiyon, Hiperinsülinemi, C-Peptid*

**Department of Cardiology, Numune Education and Resource Hospital, Ankara*

***Department of İnternal Medicine, Numune Education and Resource Hospital, Ankara*

****Department of Clinical Biochemistery Laboratory, Numune Education and Resource Hospital, Ankara*

Received: Feb 21,2001 Accepted: March 26,2001

Metabolic disorders are commonly associated with hypertension, which is a risk factor for coronary, cerebral and renal vascular diseases. Plasma glucose concentrations of patients with hypertension are higher when compared with normal individuals [1]. Hypertensive patients also have a higher incidence of glucose intolerance and prevalence of diabetes mellitus [2]. An association between hypertension and hyperinsulinemia has been recognised for many years [3,4]. Different studies have shown the hypertensive effect of hyperinsulinemia. This has been explained through sodium-resorption in renal tubular cells [5] and sympathetic nervous system overactivity [6]. Insulin is a mitogenic substance and can facilitate smooth muscle cell proliferation in the media of the arterial vessel walls [7]. These effects of insulin presumably eventuate in a rise in blood pressure that may be either a primary cause of hypertension, or, at least, a secondary potentiator.

Hyperinsulinemia is mostly suggested to be associated with the metabolic status seen with hypertension, obesity, dyslipidemia and glucose intolerance [8]. It is generally accepted that hyperinsulinemia is secondary to insulin resistance, not only in hypertension, but also in obesity and non-insulin dependent diabetes [9,10]. The combination of diabetes, lipid metabolism abnormalities and hyperinsulinemia could contribute to the increased risk of coronary artery disease associated with hypertension [11].

In this study, we aimed to investigate the correlation of hyperinsulinemia with obesity and other lipid metabolism abnormalities in essential hypertensive patients who do not have glucose intolerance or diabetes mellitus.

METHODS

The study group consisted of 50 essential hypertensive (31 females, aged 56.8±9.6 years; 19 males, aged 52.7±9.7 years) patients and 19 normotensive (8 females, aged 51.6±10.5 years; 11 males, aged 56.4±13.7 years) patients. The body mass index (BMI) of the patients was calculated using the formula weight (kg)/height $(m)^2$. Patients who had BMIs over 27% were considered as obese. Diastolic blood pressures were evaluated as mild (90-104mmHg), moderate (105-114 mmHg) and severe (≥115mmHg). Systolic blood pressures higher than 160 mmHg without elevation in diastolic blood pressures were accepted as isolated systolic hypertension. Patients with liver or renal diseases were excluded from the study. None of the patients had a diet or limitation of salt consumption. Antihypertensive medication was discontinued 72 hours before the study. Carbohydrate metabolism disorders were investigated in all patients by oral glucose intolerance test. Blood samples were obtained after fasting and 30, 60 and 120 minutes after administration of a 75g glucose-equivalent load for post-glucose-load plasma glucose determinations. Individuals with glucose intolerance and diabetes mellitus according to WHO criteria were excluded from the study [12]. After a fasting period of 12 hours, blood samples were taken in a sitting position, and plasma C-peptide and insulin, serum urea, creatinin, uric acid, aspartate aminotransferase (AST), alanine aminotransferase (ALT), gamma-glutamyl transpeptidase (GGT), very low density lipoprotein cholesterol (VLDL), low density lipoprotein cholesterol (LDL) and total high density lipoprotein cholesterol (t-HDL) levels were measured. Plasma insulin was measured using an insulin-Coat-A-Count kit, according to the principles of solid-phase 125I Radioimmunoassay (DPC). C-peptide was measured using the Double Antibody Kit of the same firm. Calculations were made using a Berthold LB951 G Gamma counter. Urea, creatinin, uric acid, AST, ALT, GGT, VLDL, LDL, and t-HDL levels were measured by autoanalyser.

Means were determined as arithmetic mean ± standard deviation. Differences between the groups were analysed using Student's t-test. The level of statistical significance was $p<0,05$.

RESULTS

BMI and biochemical blood values of hypertensive and normotensive patients are shown in Table 1. BMI and GGT values were found to be

Table 1: Body Mass Indexes and Biochemical Parameters of Hypertensive and Normotensive Patients

	Hypertensive	Normotensive	p
N	50	19	
BMI (kg/(m)^2)	27,6 ± 4,4	25,6 ± 2,9	P<0,05
Plasma C-peptide (ng/ml)	2,1 ± 2,1	1,0 ± 0,3	P<0,01
Plasma Insulin (mIU/ml)	19,96 ± 44,8	8,54 ± 6,0	NS
Urea (mg/dl)	33,0 ± 9,0	33,7 ± 8,6	NS
Creatinin (umol/l)	92,8 ± 12,6	96,7 ± 15,1	NS
Uric acid (mmol/l)	0,33 ± 0,1	0,31 ± 0,1	NS
Sodium (mmol/l)	137,5 ± 14,7	141,9 ± 4,7	NS
Potassium (mmol/l)	4,2 ± 0,5	4,4 ± 0,5	NS
Aspartate aminotransferase (U/l)	14,6 ± 4,9	15,5 ± 4,8	NS
Alanine aminotransferase (U/l)	15,3 ± 4,6	14,7 ± 4,8	NS
Gamma-glutamyl transpeptidase (U/l)	20,9 ± 16,8	12,6 ± 4,8	P<0,01
Very low density lipoprotein (mg/dl)	47,4 ± 26,9	36,5 ± 20,2	NS
Low density lipoprotein (mg/dl)	194,0 ± 61,9	171,4 ± 27,7	NS
High density lipoprotein (mg/dl)	46,7 ± 11,7	51,3 ± 8,7	NS

(NS: non-significant, BMI: Body Mass Index)

significantly higher in hypertensive patients (p<0,05 and p<0,01, respectively). There was no significant difference between the plasma insulin levels of the two groups, whereas plasma C-peptide levels were significantly higher in hypertensive patients (p<0,01).

Plasma C-peptide and insulin levels of male hypertensives were not significantly different from the levels of female hypertensives (p>0,05). There was no correlation between plasma C-peptide and insulin and the degree of severity of hypertension (p>0,05).

Plasma C-peptide and insulin levels of hypertensive and normotensive patients are shown according to obesity in Table 2. Plasma C-peptide and insulin levels were not significantly different between obese and non-obese patients (p>0,05). Plasma C-peptide and insulin levels of obese hypertensive patients were significantly higher than those of obese normotensive patients (p<0,05 and p<0,01 respectively). In addition, plasma C-peptide levels were found to be significantly higher in non-obese hypertensive patients when compared with non-obese normotensives (p<0,01). The difference in plasma insulin levels was not significant between non-obese hypertensive and normotensive patients (p>0,05). There was no correlation between serum VLDL and LDL levels and plasma C-peptide and insulin levels (p>0,05).

DISCUSSION

In this study, we determined that C-peptide levels in hypertensive individuals were elevated independently of obesity and other lipid metabolism disorders. Previous studies have reported that increased insulin levels in hypertensive patients were associated with insulin resistance [9,10]. Obesity is one of the most important causes of insulin resistance. The decrease in peripheric insulin receptors [13] and the increase of free

Table 2: Plasma C-peptide and Insulin Levels of Hypertensive and Normotensive Patients and Overall Obesity

	Normotensive		Hypertensive	
	Obese	Non-obese	Obese	Non-obese
N	8	11	27	23
C-peptide (ng/ml)	1,1 ± 0,7	0,9 ± 0,2	1,9 ± 1,7 *	2,3 ± 2,4 ‡
Insulin (μIU/ml)	6,73 ± 4,0	9,85 ± 6,8	15,26 ± 11,4 †	25,48 ± 64,4

(: p<0,05 when compared with obese normotensives, †: p<0,01 when compared with obese normotensives, ‡: p<0,01 when compared with non-obese normotensives.)*

fatty acid flux [14] are effective in the development of the resistance in obese individuals. Although hyperinsulinemia is particularly noticeable in individuals with upper body obesity [15], it is also found in non-obese hypertensives [10,16]. Insulin resistance and concomitant hyperinsulinemia are worsened not only by obesity but also by physical inactivity [17] and androgenicity [18]. Insulin resistance depends on an increase in the number of Type II B muscle fibers, which are less sensitive to insulin during physical inactivity [19]. Since the hypertensive and normotensive patients of this study were physically inactive individuals, we concluded that the elevation of C-peptide levels of the hypertensive group was not directly related to physical inactivity. Insulin resistance increases with the effects of androgen. However, the difference in plasma insulin and C-peptide levels between male and female patients was not significant in our study. Therefore, we could not suppose a combined-additive effect of androgens on hyperinsulinemia in hypertensive patients.

Dyslipidemia is commonly seen in hypertensives [20,21]. Previous studies have shown that both hyperinsulinemia and obesity are independently associated with increased serum trygliceride levels in hypertensives [22,23]. Insulin resistance resulting in hyperinsulinemia may cause hypertriglyceridemia by direct stimulation of hepatic production of VLDLs [14]. Increased free fatty acid flux might be another mechanism whereby insulin resistance could increase VLDL secretion [14]. In contrast, no correlation was found between plasma insulin and C-peptide levels and plasma VLDL levels in our study. This may be due to two reasons. Firstly, although upper body adiposity is known to be strongly associated with increased VLDL cholesterol levels, our study considered overall adiposity as obesity criteria. Secondly, the exclusion of diabetic individuals from the study may have reduced the association of hyperinsulinemia with dyslipidemia. Therefore, future prospective studies are needed in different populations and different age groups.

Previous studies have shown a positive correlation between the severity of hypertension and hyperinsulinemia [3,22]. We did not find a significant correlation between plasma insulin and C-peptide levels and the degree of severity of hypertension. Hyperinsulinemia is not the only factor causing essential hypertension. Therefore, a positive correlation between hyperinsulinemia and the degree of severity of hypertension may not always be expected. The high levels of plasma insulin in the hypertensives under treatment support this suggestion [9,24].

Another noticeable finding of our study was the presence of an insignificant elevation of plasma insulin levels with a significant increase in plasma C-peptide levels in hypertensives. C-peptide is believed to reflect the endogenous insulin

production better than plasma insulin, since it has a lower hepatic clearance than insulin [25]. In addition, hepatic insulin clearance is known to be higher in obese patients [3]. The reason for the increased levels of C-peptide only in the hypertensives in our study may be related to the higher body mass indexes of the hypertensive group.

In conclusion, our results have shown that both hyperinsulinemia and overall adiposity are independently associated with hypertension. Plasma C-peptide levels are a better indicator of insulin secretion than plasma insulin levels.

REFERENCES

1. Jarrett RJ, Keen H, McCartney M, Fuller JH, Hamilton PJS, Reid DD, Rose G: Glucose tolerance and blood pressure in two population samples: their relation to diabetes mellitus and hypertension. Int J Epidemiol 1978, 7:15-24.
2. Modan M, Halkin H, Almog S, Lusky A, Eshkol A, Shefi M *et al.*: Hyperinsulinemia: a link between hypertension, obesity and glucose intolerance. J Clin Invest 1985, 75:809-817.
3. Sechi LA, Tedde R, Marigliano A, Melis A, Pala A, Orecchioni C: Insulin resistance and ß-cell hypersecretion in essentiol hypertension. J Hypertens 1990, 8(suppl 4): S87-S89.
4. Bonora E, Moghetti P, Zenere M, Tosi F, Travia D, Muggeo M: ß-cell secretion and insulin sensitivity in hypertensive and normotensive obese subjects. Int J Obes 1990, 14: 735-742.
5. Blaustein MP: Sodium ions, Calcium ions, blood pressure regulation and hypertension: a reassessment and a hypothesis. Am J Physiol 1977, 232: C165-C173.
6. Christensen NJ: Acute effects of insulin on cardiovascular functions and noradrenalin uptake and release. Diabetologia 1983, 25: 377-381.
7. King GL, Kahn CR, Rechler MM, Nissley SP: Direct demonstration of separate receptors for growth and metabolic activities of insulin and multiplication-stimulating activity (an insulin-like growth factor) using antibodies to the insulin receptor. J Clin Invest 1980, 66: 130-140.
8. Barret-Connor E, Criqui MH, Klauber MR, Holdbrook M: Diabetes and hypertension in a community of older adults. Am J Epidemiol 1981,113: 276-284.
9. Shen DC, Shieh SM, Fuh MMT, Wu A, Chen YDI, Reaven GM: Resistance to Insulin-stimulated-Glucose uptake in patients with hypertension. J Clin End Met 1988, 66: 580-583.
10. Pollare T, Lithell H, Berne C: Insulin resistance is a characteristic feature of primary hypertension independent of obesity. Metabolism 1990, 39: 167-174.
11. Stamler J, Stamle R, Liu K: High blood pressure: Role in coronary heart disease and implications for prevention and control. In Coronary Heart Disease. Edited by Connor W, Bristow D: Philadelphia, PA, Lippincott; 1985: 85-109.
12. World Health Organization: WHO Expert Committee on Diabetes Mellitus: second Report. Techn Rep Ser 646. Geneva: WHO. 1980.
13. Guyton AC: Insulin, glucagon and diabetes mellitus. In Textbook of Medical Physiology. Edited by Wonsiewicz MJ Philadelphia: W.B. Saunders Company; 1991: 855-867.
14. Reaven GM, Greenfeld MS: Diabetic hypertriglyceridemia: Evidence for three clinical syndromes. Diabetes 1981, 30(suppl 2): 66-75.
15. Kaplan NM: The deadly quartet. Upper-body obesity glucose intolerance, hypertriglyceridemia and hypertension. Arch Intern Med 1989, 149: 1514-1520.
16. Christlieb AR, Krotewski AS, Warram JH, Soeldner JS: Is insulin the link between hypertension and obesity? Hypertension 1985, 7(suppl II): 54-57.
17. Yalow RS, Rose HG, Bauman WA: Hyperinsulinemia. Am J Med 1988, 85: 22-30.
18. Kissebah AH, Freedman DS, Peiris AN: Health

risks of obesity. Med Clin North Am 1989, 73: 111-138.

19. Lillioja S, Young AA, Culter CL, Ivy JL, Abbott WG, Zawadzki JK, et al.: Skeletal muscle capillary density and fiber type are possible determinants of in vivo insulin resistance in man. J Clin Invest 1987, 80: 415-424.
20. Zavaroni I, Bonora E, Pagliara M, Dall'Aglio E, Luchetti L, Buonanno G, et al.: Risk factors for coronary artery disease in healthy persons with hyperinsulinemia and normal glucose tolerance. N Eng J Med 1989, 320: 702-706.
21. Fuh MM, Shieh SM, Wu DA, Chen YD, Reaven GM: Abnormalities of carbohydrate and lipid metabolism in patients with hypertension. Arch Intern Med 1987, 147: 1035-1038.
22. Haffner SM, Fong D, Hazuda HP, Pugh JA, Patterson JK: Hyperinsulinemia, upper body adiposity, and cardiovascular risk factors in non-diabetics. Metabolism 1988, 37: 338-345.
23. Orchard TJ, Becker DJ, Bates M, Kuller LH, Drash AL: Plasma insulin and lipoprotein cholesterol concentrations: An atherogenic association? Am J Epidemiol 1983, 118: 326-337.
24. Nilsson P, Lindholm L, Schersten B: Hyperinsulinaemia and other metabolic disturbances in well-controlled hypertensive men and women: an epidemiological study of the Dalby population. J Hypertens 1990, 8: 953-959.
25. Polonsky KS, Pugh W, Jaspan JB, Cohen DM, Karrison T, Tager HS, et al.: C-peptide and insulin secretion. J Clin Invest 1984, 74: 1821-1829.

JOURNAL OF ANKARA MEDICAL SCHOOL Vol 23, No 2, 2001 129-135

THE RELATIONSHIP BETWEEN TIME OF ONSET AND SHORT - AND LONG - TERM PROGNOSIS IN MYOCARDIAL INFARCTION

Ahmet Temizhan* ✣ Candan Avan Özen** ✣ İzzet Tandoğan** ✣ Özgül Uçar** ✣ Turgut Karabağ* ✣ Sinan Aydoğdu**

SUMMARY

Aim: *It is not known whether chronobiological changes have an impact on the prognosis of acute ischemic events or not. The aim of this study was to investigate the differences in the short-term and long-term end-points of patients who experience acute myocardial infarction (AMI) during morning hours and those whose AMI occurs at other times of the day.*

Material and methods: *One hundred seventeen patients admitted to our hospital with AMI were grouped according to the time of onset of AMI (06.00-12.00, 12.00-18.00, 18.00-24.00 and 24.00-06.00. Mortality and morbidity rates during their hospital stay and at one month, six months and one year after AMI were compared. Patients who experienced chest pain between 06.00-12.00 had a higher rate of trombolytic treatment when compared to the other groups (p<0.05). The number of affected vessels and the onset of chest pain between 06.00-12.00 were depicted as independent variables that increased 1-year mortality (R=0.33, Exp B=8.24, p=0.003 and R=0.18, Exp B=3.54, p=0.048 respectively). The onset of chest pain between 12.00-18.00 was found to be an independent variable that decreased the mortality rate (R=-0.21, Exp B=0.35, p=0.034).*

Conclusion: *As a result of investigating the effects of circadian factors on ischemic events, we can collect information regarding the onset of the process as well as its prognosis.*

Key words: *Circadian Rhythm, Acute Myocardial İnfarction*

ÖZET

AKUT MİYOKARD İNFARKTÜSÜ BAŞLANGIÇ ZAMANININ ERKEN VE GEÇ DÖNEM PROGNOZLA İLİŞKİSİ

Amaç: *Kronobiolojik değişikliklerin akut iskemik olayların prognozu üzerinde bir etkisinin olup olmadığı bilinmemektedir. Bu amaçla, sabah saatlerinde akut miyokard infarktüsü geçiren hastalar ile günün diğer saatlerinde akut miyokard infarktüsü geçiren hastalar arasında kısa ve uzun dönem sonlanımlar açısından bir fark olup olmadığını araştırmayı amaçladık.*

Yöntem ve bulgular: *Akut miyokard infarktüsü tanısı ile başvuran 117 hasta göğüs ağrısının başlangıç saatine göre 06:00-12:00, 12:00-18:00, 18:00-24:00 ve 24:00-06:00 zaman dilimleri arasında gruplandırıldı. Hastane içi, bir ay, altı ay ve bir yıl sonraki morbidite ve mortalite oranları karşılaştırıldı. Göğüs ağrısı saat 06:00-12:00 arasında başlayan hastalara diğer zaman dilimindeki hastalara göre trombolitik tedavinin daha yüksek oranda uygulandığı saptandı (p<0.05). Hastalıklı damar sayısı ve göğüs ağrısının saat 06:00-12:00 arasında başlaması bir yıllık mortaliteyi arttıran bağımsız değişkenler olarak belirlendi (sırasıyla R=0.33, Exp B=8.24, p=0.003 ve R=0.18, Exp B=3.54, p=0.048). Göğüs ağrısının saat 12:00-18:00 arasında başlaması ise mortalite oranını azaltan bağımsız değişken olarak saptanmıştır (R=-0.21, Exp B=0.35, p=0.034).*

Sonuç: *Sirkadiyan etkenlerin iskemik olaylar üzerine olan etkilerinin incelenmesi sayesinde akut koroner olayların başlangıcı hakkında bilgi edinilebildiği gibi sonlanımı hakkında da bilgi sahibi olunabileceğini düşünmekteyiz.*

Anahtar kelimeler: *Sirkadiyan Ritim, Akut Miyokard İnfarktüsü*

**Selçuk University, Faculty of Medicine, Dept. of Cardiology*
***Ankara Numune Education and Researds Hospital, Dept. of Cardiology, Ankara*

Received: April 25,2001 Accepted: May 28,2001

AIM:

Angina pectoris, myocardial infarction and sudden death are the most serious complications of coronary artery disease. The results obtained from epidemiological studies and large clinical trials revealed that these undesirable events increase during the morning hours with the circadian rhythm (1-4). These events were thought to be related to the increased activity of plasminogen activator inhibitor (5), tissue plasminogen activator antigens (6), platelet aggregation (7), plasma epinephrine and norepinephrine levels (8,9).

Due to increased trombogenicity and decreased fibrinolytic activity during these hours of the day, thrombolytic therapies should be administered at higher doses (10,11), and patients who go through coronary angioplasty should be followed up more closely for early complications (12). Although these treatment approaches are tailored by taking the possible effects of circadian triggering factors into account, we do not know whether such chronobiological changes have an effect on the prognosis of acute ischemic events. We aimed to investigate the differences between patients who experienced acute myocardial infarction (AMI) in morning hours and those whose AMI occurred at other hours of the days in terms of short- and long-term prognosis.

PATIENTS AND METHOD:

A total of 117 patients (94 males, 23 females) admitted to the coronary care unit of the Ankara Numune Hospital Department of Cardiology between April 1999 and February 2000 were included in this study. The diagnosis of AMI was established through personal history, physical examination, cardiac enzyme levels and electrocardiograph (ECG) criteria. The detection of at least one of the following changes on ECG was accepted as a positive criterion: 2mm ST segment elevation 0.08 seconds after J-point on at least two derivations; newly developed Q-wave on at least two leads; newly developed significant R-wave.

Cardiovascular risk factors such as smoking, diabetes, hypertension and hypercholesterolemia and a previous history of myocardial infarction and angina pectoris were considered in the study. Patients who smoked more than five cigarettes per day were classified as smokers. Those who had never smoked and those who had discontinued smoking for over two years were classified as non-smokers, based on the Framingham study's (13) equalization of these two groups in terms of risk of cardiovascular event. Patients with a history of diabetes, patients receiving anti-diabetic medication and patients with fasting hyperglycemia were considered as diabetics.

Patients with a history of hypertension, patients receiving anti-hypertensive treatment, patients with identified left ventricular hypertrophy (by ECG and echocardiography) and those with blood pressure of >140/90 mmHg were accepted as hypertensive. Patients whose serum cholesterol level measured above 200 mg/dl were considered to have hypercholesterolemia. Previous myocardial infarction was confirmed by personal history, ECG and echocardiography.

All the patients had undergone coronary angiography within 7±2 days using a percutaneous femoral approach and Judkins technique. Right-left coronary arteries were selectively approached, and multiple projections were obtained. Localization and the numbers of diseased coronary arteries (epicardial coronary arteries with >50% stenosis) were investigated.

Patients were classified by time of onset of chest pain as follows: 06.00-12.00, 12.00-18.00, 18.00-24.00, 24.00-06.00. The time of onset for MI was confirmed by creatine kinase enzyme peak. The time elapsed between the time of onset of pain and admission to the coronary care unit was recorded. Patients who received trombolytic treatment were grouped as follows: those receiving treatment within the first six hours, those receiving treatment between 6-12 hours and those receiving treatment after 12 hours. Patients who underwent percutaneous transluminal coronary angioplasty (PTCA) or coronary artery bypass grafting operations (CABG) during a one-year follow-up period were recorded. Patients

who had experienced primary or rescue PTCA, renal insufficiency, hepatic insufficiency, previous heart failure and valvular heart disease were excluded from the study.

During the first week in hospital, patients were closely followed-up for newly developing conduction disturbances (atrioventricular block, bundle branch block), atrial fibrillation, sustained ventricular tachycardia, re-infarction, post-infarction angina pectoris, mechanical complications, heart failure, and cardiac death. Re-infarction and cardiac death rates were evaluated at one month, six months and 12 months.

Statistical analysis:

Data was evaluated using SPSS statistical program. Student t-test (two-tailed) was used to compare means of continuous variables, and X^2 test was used for categorical variables. The effect of independent variables on mortality and morbidity was tested using multivariate logistics regression analysis. P<0·05 was accepted as statistically significant.

RESULTS:

The clinical characteristics of patients grouped according to time of onset of chest pain are summarized in Table 1. There was no statistically significant difference between the groups in terms of age, sex, frequency of diabetes, hypertension, hypercholesterolemia or smoking. Rates of patients with a history of angina pectoris and myocardial infarction did not differ between the groups, nor did the time elapsed between onset of chest pain and admittance to the intensive coronary unit. All patients received aspirin and anticoagulants during their hospital stays. Nitrates, beta-blockers, angiotensin converting enzyme inhibitors, calcium channel blockers and digital preparations were administered in similar rates in all groups. The number of patients receiving trombolytic treatment was higher in those patients who experienced chest pain between 06.00-12.00 when compared to other groups. The time of administering trombolytic treatment and the frequency of performing PTCA and CABG did not differ significantly.

Coronary angiography characteristics of the patients are shown in Table 2. Localization of infarct, distribution of lesions on the coronary arteries (left main coronary artery, left ant descending, left circumflex, right coronary artery) and the number of affected vessels showed no statistically significant difference between the groups. During a one-year follow-up period, 35 patients (30%) developed post-infarction angina pectoris, 10 (8%) had conduction disturbances, 7(6%) had sustained ventricular tachycardia, seven (6%) had re-infarction, six (5%) had atrial fibrillation and five (4%) had heart failure. Nine patients (8%) died due to cardiac-related causes.

Multiple logistics regression analysis of the independent variables affecting one-year total mortality is shown in Table 3. They were: number of diseased arteries; administration of thrombolytic treatment; time of trombolytic treatment; previous myocardial infarction; time of onset of chest pain. Independent variables increasing mortality were number of affected vessels and the onset of chest pain between 06.00-12.00 (R=0.33, Exp. B=8.24, p=0.003 and R=0.18, Exp B= 3.54, p=0.048 respectively). The onset of chest pain between 12.00-18.00 was an independent variable decreasing mortality (R=-0.21, Exp B=0.35, p=0.034).

Multiple logistic regression analysis of the independent variables influencing one-year total mortality and morbidity are summarized in Table 4. Independent variables were: number of affected vessels; administration of trombolytic treatment; time of administration of thrombolytic agents; previous myocardial infarction; time of onset of chest pain. The number of affected vessels was the only independent variable increasing total mortality and morbidity (R=0.16, Exp B=1.95, p=0.025 and R=0.16).

DISCUSSION:

Our study found myocardial infarction onset during morning hours and the number of affected vessels to be independent risk factors affecting one-year total mortality. While no similar studies have appeared in the literature, Kurnik stated that patients admitted with and treated for acute

Table 1: Clinical characteristics of patients according to time interval

	00-06	06-12	12-18	18-24	P value
N	28	32	31	26	
Age, year	56,3 ± 12	55,1 ± 11	56,8 ± 10	58,7 ± 10,4	NS
Male (%)	80	93	79	68	NS
Diabetes (%)	28	14	21	23	NS
Hypertension (%)	36	27	24	46	NS
Hypercholesterolemia (%)	28	36	20	46	NS
Current smokers (%)	64	75	63	46	NS
History of previous angina (%)	44	34	57	61	NS
Previous myocardial infarction (%)	4	9	12	8	NS
Time to hospitalization, hour	7,5 ± 8,8	5,6 ± 6,5	7,6 ±8,3	8,1 ± 7,8	NS
Medication (%)					NS
Aspirin	100	100	100	100	
Anti-coagulan	100	100	100	100	
Beta blocker	76	75	75	78	
Angiotensin converting enzyme inhibitor	56	55	58	56	
Calcium channel blocker	10	8	11	10	
Nitrates	80	81	78	80	
Digital	2	1	3	1	
Trombolytic treatment	68	85	61	50	<0,05
Time to trombolytic treatment					NS
first 6 hour	56	69	55	46	
6 – 12 hour	8	9	6	4	
Late phase	36	21	39	50	
PTCA or CABG (%)	40	46	49	31	NS

(PTCA:percutaneous transluminal coronary angioplasty, CABG:coronary artery bypass grafting, NS: non-significant)

myocardial infarction between 24.00-12.00 and 12.00-24.00 did not differ in terms of hospital mortality (4.5%) or re-infarction rates (10). Although its necessity was emphasized, long-term follow-up for prognosis was not conducted.

An onset of myocardial infarction between 12.00-18.00 was an independent variable decreasing one-year total mortality. It is thought that different triggering factors might play a role at different times of the day and in different infarct types (14). This view is supported by the absence of a circadian rhythm in patients with previous myocardial infarction and non-Q myocardial infarction, at advanced ages, in diabetics and in non-smokers (15,16). Although these subgroups were included in our study, they were present at similar rates in the different time-interval groups. Furthermore, the frequency of hypertension, hypercholesterolemia and the

Table 2: Coronary angiographic features of patients

	Time of onset of chest pain				
	00-06	06-12	12-18	18-24	p value
Infarct localization(%)					NS
Anterior	44	49	36	57	
Inferior	40	46	49	30	
Non-Q	16	6	15	23	
Left main coronary artery (%)	1	2	1	1	NS
LAD (%)	48	46	40	51	NS
LCx (%)	24	21	21	28	NS
RCA (%)	30	33	37	29	NS
Diseased vessels (%)					NS
One vessel	48	39	55	39	
Two vessel	40	33	25	34	
Three vessel	12	27	21	27	

(LAD: left anterior descending coronary artery, LCx: left circumflex coronary artery, RCA: right coronary artery, NS: non-significant)

Table 3: Multiple logistic regression analysis of independent variables affecting 1-year mortality.

Mortality rates	Coefficient B	Standard Deviation	p	R	Exp. B
Number of vessel diseased	2,28	0,77	0,003	0,33	8,24
Thrombolytic treatment	3,5	2,1	0,091	0,12	34,15
Time to trombolytic treatment	0,82	1,01	0,427	0,00	2,27
Previous MI	-1,19	1,44	0,407	0,00	0,30
Previous angina	-0,31	0,91	0,736	0,00	0,74
MI onset between 00 – 06	0,23	0,60	0,702	0,00	1,26
MI onset between 06 – 12	1,27	0,64	0,048	0,18	3,54
MI onset between 12 – 18	-1,05	0,49	0,034	-0,21	0,35
MI onset between 18 – 24	-0,28	0,56	0,615	0,00	0,76

(MI: myocardial infarction)

number of vessels involved did not differ significantly between the groups. For these reasons, we believe that the circadian triggering factors influencing the onset of myocardial infarction might play a similar role in its prognosis as do other atherosclerotic risk factors. Although the number of patients who received thrombolytic treatment was higher among the patients experiencing

Table 4: Multiple logistic regression analysis of independent variables affecting the development of 1-year mortality and morbidity.

Mortality and morbidity rates	Coefficient B	Standard Deviation	p	R	Exp. B
Number of diseased vessels	0,67	0,30	0,025	0,16	1,95
Trombolytic treatment	1,27	1,03	0,216	0,00	3,56
Time to trombolytic treatment	1,00	0,53	0,058	0,11	2,72
Previous MI	-0,11	0,81	0,890	0,00	0,89
Previous angina	0,02	0,49	0,962	0,00	1,02
MI onset between 00 – 06	0,23	0,31	0,455	0,00	1,26
MI onset between 06 – 12	0,12	0,29	0,661	0,00	1,13
MI onset between 12 – 18	-0,22	0,26	0,392	0,00	0,80
MI onset between 18 – 24	-0,08	0,29	0,773	0,00	0,92

(MI: myocardial infarction)

myocardial infarction during the morning hours (06.00-12.00), it is interesting that this time interval has been identified as a risk factor increasing mortality. This shows us that, as a result of circadian influences, thrombolytic treatment has a limited success rate at this time of the day. Previous studies found that the increased thrombogenicity and decreased fibrinolytic activity that occurred during morning hours had a negative impact on the success of thrombolytic treatment and noted that treatment needed to be provided at higher doses in such cases (10, 11).

In conclusion, elimination of long-term risk factors such as hypertension, diabetes mellitus, hypercholesterolemia and smoking can reduce the risk of cardiovascular disease. Reducing the circadian triggering factors with short-term effects on the development of thrombosis, such as hypercoagulability, catecholamine secretion and platelet aggregation, can prevent acute coronary occlusions (10). By analyzing the effects of circadian factors on ischemic events, we can gain information regarding the onset of acute coronary events as well as their prognoses.

REFERENCES

1- Mulcahy D, Keegan J, Cunningham D, et al. Circadian variation of total ischemic burden and its alteration with anti-anginal agents. Lancet, 1988; 2:755-9.

2- Muller JE, Stone PH, Turi ZG, et al. Circadian variation in the frequency of onset of acute myocardial infarction. N Engl J Med, 1985; 313:1315-22.

3- Thompson DR, Blandford RL, Sutton TW, Marchant PR. Time of onset of chest pain in acute myocardial infarction. Int J Cardiol, 1985; 7:139-48.

4- Muller JE, Ludmer PL, Willich SN, et al. Circadian variation in the frequency of sudden cardiac death. Circulation, 1987; 75:131-8.

5- Angleton P, Chandler WL, Schmer G. Diurnal variation of tissue-type plasminogen activator and its rapid inhibitor (PAI-1). Circulation, 1989; 79:101-6.

6- Bridges AB, Mc Laren M, Scott NA, et al. Circadian

variation of tissue plasminogen activator and its inhibitor, von Willebrand factor antigen, and prostacyclin stimulating factor in men with ischaemic heart disease. Br Heart J, 1993; 69:121-4.

7- Tofler GH, Brezinski DA, Schafer AI, et al. Concurrent morning increase in platelet aggregability and the risk of myocardial infarction and sudden cardiac death. N Engl J Med, 1987; 316:1514-8.

8- Linsell CR, Lightman SL, Mullen PE, et al. Circadian rhythms of epinephrine and norepinephrine in man. J Clin Endocrinol Metab, 1985; 60:1210-5.

9- Millar-Craig MW, Bishop CN, Raftery EB. Circadian variation of blood pressure. Lancet, 1978; 1:795-7.

10- Kurnik PB. Circadian variation in the efficacy of tissue-type plasminogen activator. Circulation, 1995; 91:1341-6.

11- Fujita M, Araie E, Yamanishi K, Miwa K, Kida M, Nakajima H. Circadian variation in the success of intracoronary trombolysis for acute myocardial infarction. Am J Cardiol 1993; 71: 1369-1371

12- Temizhan A, Dinçer I, Pamir G, Alpman A, Oral D. Is there any effect of chronobiological changes on coronary angioplasty? J Cardiovasc Risk 2001; 8: 15-19.

13- Gordon T, Kannel WB, McGee D, Dawber TR. Death and coronary attacks in man after giving up cigarette smoking. A report from the Framingham study. Lancet 1974;ii:1345-8

14- Ridker PM, Manson JAE, Buring JE, Muller JE, Hennekens CH. Circadian variation of acute myocardial infarction and the effect of low-dose Aspirin in a randomized trial of physicians. Circulation 1990; 82: 897-902.

15- Hjalmarson A, Gilpin EA, Nicod P, Dittrich H, Henning H, Engler R, et al. Differing circadian patterns of symptom onset in subgroups of patients with acute myocardial infarction. Circulation 1989; 80: 267-275.

16- Kleinman NS, Schechtman KS, Young PM, et al. Lack of diurnal variation in the onset of non-Q-wave infarction. Circulation 1990; 81: 548-555.

JOURNAL OF ANKARA MEDICAL SCHOOL Vol 23, No 2, 2001 137-142

QT DISPERSION IN RHEUMATOID ARTHRITIS

Mete Alpaslan* ✣ Serap Alpaslan** ✣ Ersel Onrat*
✣ Deniz Evcik*** ✣ Nihal Taş

SUMMARY

Objective: *To assess whether rheumatoid arthritis (RA) is associated with an increased QT length or dispersion.*

Methods: *64 patients with RA and 25 healthy adults participated in this study. RA was diagnosed according to the 1987 revised criteria of ARA. QT dispersion was assessed by 12-lead surface electrocardiography.*

Results: *Mean heart rate and systolic and diastolic blood pressures were not significant between the two groups (p >0.05). Body mass index was 27 ± 4 kg/m^2 in both RA and control group. Some of the QT parameters were significantly different between the two groups (minimum QT 338 ± 28 and 352 ± 26 ms; QT dispersion 56 ± 24 and 40 ± 15 ms; maximum QTc 459 ± 30 and 436 ± 28; and QTc dispersion 65 ± 27 and 45 ± 19 ms in RA patients and controls, respectively).*

Conclusion: *Patients with RA appear to be associated with a significant increase in QT length and QTc dispersion when compared with healthy adults. However, this association does not correlate with the duration of disease.*

Key words: *Rheumatoid Arthritis, Electrocardiography, QT Dispersion*

ÖZET

ROMATOİD ARTRİTTE QT DİSPERSİYONU

Amaç: *Romatoid artrit (RA) hastalarında QT uzunluğunun veya dispersiyonunun artıp artmadığını belirlemek.*

Metod: *RA'li 64 hasta (ortalama yaş 50 ± 9) ve 25 sağlıklı yetişkin (ortalama yaş 45 ± 14) çalışmaya katıldı. RA tanısı 1987 ARA kriterlerine göre kondu. QT dispersiyonu 12-derivasyonlu yüzey elektrokardiyografisinden değerlendirildi.*

Bulgular: *Her iki grup arasında sistolik ve diyastolik kan basınçları yönünden anlamlı farklar bulunmadı (p >0.05). Vücut kütle indeksi (BMI) hem RA hem de kontrol grubunda 27 ± 4 kg/m^2 idi. Bazı QT parametreleri iki grup arasında anlamlı derecede farklı bulundu (RA ve kontrol gruplarında sırasıyla minimum QT 338 ± 28 ve 352 ± 26 ms; QT dispersiyonu 56 ± 24 ve 40 ± 15 ms; maksimum QTc 459 ± 30 ve 436 ± 28 ms; QTc dispersiyonu 65 ± 27 ve 45 ± 19 ms idi).*

Sonuç: *Sağlıklı yetişkinlerle kıyaslandığında RA'li hastalarda QT uzunluğu ve QTc dispersiyonu artmış görünmektedir. Ancak bu durum hastalığın süresi ile korelasyon göstermez.*

Anahtar kelimeler: *Romatoid Artrit, Elektrokardiyografi, QT Dispersiyonu*

*Department, Afyon Kocatepe University, Afyon.

**Physical Medicine and Rehabilitation, Faculty of Medicine, Gazi University, Ankara.

***Physical Medicine and Rehabilitation, Afyon Kocatepe University, Afyon.

Received: March 12,2001 Accepted: April 16,2001

Rheumatoid arthritis (RA) is a multisystemic disease that can involve heart in several ways. Pericarditis, coronary arteritis, myocarditis, valvular dysfunction and conduction system abnormalities are among the cardiac manifestations of this disease.[1-6]

QT dispersion is defined as the difference in QT intervals of various leads on surface electrocardiogram (ECG). It is known that disparity of repolarization of adjacent myocardial segments may result in reentry, which in turn may cause ventricular arrhythmias.[7] Therefore, it is suggested that an increase in QT dispersion may be associated with reentry mechanisms resulting in ventricular fibrillation.[8] In patients with chronic ischemic heart disease, prolongation of QTc interval has also been shown to predict sudden death.[9]

Although various cardiac manifestations of RA are well known, QT dispersion in this disease is not investigated thoroughly. Our aim in this study was to evaluate QT length and dispersion in patients with RA and to search for the presence of a correlation between duration of RA and dispersion of corrected QT.

Material and Methods

Sixty-four patients with rheumatoid arthritis participated in this study. Twenty-five healthy adults of similar ages formed the control group. RA was diagnosed according to the 1987 revised criteria of the American Rheumatism Association.[10]

All subjects underwent complete physical examination. Subjects with hypertension, diabetes mellitus, heart failure, atrial fibrillation, clinically significant valvular heart disease and established coronary artery disease were excluded from the study. Patients with clinically overt cardiac disease were evaluated and excluded noninvasively by clinical history and detailed physical examination. Patients with RA were not under treatment by potentially cardiotoxic drugs or drugs that could affect QT interval.

QT dispersion was evaluated by 12-lead surface ECG, which was recorded at a paper speed of 25mm/s. QT interval was measured manually by a cardiologist. The cardiologist was blinded to the clinical diagnosis of the subjects. The onset of Q wave was regarded as the onset of QT interval. The end of QT interval was the point where the T wave intersects the isoelectric TP segment. The leads were excluded from analysis if the onset and end points of QT interval were undetectable. Subjects were included in the study if at least 8 leads could be analyzed. QT dispersion (QTd) was calculated as the difference between maximum and minimum QT intervals. QT interval was corrected by heart rate (QTc) according to the Bazett's formula ($QTc=QT/[RR]^{1/2}$). Corrected QT dispersion (QTcd) was also calculated as the difference between maximum and minimum QTc.

Statistical analysis. Data was presented as mean $\pm$ SD (standard deviation). Statistical analysis was made with the "SPSS for windows" software. Comparison of means between the two groups was made by Mann-Whitney U test. $P < 0.05$ was accepted to be statistically significant. The relationship between QTcd and the duration of rheumatoid arthritis was assessed by correlation and linear regression analysis.

Results

The duration of disease was 7 $\pm$ 8 years in the RA group. Clinical features of subjects are shown in Table 1. The mean age of subjects in RA group and the controls were not significantly different (50 $\pm$ 9 years and 45 $\pm$ 14 years respectively, $p > 0.05$). Systolic and diastolic blood pressures also were not significantly different between the two groups (p value was >0.05 for both). Mean heart rate was significantly higher in the RA group when compared with those of the controls (82 $\pm$ 12 /min. and 74 $\pm$ 13 /min. respectively, $p=0.005$). However, there was no apparent cause for this difference. There was no correlation between the duration of RA and the heart rate ($r=0.12$ and $p > 0.05$).

The values of QT parameters are depicted in Table 2. Maximum QT interval length was 394 $\pm$ 14 ms in the RA group and 393 $\pm$ 25 ms in the

Table 1. Characteristics of study subjects.

	Rheumatoid arthritis (n=64)	Controls (n=25)	P value
Sex (male/female)	21/43	12/13	
Age, years	50 ± 9	45 ± 14	0.127
Heart rate, /min.	82 ± 12	74 ± 13	0.005 *
Systolic BP, mmHg	123 ± 15	124 ± 18	0.954
Diastolic BP, mmHg	77 ± 11	75 ± 11	0.524
Weight, kg	74 ± 11	72 ± 13	0.366
Height, cm	163 ± 7	162 ± 7	0.524
Body mass index, kg/m^2	27 ± 4	27 ± 4	0.485
Duration of disease, years	7 ± 8	-	-

* significant (p <0.05). Data are mean ± SD. BP=blood pressure.

controls. The minimum QTc was 394 ± 24 ms in the RA group and 391 ± 29 ms in the control group. Both maximum QT interval length and the minimum QTc were not significantly different between the two groups (p values were > 0.05 for both).

Minimum QT interval, QTd, maximum QTc and QTcd were all significantly different between the two groups (Table 2, Figures 1-4). Minimum QT interval was 338 ± 28 ms in the RA group while it was 352 ± 26 ms in the control group (p=0.006). This might be the result of a higher heart rate in patients with RA. QT dispersion was 56 ± 24 ms in the RA group and 40 ± 15 ms in the controls (p=0.005). Maximum QTc was 459 ± 30 ms in the RA group while it was 436 ± 28 ms in the controls (p=0.001). QTcd was 65 ± 27 ms in the RA group and 45 ± 19 ms in the controls (p=0.000).

In order to analyze the correlation between QTcd and the duration of RA, the correlation and linear regression analysis were performed. There was no correlation between QTcd and the duration of RA. The regression coefficient was r=0.14 and p=0.184. The regression equation was QTcd=57.16 + 0.47 duration of RA (Figure 5).

Table 2. QT parameters in patients with rheumatoid arthritis and controls.

	Rheumatoid arthritis (n=64)	Control group (n=25)	P value
Minimum QT, ms	338 ± 28	352 ± 26	0.006 *
Maximum QT, ms	394 ± 36	393 ± 25	0.330
QT dispersion, ms	56 ± 24	40 ± 15	0.005 *
Minimum QTc, ms	394 ± 24	391 ± 29	0.414
Maximum QTc, ms	459 ± 30	436 ± 28	0.001 *
QTc dispersion, ms	65 ± 27	45 ± 19	0.000 *

* significant (p <0.05). QTc=corrected QT.

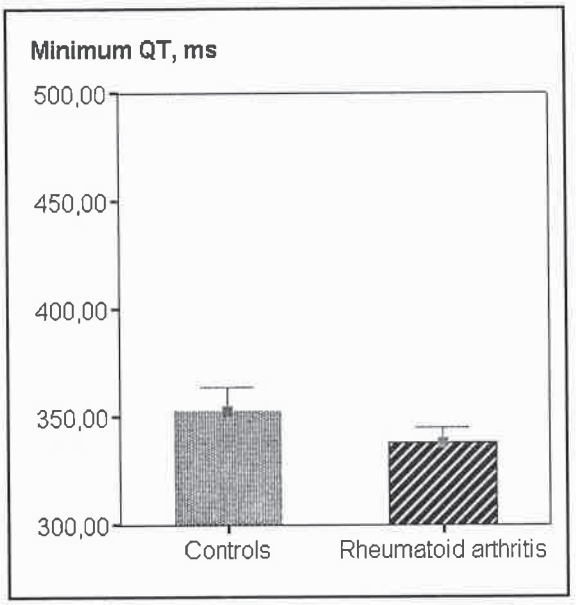

Figure 1. Minimum QT interval was significantly lower in the rheumatoid arthritis group ($p < 0.05$).

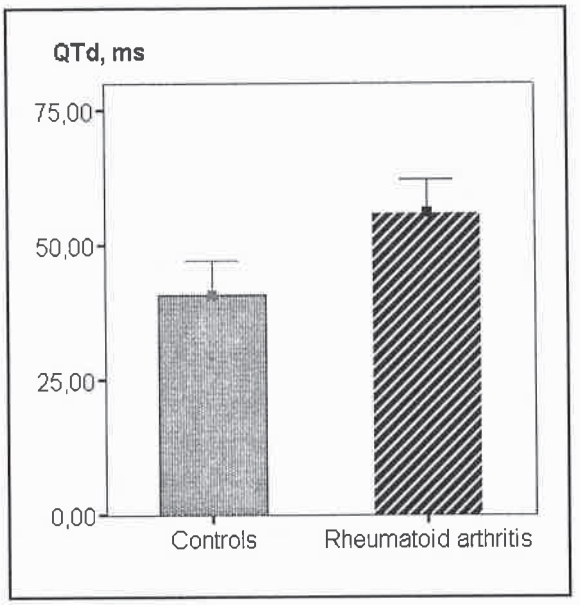

Figure 2. QT dispersion was significantly higher in patients with rheumatoid arthritis ($p < 0.05$).

Duration of RA also was not correlated with any of the QT parameters.

Discussion

RA is a chronic multisystem disease that can have various types of cardiac involvement. Although pericarditis is the most common manifestation of cardiac involvement in RA, coronary arteritis, myocarditis, valvular dysfunction and conduction system disease can also be observed.[1-6] On the other hand, QT dispersion in RA is not thoroughly investigated.

In this study, we observed that the heart rate

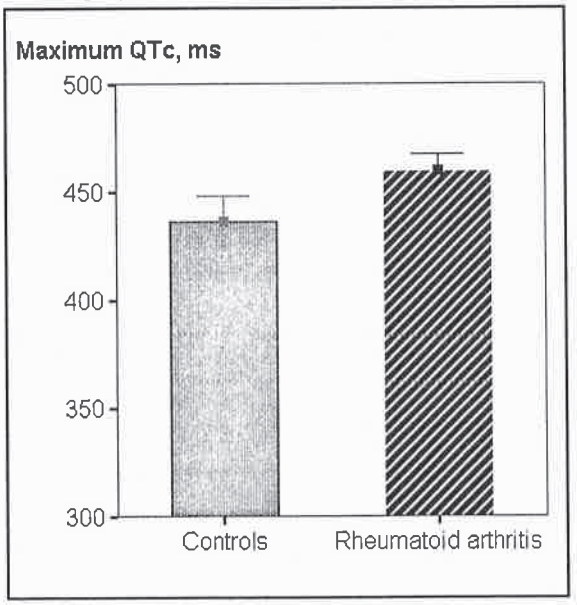

Figure 3. Maximum QTc was significantly higher in the rheumatoid arthritis group ($p < 0.05$).

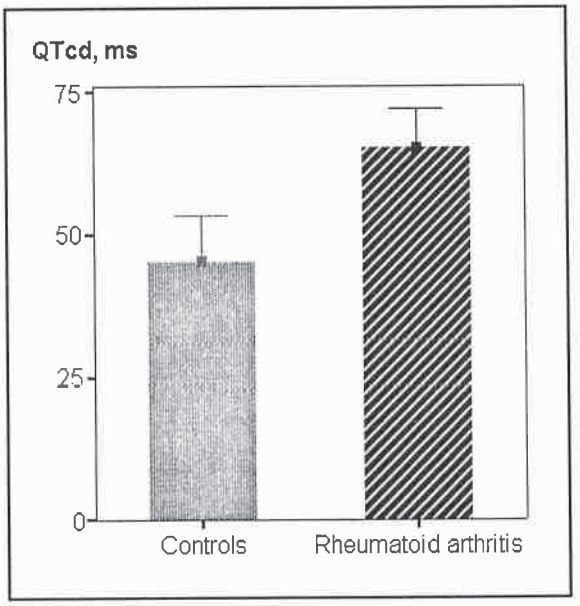

Figure 4. QTc dispersion was significantly higher in patients with rheumatoid arthritis ($p < 0.05$).

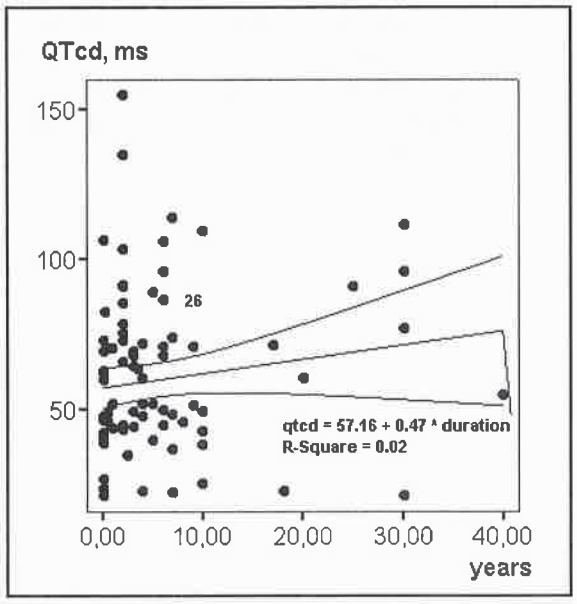

Figure 5. Linear regression between QTcd and the duration of rheumatoid arthritis.

was significantly higher in patients with rheumatoid arthritis. Although our study did not aim to identify its cause, we think that this may be related to the rheumatoid arthritis itself since the systolic and diastolic blood pressures are not significantly different between the two groups. Another cause may be the relatively smaller number of control subjects. Because of this relatively higher heart rate, we found the minimum QT to be significantly lower in the RA group.

In addition, we found that QT dispersion, maximum QTc and QTcd were significantly higher in patients with rheumatoid arthritis. This may suggest that patients with RA have inhomogenous ventricular repolarization and are at an increased risk of ventricular arrhythmias. In fact, our results are in accordance with a recent study which also concluded that QT dispersion is increased in patients with rheumatoid arthritis.[11] In their study Goldeli et al. found that the premature ventricular repolarization complexes on 24-hour ambulatory ECG recordings were correlated with dispersion variables.[11]

Duration of rheumatoid arthritis and its correlation with QTcd has not been mentioned in previous studies. Although our results show a significant increase in QTcd among RA patients, there was no correlation of this QT parameter with the duration of RA. This raises the possibility that mechanisms other than the direct effects of RA on myocardium may be responsible for the increase in QTcd. Further studies are needed to determine the pathogenesis of this increase in QTcd in patients with RA.

REFERENCES

1. Maione S, Valentin G, Giunta A, et al. Cardiac involvement in rheumatoid arthritis: an echocardiographic study. Cardiology 1993;83:234-9.
2. Leibowitz W B. The heart in rheumatoid arthritis (rheumatoid disease). A clinical and pathological study of 62 cases. Ann Intern Med 1963;58: 102-23.
3. Ahern M, Lever J V, Cosh J. Complete heart block in rheumatoid arthritis. Ann Rheum Dis. 1983;42:389-97.
4. Roberts W C, Kehoe J A, Carpenter D F, Golden A. Cardiac valvular lesions in rheumatoid arthritis. Arch Intern Med 1968;122:141-6.
5. Thould A K. Constrictive pericarditis in rheumatoid arthritis. Ann Rheum Dis 1986;45:89-94.
6. Slack J D, Waller B. Acute congestive heart failure due to the arteritis of rheumatoid arthritis: early diagnosis by endomyocardial biopsy: a case report. Angiology 1986;37:477-82.
7. Merx W, Yoon M S, Han J. The role of local disparity in conduction and recovery time on ventricular vulnerability to fibrillation. Am Heart J 1977;94:603-10.
8. Karjalainen J, Reunanen A, Ristola P, Viitasalo M. QT interval as a cardiac risk factor in a middle aged population. Heart 1997;77:543-8.
9. Puddu P E, Bourassa M G. Prediction of sudden death from QTc interval prolongation in patients with chronic ischemic heart disease. J Electrocardiol 1986;19:203-11.
10. Arnett F C, Edworthy S M, Bloch D A, et al. The

American Rheumatism Association 1987 revised criteria for the classification of rheumatoid arthritis. Arthritis Rheum 1988; 31: 315-24.

11. Goldeli O, Dursun E, Komsuoglu B. Dispersion of ventricular repolarization: a new marker of ventricular arrhythmias in patients with rheumatoid arthritis. J Rheumatol 1998; 25:447-50.

JOURNAL OF ANKARA MEDICAL SCHOOL Vol 23, No 2, 2001 143-147

AN UNUSUAL TUMOR OF THE CHEST WALL - PLEURAL LIPOMA REPORT OF TWO CASES

Murat Kara* ✣ Dalokay Kılıç ✣ Ayten Kayı Cangır* ✣ Serpil Dizbay Sak**** ✣ Şevket Kavukçu*****

SUMMARY

Intrathoracic lipomas are quite rare tumors, with those originating from pleural fat tissue being the least common. Two cases of pleural lipomas are presented with the features of this tumor. They should be considered in the differential diagnosis of pleural tumors. Total excision of the tumor enables histologic diagnosis as well as surgical treatment. Although they are classified as deep-seated lipomas, recurrence is unlikely.

Key words: *Intrathoracic, Pleural Lipoma*

ÖZET

GÖĞÜS DUVARININ NADİR BİR TÜMÖRÜ: PLEVRAL LİPOMA

İntratorasik lipomlar nadir tümörlerdir ve plevradan köken alan daha az görülürler. Bu makalede iki olgunun özellikleri sunulmuştur. Plevral tümörlerin ayırıcı tanısında göz önünde tutulması gereken bu lezyonların total eksizyonu tümörü hem tedavisine ve hem de tanısını sağlar. Derin yerleşimli lipomlar arasında yer almalarına karşın nüks olgularda beklenmeyen bir durumdur.

Anahtar Kelimeler: *Plevra, Lipoma*

Although lipomas are the most common benign neoplasms, intrathoracic lipomas are quite rare. Even rarer are occurrences of pleural lipomas. Most of these lesions are asymptomatic and discovered incidentally on chest roentgenograms (1).

Herein we present two cases of pleural lipomas that were operated on in our clinic during the past six years, as well as the clinicopathological features of this tumor.

Case reports

Case 1. A 23-year-old male patient without complaints was referred to our clinic because of an abnormal chest film. His past history was unremarkable. Physical examination and laboratory data were unrevealing. A chest roentgenogram revealed a well-circumscribed mass shadow, superposing with the medial border of the scapulae in the left upper lung field. Computer tomography (CT) showed a soft tissue mass of -110 Hounsfield Units (H.U.) lying

*Assistant Professor, Department of Thoracic Surgery, Kırıkkale University School of Medicine, Kırıkkale

**Fellow, Department of Thoracic Surgery, Ankara University School of Medicine

***Staff surgeon, Muhittin Ülker Emergency and Traumotology Hospital, Balgat, Ankara

****Associate Professor, Department of Pathology, Ankara University School of Medicine

*****Professor, Department of Thoracic Surgery, Ankara University School of Medicine

Received: May 24,2000 Accepted: Oct 23,2000

beneath the pleura in the left upper zone (Fig. 1). A thoracotomy revealed a 4-cm soft tissue mass located subpleurally in the area of the third interspace in the mid-axillary line, macroscopically consistent with lipoma, which was totally excised. The specimen was a lobulated, pale-yellow mass consisting of mature fatty tissue separated by thin, fibrous septa and was diagnosed as lipoma. The parietal pleura was intact, and no pathological change was observed in either the lung or the bony structure. Post-operative course was uneventful. There has been no recurrence in a six-year follow-up.

Case 2. A 47-year-old male patient with a six-month history of chest-wall pain was found to have a mass in his right hemithorax and was referred to our clinic. Physical examination was within normal limits. No abnormal laboratory finding was observed. A chest roentgenogram revealed a homogenous mass density in the right upper lung field, superposing with the mid-portion of the clavicle (Fig. 2). CT showed a 5-cm mass composed of fatty tissue (-123 H.U.) that was in close contact with the pleura at the right upper apical segment localization of the lung (Fig. 3). Bone scan was within the normal limits. A thoracotomy revealed an apical subpleural mass located at the second intercostal space and consistent with the appearance of a lipoma. There was no evidence of invasion of the tumor. Total excision was performed. Histologically, it was confirmed to be a lipoma. The patient remains well five months after surgery.

Discussion

Lipomas are extremely common benign tumors arising from subcutaneous tissue. In addition to the common superficial localizations of neck, trunk, face, hands and feet, they also occur rarely in deeper structures such as the retroperitoneum, skeletal muscle, mediastinum and gastrointestinal tract. They are usually found as solitary lesions (2).

Intrathoracic lipomas can be classified as follows: 1) endobronchial, 2) parenchymal, 3) cardiac, 4) mediastinal, 5) pleural (1). They are relatively rare, and those originating from pleural fat tissue are the least common. There are about 32 reported cases of pleural lipoma in the world literature from the past 10 years, including the recently reported giant lipoma (3). Pleural lipomas originate from the submesothelial layer of

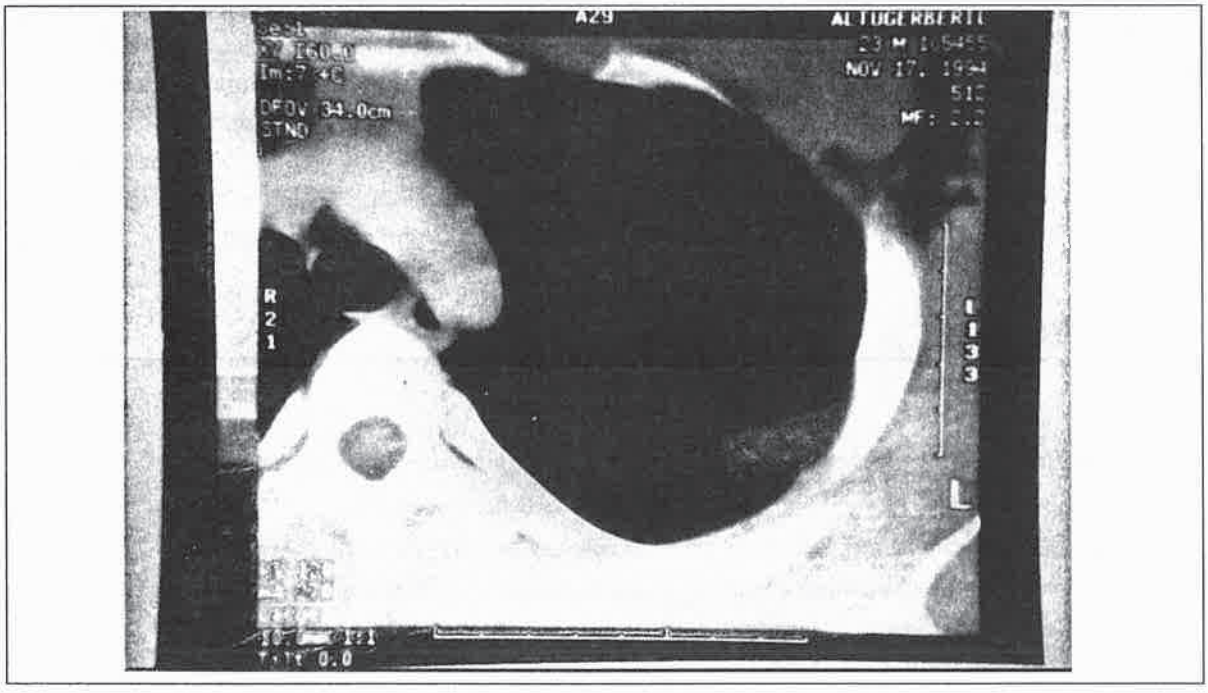

Figure 1. CT scan revealing a pleural-based mass in the left hemithorax

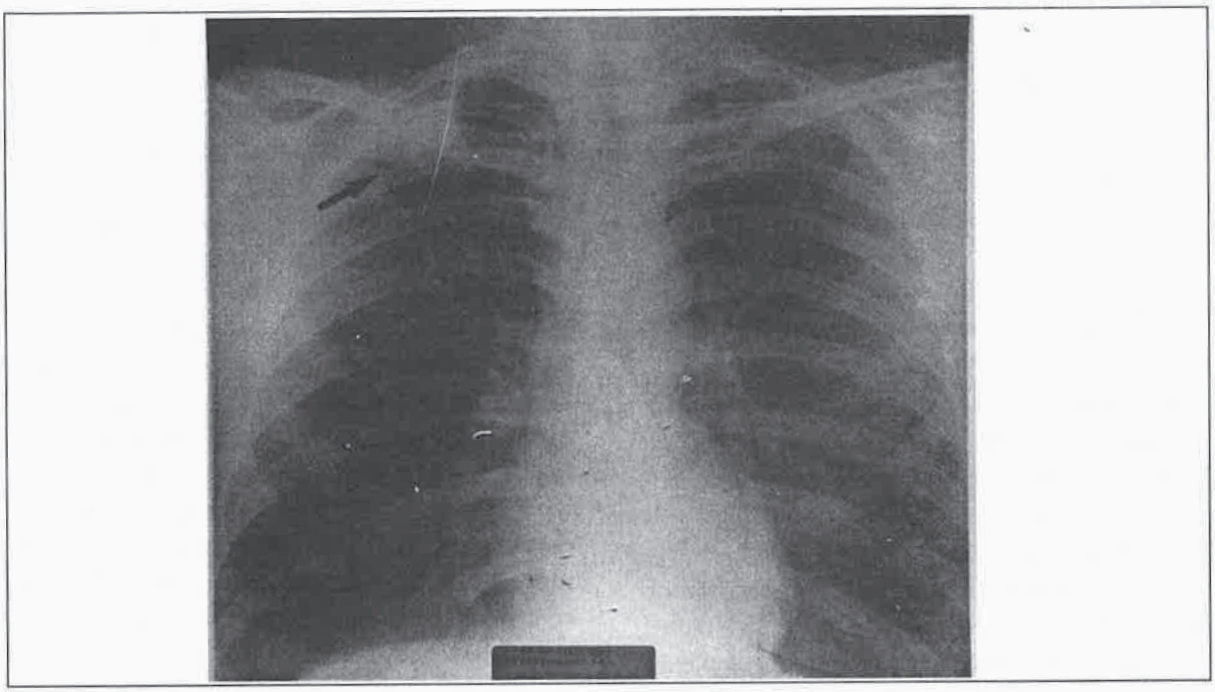

Figure 2. Chest X-ray showing a homogenous mass density (arrow) in the right upper lung field

the pleura and enlarge towards the pleural space and extrapleural area. They are mostly located beneath the parietal pleura and sometimes visceral (4) or diaphragmatic pleura (5). Pleural lipomas possess a more irregular configuration and tend to be less well-circumscribed than superficial lipomas. Their contours are usually determined by the spaces they occupy, but they may

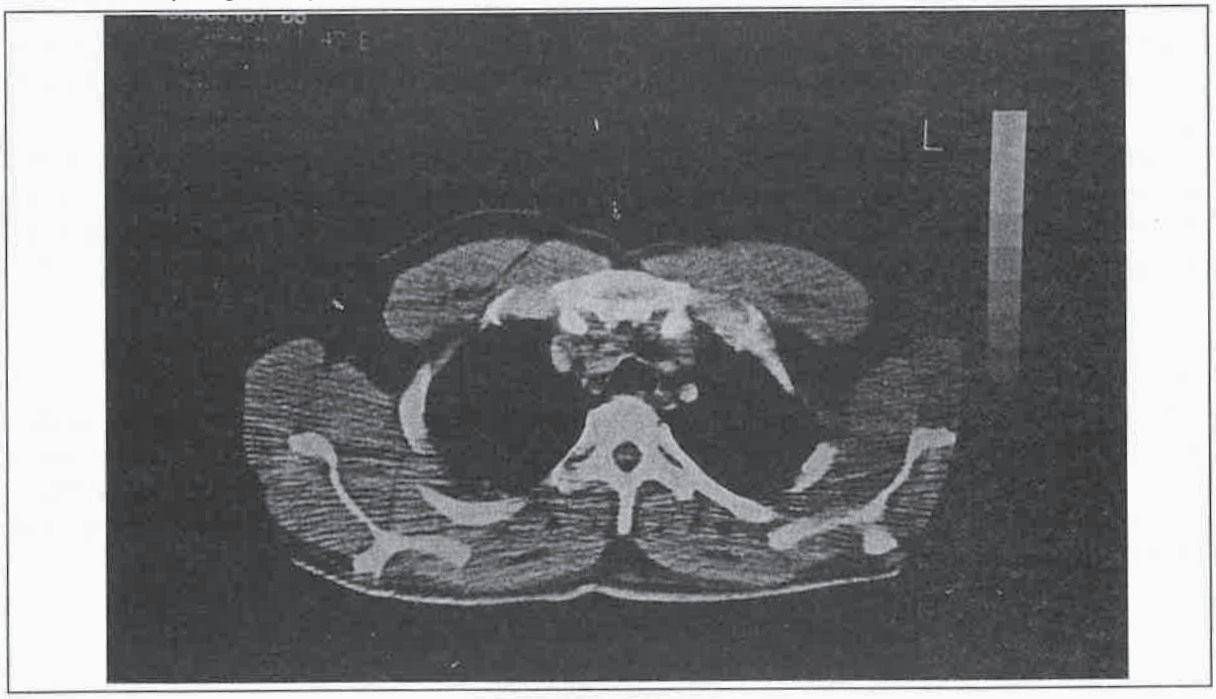

Figure 3. CT scan showing a peripherally located tumor, highly suggestive of pleural origin with fatty tissue density (-123 H.U.)

have areas of projection into the surrounding fatty tissues (2).

Pleural lipomas are usually discovered on routine chest films as asymptomatic masses. They may produce symptoms in the case of pressure to the contagious structures such as heart, lung or chest wall. Our second case featured chest-wall pain that revealed no involvement of the bony structure and was possibly the result of nerve compression.

On chest radiographs, pleural lipomas present themselves as well-circumscribed areas of increased density, in contrast to lung. They may also contain punctate or linear calcifications. Bone erosion, cortical thickening and hyperosteosis of the ribs caused by extrinsic pressure of the tumor may exist, depending on the size of the tumor (6). It has been noted that localized pleural tumors are often pedunculated, rendering these tumors mobile. Hence, marked changes in shape and density of the mass will occur on comparable projections. Recognition of pedunculation indicates with certainty that a mass is of pleural origin (7). Both of our cases were non-pedunculated tumors.

CT shows a well-defined mass of homogeneous fat density (between -50 and -150 H.U.) at obtuse angles with the chest wall and displacing adjacent pulmonary parenchyma and vessels (6,8). Pleural lipomas can be distinguished from other lipid-containing entities such as thymolipomas, angiolipomas, fibrolipomas and teratomas by their homogeneous density and lack of soft tissue islands interspersed within the fat tissue. Differential diagnosis with liposarcomas is based on the facts that liposarcomas are rarely located in the thoracic cavity and are usually large, symptomatic and infiltrative heterogeneous tumors with attenuation coefficients greater than -50 H.U. (9). Magnetic resonance imaging might be helpful in the diagnosis as well as in differential diagnosis from liposarcoma (10).

Preoperative diagnosis still remains difficult. Percutaneous needle biopsy may be of benefit, but is sometimes unyielding (1). CT may be useful for accurate diagnosis, if specific criteria are met (9). In our cases, CT showed both of the tumors had a density consistent with adipose tissue. However, it was necessary to confirm the benign nature of the lesion; therefore, we performed a thoracotomy. If the tumor has a significantly unclear capsule, a wider excision including the surrounding intercostal muscles is recommended (11). In our cases, the tumors were well-demarcated; and wider excision was not necessary. Patients with limited cardiopulmonary reserve may undergo videothoracoscopic excision (12).

Lipomas differ little in microscopic appearance from surrounding fat tissue. Like fat, they are composed of mature fat cells, but the cells vary slightly in shape and size, being somewhat larger, measuring up to 200_ in diameter. Occasionally, secondary changes may occur as the result of impaired blood supply, traumatic injuries such as infarction and hemorrhage, and calcification or cyst-like changes (2). In our cases, secondary changes were not prominent.

Although, deep-seated lipomas have a greater tendency to recur, presumably because of the difficulty of complete surgical removal (2), no report of recurrence in pleural lipomas has appeared in the presented cases to date.

In conclusion, lipomas should be considered in the differential diagnosis of pleural tumors. CT and needle biopsy may be helpful in the diagnosis, but are not always adequate for confirming the final diagnosis. Total excision of the tumor enables both histologic diagnosis and surgical treatment in pleural lipomas.

REFERENCES

1. Politis J, Funahashi A, Gehlsen JA, Decock D, Stengel BF, Choi Hongyung. Intrathoracic lipomas. J Thorac Cardiovasc Surg. 1979; 77:550-6.
2. Enzinger FM, Weiss SW. Benign lipomatous tumors. In: Soft Tissue Tumors. 3rd ed. St. Louis: Mosby, 1995:384-9.
3. Corbi P, Boufi M, Thierry G, Menu P. Giant pleural lipoma. Eur J Cardio - Thorac Surg. 1999; 16:249-50.
4. Naccarato AG, Viacava P. Visceral pleura lipoma: a previously undescribed localization and review of the literature on pleural lipomas. Pathologica. 1998; 90:298-301.
5. Eyck EAT. Subpleural lipoma. Radiol. 1960; 74:295-7.
6. Buxton RC, Tan CS, Khine NM, Cuasay NS, Shor MJ, Spigos DG. Atypical transmural thoracic lipoma: CT Diagnosis. J Computer Asisted Tomography. 1988; 12:196-8.
7. Berne As, Heitzman ER. The roentgenologic signs of pedunculated pleural tumors. Amer J Roentgenol Rad Ther and Nuclear Med. 1962; 87:892.
8. Epler GP, Mcloud TC, Munn CS, Colby TV. Pleural lipoma: Diagnosis by computed tomography. Chest 1986; 90:265-8.
9. Storey TF, Narla LD. Pleural lipoma in a child - CT evaluation. Pediatr Radiol. 1991; 21:141-2.
10. Matsumoto K, Hukuda S, Ishizawa M, Chano T, Okabe H. MRI findings in intramuscular lipomas. Skeletal Radiol 1999; 28:145-52.
11. Tokitsu K, Tachibana S, Kawakami M, et al. Two surgical cases of intrathoracic lipoma. Kyobu Geka. 1999; 52:251-3.
12. Furrer M, Inderbitzi R. Case report: endoscopic resection of a 5 cm intrathoracic lipoma. Pneumologie 1992; 46:334-5

JOURNAL OF ANKARA MEDICAL SCHOOL Vol 23, No 2, 2001 149-153

SPOROTRICHOID LEISHMANIASIS

Pelin K. Ekmekçi* ✣ Rana Anadolu* ✣ Tuğba Oskay ✣ Erbak Gürgey*

SUMMARY

Although cutaneous leishmaniasis having sporotrichoid pattern has been increasing in the United States since 1970, it is still very few reported in the Middle East. This form of the disease is mostly caused by Leishmania Brasiliensis and the sporotrichoid presentation is thought to be due to the lymphatic spread of the infection. Endemic tropical patogens like cutaneous leishmaniasis should be considered in the differential diagnosis of any chronic skin lesion resembling sporotrichoid pattern especially in a person who has been in an endemic area.

Key words *: Sporotrichosis, Cutaneous Leishmaniasis.*

We present a patients with wtaneous Leishmaniasis with a Sporotrichoid pathern.

ÖZET

SPOROTRİKOİS LEISHMANİASİS

Sporotrikoid klinik gösteren kutanöz leishmaniasis 1970'lerin sonundan itibaren özellikle Amerika'da çok sayıda bildirilmiş olmakla birlikte bu sayı Ortadoğu'da oldukça azdır. Yapılan araştırmalarda bu tablonun genellikle Leishmania Brasiliensis tarafından oluşturulduğu ve infeksiyonun lenfatiklere yayılımı sonucu meydana geldiği saptanmıştır. Özellikle endemik bölgelerde bulunan ve belirli bir inkübasyon periyodunu takiben oluşan sporotrikoid patterndeki lezyonlar sporotrikozis dışında endemik tropikal patojenleri de akla getirmelidir.

Anahtar kelimeler: *Sporotrikozis, Kutanöz Leishmaniasis.*

CASE REPORT

A 52 years old male admitted to our clinic for nodular lesions with central ulceration sited on the flexural surfaces of his right wrist. He had a history of a traffic accident during which many spines pricked his wrist where the first nodular lesion developed shortly after. Two new lesions followed this first nodule and they all became ulcerated approksimately in a month.

On his dermatological examination three nodular lesions with central ulceration, red to violaceus in color were revealed on the flexural surfaces of his right wrist. The lesions were arrranged in a lineer presentation typically parallel to the lymphatic drenaige resembling sporotrichoid pattern (Fig1). There were no axilllary or epitrochlear palpable lymph nodes and further physical examination revealed no other pathological findings.

Routine laboratory parameters including complete blood cell count, serum chemistry and electrolytes were all within normal limits.

The diagnosis of sporotrichosis, leishmaniasis and deep fungal infections were suggested clinically and a biopsy was taken from his first lesion

Ankara University, Faculty of Medicine Department of Dermotology

Received: Aug 23,2000 Accepted: Oct 23,2000

Fig 1. Multiple nodular lesions on the flexural surface of the right wrist.

Dermatopathological examination of the biopsy material stained with hematoxylen eosin showed pseudoepiteliamateous hyperplasia, spongiosis, neutrophilic cell foci and heamoragic crust formation in the epidermis. There was a dense inflamatuar cell infiltration composed of large histiocytes forming nodular foci and many mononuclear cells around these nodules. There were clusters of basophilic granules within the cytoplasm of the dermal macrophages and around the neutrophilic foci in the epidermis. These granules were established to be leishmania microorganisms (Fig 2). The smear obtained from the edge of the ulcerated nodule also demonstrated abundant organisms within the histiocytes and free in extracellular location (Fig 3).

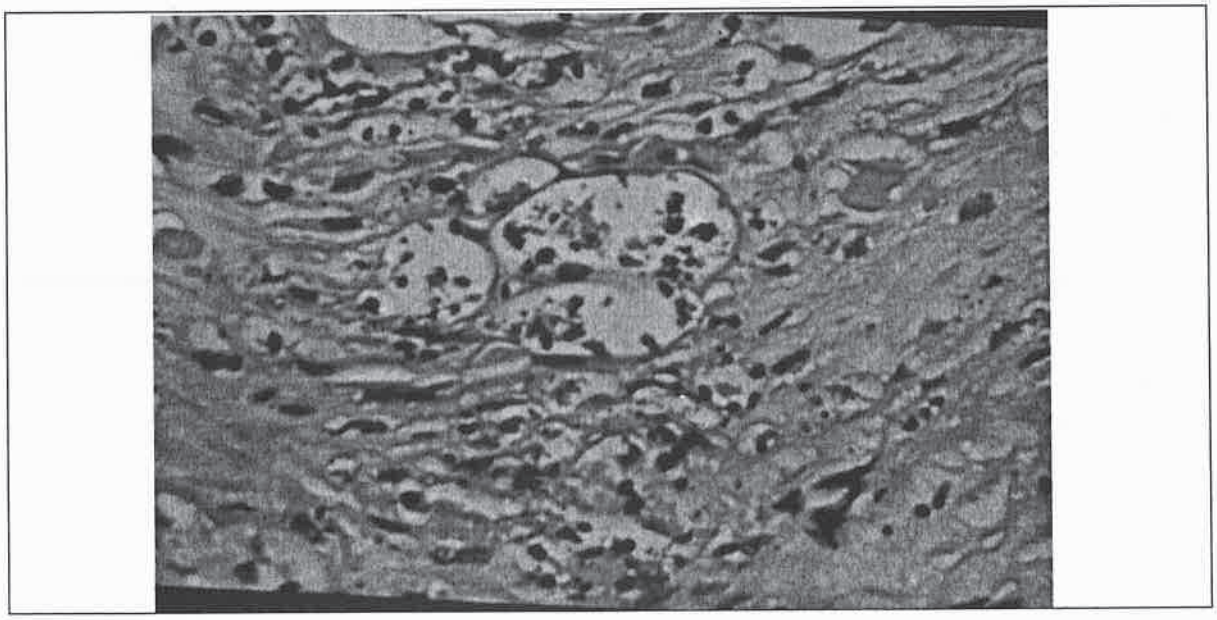

Fig 2. Clusters of basophilic granules within the cytoplasm of dermal macrophages.

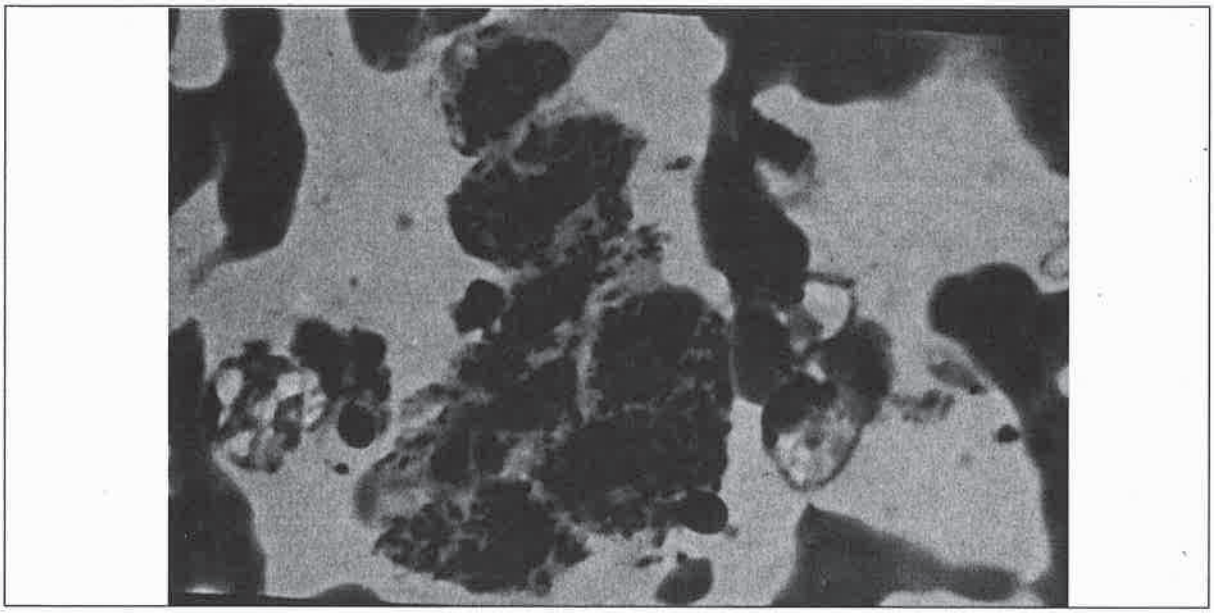

Fig 3. The smear demonstrating abundant amount of organisms within the histiocytes.

According to these findings, the diagnosis of sporotrichoid leishmaniasis was given to the patient as he had clinical similarities with sporotrichosis but dermatopathologic proof of leishmaniasis.

DISCUSSION

Cutaneous leishmaniasis is an endemic disease in the central and south America, Middle East and in most parts of tropical and subtropical Africa and Asia. The parasites are transmitted by the bite of ground dwelling sand flies. Between 2 to 24 weeks later, a small nodule appears at the inoculation site that usually evolves into a well-demarcated ulcer. Satellite lesions can appear around the original lesion. Although regional lymhadenopathy occasionally develops, systemic symptoms rarely occur (1,2).

The classical clinicopathologic picture of cutaneous leishmaniasis is variable and depends upon many factors, including host-parasite interactions. The lesions typically appear on exposed areas of the body where inoculation occurs. In the acute form, the disease begins as a small erythematous papule, which may appear immediately after the bite of the sand fly but usually 2 to 4 weeks later. The papule slowly enlarges in size over a period of several weeks. This is then followed by central softening and possible ulceration. Healing begins in the center of the ulcer, leaving behind a permanent depressed and disfiguring scar. In the chronic form, the lesions, if multiple, may be symmetric and do not ulcerate but follow a chronic indolent course. In the recidivan type on the other hand papules similar to those described in the acute phase appear around the preexisting scar of the primary lesion (2).

Except these classical forms of leishmaniasis there has also atypical, rare cases been reported in the last several decades including sporotrichoid leishmaniasis (3,4,5).

Cutaneous leishmaniasis is one of the several disorders that may resemble sporotrichosis. There are also cases of tuberculosis, syphilis, cat-scracth disease, localized pyogenic infections, tularemia, deep fungal infections and atypical mycobacterial infections which has presented in a sporotrichoid pattern (1). The diagnosis of cutaneous leishmaniasis depends on finding parasites. The organisms may be identified in smears or in tissue sections, or cultured. The lesions should be carefully and repeatedly cleaned

before aspiration and biopsy. An aspirate and biopsy specimen should be taken from the margin of the lesion. The most effective method is detecting parasites in tissue smears stained with a Wright-Giemsa preparation, or alternatively Leishman bodies may be seen within enlarged histiocytes in histopathological sections stained with H&E. Aspirates and biopsy materials can also be cultured in Novy-Mac Neal-Nicolle biphasic medium, since amastigotes may be sparse, particularly if the lesion is long-standing (2,5).

Since our patient was not in an endemic area, and the lesions occured in the spike-bitten localization during a trauma, and presented in a linear pattern, parallel to the lymphatic drainage, it was thought to be sporothricosis clinically, however typical dermatopathologic findings of the biopsy material revealing leishmania microorganisms confirmed the diagnosis of cutaneous leishmaniasis.

REFERENCES

1. Jay R. Kostman, Mark J. DiNubile: Nodular lymphangitis: A distinctive but often unrecognised syndrom. Ann. Int. Med. 118;883-888,1993
2. Thomas B. Fitzpatrick, Arthur Z. Eisen, Klaus Wolff, Irwın M. Freedberg. Dermatology in general medicine. 4th Edit., Mc Graw Hill Inc., United States of America. 2772-77,1993.
3. 1993Abdul-Ghani Kibbi, Paulette G. Karam, Amal K. Kurban: Sporotrichoid leishmaniasis in patients from Saudi Arabia ; Clinical and histologic features. J. Am. Acad. Deratol. 17; 759-64,1987.
4. Kerdel- Vegas F.: American Leishmaniasis. Int. J. Dermatol. 21;291-303, 1982.
5. James P. Willems, Suzanne M. Schmidt, Henneth E. Greer, Calvin O. McCall et al. Sporotrichoid cutaneous leishmaniasis in a traveler. South. Med. J. 90;325-327,1997.

JOURNAL OF ANKARA MEDICAL SCHOOL Vol 23, No 2, 2001 155-160

A CASE OF EPIDERMOLYSIS BULLOSA ACQUISITA WITH A STRIKING CLINICAL RESEMBLANCE TO BULLOUS PEMPHIGOID

Hatice Şanlı* ✣ Rana Anadolu* ✣ Ayşe Boyvat* ✣
Erdinç Terzi* ✣ Erbak Gürgey* ✣ Mine Erbil** ✣ Ruhser Başer**

SUMMARY

In 1994, a 41 - year - old woman presented with multiple erosions and blisters on the oral mucosa, trunk and extremities for one week. A biopsy specimen showed a subepidermal cleft with an inflammatory infiltrate consisting mainly of neutrophils and eosinophils in the upper dermis. Immunohistochemistry revealed linear deposits of IgG and C3 at the dermal - epidermal basement zone. Treatment with 80 mg prednisolone and 150 mg azathioprine was initiated with the diagnosis of bullous pemphigoid. In 1995, the patient complained of difficulty in swallowing solid food. Oesophagoscopy revealed multiple erosions and a web - like stenosis of the upper oesophagus. At that time, the skin lesions were not associated with trauma, showed no scarring and milia formation was not noted. In June 1999, the patient presented with bullous lesions over areas of trauma, scarring from previous lesions and milia formation. The diagnosis of epidermolysis bullosa acquisita was confirmed by NaCl split skin and electron microscopy that revealed blister formation beneath the lamina densa of the basement membrane zone. This report highlights the similarity between the clinical, dermatopathologic and immunohistochemical findings of epidermolysis bullosa acquisita and bullous pemphigoid and the need for electron microscopic or modern immunologic investigations in the diagnosis of bullous diseases.

Key words: *Bullous Pemphigoid, Epidermolysis Bullosa Acquisita.*

ÖZET

41 yaşında bayan hasta 1994 yılında bir hafta önce başlayan oral mukoza, gövde ön - arka yüzü, üst ve alt ekstremitelerin distal kısmında yaygın erode alanlar ve eritemli zeminde gelişen büllöz lezyonlar şikayetiyle kliniğimize başvurdu. Alınan deri biopsisinin dermatopatolojik incelemesinde subepidermal bül oluşumu, üst dermiste nötrofil ve eozinofillerden oluşan infiltrasyon saptandı. Perilezyoner deriden yapılan immunhistokimyasal incelemelerde dermoepidermal bileşkede lineer Ig G ve C 3 depolanması belirlendi. Hastaya büllöz pemfigoid tanısıyla 80 mg prednizolon ve 150 mg azathioprine baslandı. 1995 yılında hastada katı gıdalara karşı disfaji gelişti. Yapılan özefagoskopide, özefagus üst kısmında web benzeri stenoz ve multiple erozyonlar saptandı. Haziran 1999'da hastada oral mukoza, gövdede, üst ve alt ekstremitede travma sonrasında gelişen büllöz lezyonlar ve erode alanların yanısıra iyileşen lezyonların üzerinde milia formasyonu ve skatris gözlendi. Elektron mikroskobu ve NaCl split skin incelemesiyle bazal membran bölgesinde sublamina densada bül oluşumunun gösterilmesiyle epidermolizis bülloza acquisita tanısı konuldu. Epidermolizis bülloza ve büllöz pemfigoidin klinik, dermatopatolojik ve immunhistokimyasal bulgularının benzer özellik göstermesi nedeniyle bu iki hastalığın ayırıcı tanısında elekron mikroskopisi ve modern immunolojik incelemelere gereksinim duyulmaktadır.

Anahtar kelimeler: *Büllöz Pemfigoid, Epidermolizis Bülloza.*

Epidermolysis bullosa acquisita (EBA) is a subepidermal blistering disease characterized by autoantibodies specific for type VII collagen which is specifically localized to anchoring fibrils of the basement membrane zone (1). Typical clinical features of EBA include skin fragility, ero-

*Department of Dermatology, Ankara University Faculty of Medicine, Ankara, Turkey.

**Department of Anatomy, Hacettepe University Faculty of Medicine, Ankara, Turkey.

Received: Aug 15,2000 Accepted: Oct 23,2000

sions, and bullous lesions that heal with scarring and milia. EBA and bullous pemphigoid (BP) are both chronic bullous disorders of the skin characterized by linear deposition of IgG and C3 along the basement membrane zone. Differential diagnosis of EBA and BP may be difficult because of the similarity of the clinical features, histopathologic and immunohistochemical findings. In this report we present a case of an EBA with clinical, dermatopathologic and immunohistochemical findings similar to BP and in whom definitive diagnosis of EBA was made by NACl split skin and electron microscopic studies. The subepidermal separation was within the lamina densa of the basal membran zone. Ig G deposition was on the dermal side of the NACl split skin substrate.

CASE REPORT

In October 1994, a 41 - year - old woman presented with multiple erosions on the oral mucosa, and blisters that arise on erythemathous skin on trunk and distal parts of upper and lower extremities for one week (Figure 1).

A biopsy specimen showed a subepidermal cleft with an inflammatory infiltrate consisting mainly of neutrophils and eosinophils in the upper dermis. Immunohistochemistry revealed linear deposits of IgG and C3 at the dermal - epidermal basement zone. Treatment with 80 mg prednisilone and 150 mg azathioprine was initiated with the diagnosis of bullous pemphigoid. Disease activity decreased, however psychosis due to prednisolone therapy was noted and new lesions developed with the reduction of the prednisolone dosage. After seven months, the patient complained of difficulty in swallowing solid food. Oesophagoscopy revealed multiple erosions and a web - like stenosis of the upper oesophagus. At that time, skin lesions were not associated with trauma, showed no scarring and milia formation. Dapsone 100 mg / day was initiated in combination with the prednisilone - azathioprine treatment. The therapy proved initially successful, but dapson could not be administered in full dose because of methemoglobuliemi, that occured each time the drug was administered and after two months dapsone therapy had to be discontinued. Sulphamethoxypridine, tetracycline and nicotinamide therapies all proved ineffective. After two years, the patient presented with bullous lesions and erosions on oral mucosa, trunk, upper and lower extremities (Figure 2, 3).

Bullous lesions were associated with trauma and scarring from previous lesions and milia formation was prominent. A biopsy was taken with the clinical diagnosis of EBA. Dermatopathologic examination of the biopsy specimen revealed

Figure·1: In 1995 the patient presented with tense bullous lesions on an erythematous base.

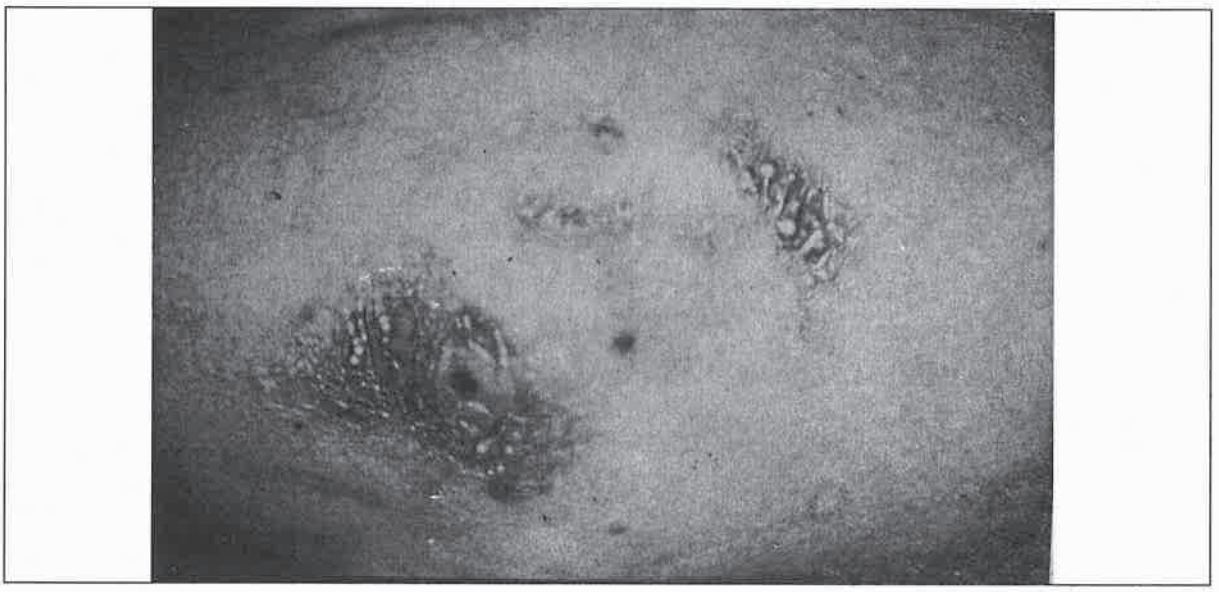

Figure 2: Milia formation and scaling on the elbow.

subepidermal cleft with an inflammatory infiltrate consisting mainly of neutrophils and eosinophils in the upper dermis (Figure 4).

Immunohistochemical evaluation of the biopsy taken from the perilesional skin revealed linear IgG and C3 deposition. Since these immunohistochemical findings are identical in EBA and BP, and the clinical findings of our patient were consistent with EBA, electron microscopic evaluation and NACl split skin test were carried out. The subepidermal separation was within the lamina densa of the basal membran zone. Ig G deposition was on the dermal site of the NACl split skin substrate (Figure 5).

Laboratory investigations for urinanalysis and blood chemistry were normal. Full blood count showed values of Hb: 9,2 gr / dl (12 - 16 gr / dl) and Htc: 28.3 (% 37 - 47). Erythrocyte sedimentation rate was 38 mm / h. Serum iron level was 17 ug / dl (50 - 150 ug / dl), serum total iron bind-

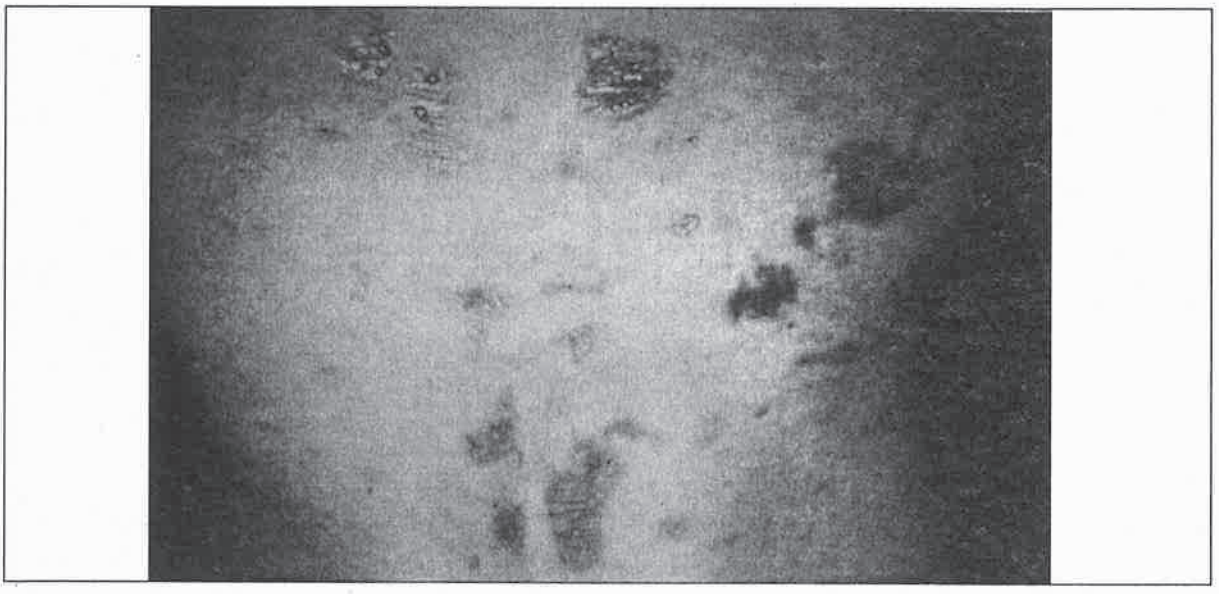

Figure 3: Milia formation and scaling on the lumbosacral area.

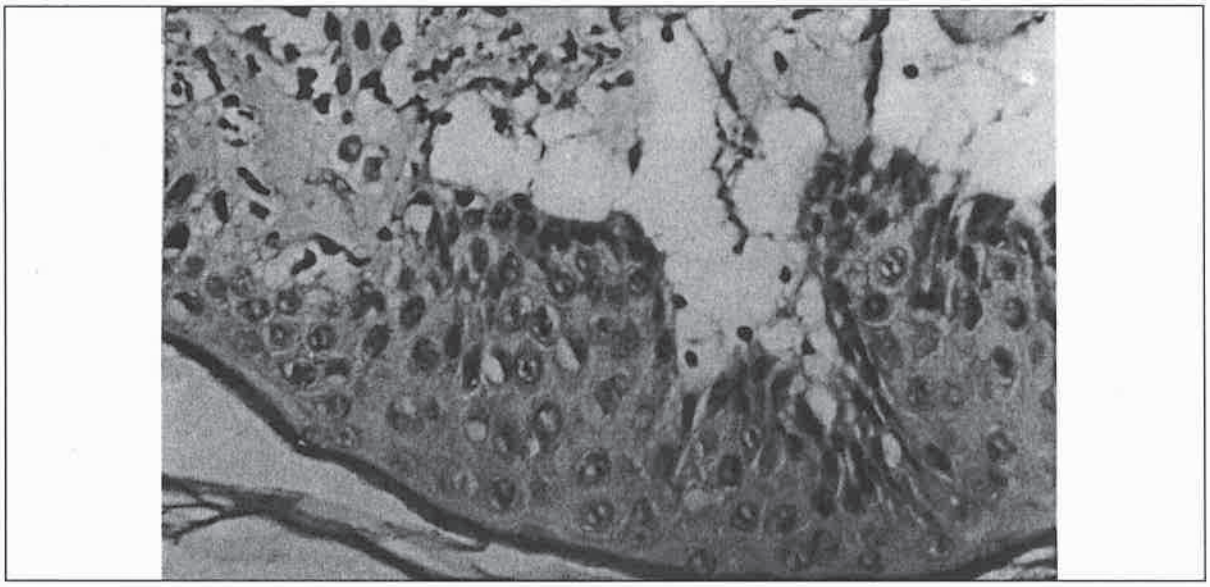

Figure 4: Subepidermal bullae formation, with many neutrophils, nuclear dust and eosinophils within the papillary dermis (HE, X 400).

ing capacity was 278 ug / dl (250 - 410 ug / dl), transferrin saturation was % 6 (% 20 - 55) and ferritin level was 12,5 ng / ml (18 - 370 ng / ml). Stool examinations for occult blood and parasites were negative. Viral markers for hepatitis and ANA were negative. Thyroid function tests and immunologic tests were normal. Urine analysis for Bence - Jones protein was negative. Tumor markers were normal except Ca 19 - 9. Toracoabdominal CT showed two hemanjiomas of 2 cm diameter localized in the right lob posterior of liver. Mammography revealed two low density noduler opacities, both 6 mm in diameter in superior medial quadrant of left mammary gland. Thin needle aspiration biopsy from these lesions showed cystic mammopathy. The patient is currently being followed up by medical oncology department for elevated Ca 19 - 9 levels.

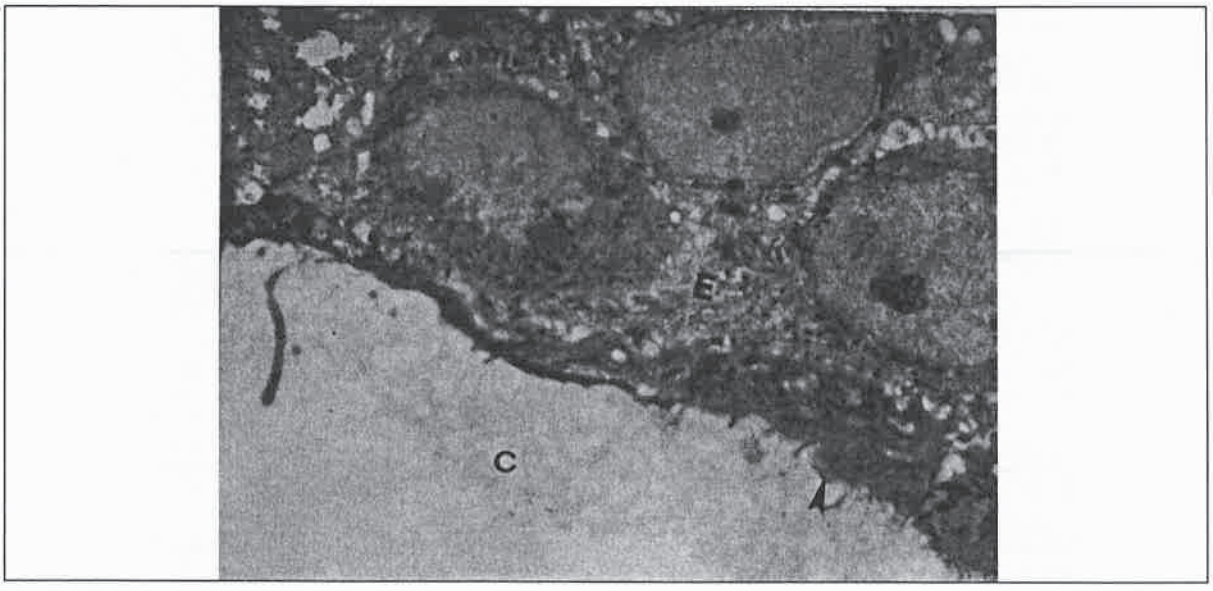

Figure 5: C; Bullae cavity, E; Epidermal keratinocyte, Sublamina densa of BMZ.

DISCUSSION

Epidermolysis bullosa acquisita (EBA) is a chronic bullous disease characterized by autoantibodies specific for type VII collagen that is specifically localized to anchoring fibrils of the basement membrane zone. Because of the similarities in the clinical features, EBA must be differentiated from other subepidermal bullous diseases such as bullous pemphigoid, cicatricial pemphigoid, Brunsting - Perry cicatricial bullous pemphigoid, bullous SLE and porphiria cutanea tarda. Cicatricial pemphigoid resembles EBA in that both diseases are associated with mucosal involvement and both present with lesions that heal with scarring. Dermatopathologic findings of cicatricial pemphigoid are subepidermal bullae formation, inflammatory infiltrate in the dermis composed of mononuclear cells, histiocytes and plasma cells, and in late stages, fibroblast proliferation and fibrosis. Direct immunofluorescence findings are similar to the findings of EBA, but electron microscopic investigation reveals seperation within the lamina lucida. Even though our patient has cicatricial pemphigoid - like clinical presentation with mucosal involvement and web - like stenosis of the oesophagus, EM findings distinguished these diseases. Some authors suggest that Brunsting - Perry cicatricial bullous pemphigoid may represent a clinical variant of EBA, since immuno - electron microscopic examination of both diseases show linear IgG and C3 deposition below the lamina densa, but the lesions of Brunsting - Perry cicatricial bullous pemphigoid are localized (2). Our patient has clinical similarities with porphyria cutanea tarda due to the acral distribution of the lesions located on the extremities and milia formations, but photosensitivity was not noted in our patient, bullous lesions were also present on the oral mucosa and DIF showed findings consistent with EBA, while deposition of IgG and C3 in the vessel walls was not found. Bullous SLE and EBA both are characterized by autoimmunity to type VII collagen, but bullous SLE may be differentiated from EBA by ANA, anti-ds DNA, lupus band test and ARA criteria. Bullous pemphigoid, which is one of the diseases that present the greatest diagnostic problems, is characterized by bullous lesions which appear on normal skin or on erythemathous bases which heal without scarring. BP - like clinical presentation has been reported in as many as 50 % of patients with EBA (3). Even though the clinical manifestations of EBA may mimic BP, some of these evolve into a more typical mechanobullous picture later in the course of the disease. It may not be possible to distinguish EBA and BP according to dermatopathologic and DIF findings, because both diseases present with subepidermal bullae formation and in both diseases DIF examination reveals linear IgG , C3 and occasionally IgA and IgM deposition along the basement membrane zone. Because of the identical clinical, dermatopathologic and DIF findings, the use of electron microscopy and immun electron microscopy may be needed to discriminate these diseases. Electron microscopic examination reveals cleavage at the lamina lucida in BP, whereas cleavage is in the sublamina densa in EBA. Immun electron microscopy shows IgG antibodies that bind to anchoring fibrils within the sublamina densa in patients with EBA. On the other hand the deposits in BP are higher up in the hemidesmosome area or lamina lucida.

Since the initial bullous lesions of our patient occurred on erythemathous bases and DIF examination revealed linear IgG and C3 along the BMZ, a misdiagnose of BP was made. However, later in the course of the disease due to the bullous lesions over traumatized areas which healed by milia and scarring, the patient was reevaluated and the clinical diagnoses of EBA was confirmed by EM, which revealed separation in the sublamina densa. Immun electron microscopy could not be performed because of technical inadequacies.

In our patient a web - like stenosis of the upper oesophagus was detected. Even though esophageal pathology is common in dystrophic

forms of epidermolysis bullosa, esophageal involvement is not a typical finding of EBA. Recently a few cases EBA with esophageal involvement is reported (4, 5) and it seems to be a new association, also indicating the great clinical heterogeneity of the disease.

A number of reports published in the literature indicate that EBA may be associated with a number of systemic diseases such as systemic lupus erthematosus, autoimmune tyroiditis, inflammatory bowel disease, multiple endocrinopathy syndrome, rheumatoid arthritis, thymoma, diabetes and others. No associated systemic disease was detected in our patient (1).

EBA is a very difficult disease to treat. The classical mechanobullous form of EBA is usually resistant to various treatment modalities such as high dose corticosteroids, azathioprine, methotrexate and cyclosporine. On the other hand, the inflammatory form of EBA which is more reminiscent of BP than a mechanobullous disorder, may respond to the treatments listed above and also improve on dapsone. Colchicine may also be beneficial. The refractory cases may respond to high dose intravenous immunglobulin (6, 7). In our case, even though good result was obtained with dapsone therapy, effective doses could not be administered because of methemoglobinemia.

In subepidermal bullous diseases, which share clinical, dermatopathologic and DIF findings, EM and Immun EM should be performed early in the course of the disease, in order to initiate the effective therapies as soon as possible and to minimize the possible complications, especially in diseases such as EBA which has a high potential for scarring.

REFERENCES

1. Epidermolysis bullosa acquisita. Fitzpatrick TB, Eisen AZ, Wolff K, Feedberg IM, Austen KF eds. Dermatology in General Medicine, 5th ed. New york McGraw Hill Inc 1999; 702 - 709.
2. Brunsting - Perry cicatricial bullous pemphigoid: A clinical variant of localized acquired epidermolysis bullosa ? Joly P, Ruto F, Thomine E, et al. J Am Acad Dermatol 1993; 28: 89 - 92.
3. Bryan K. Pang, Y . S . Lee, K . V . Ratnam. Floor - pattern salt - split cannot distinguish bullous pemphigoid from epidermolysis bullosa acquisita. Arch Dermatol 1993; 129 : 744 - 746.
4. Sachiko Miyagawa, Takashi Iıda, Hiroshi Hachisuka. Epidermolysis bullosa acquisita with oesophageal stenosis. Br J Dermatol 1992; 127: 172 - 176.
5. Weinman D, Steward MI, Woodley DT, et al. Epidermolysis bullosa (EBA) and oesophageal webs: a new association. Am J Gastroenterol 1991; 91: 1518 - 1522.
6. Epidermolysis bullosa acquisita: Efficacy of high - dose intravenous immunoglobulins. Meier F, Sönnichsen K, Schaumburg - Lever G, et al. J Am Acad Dermatol 1993; 29: 334 - 337.
7. Intravenous immunoglobulin treatment in therapy - resistant epidermolysis bullosa acquisita. Kofler H, Wambacher - Gasser B, Topar G, et al. J Am Acad Dermatol 1996; 34: 331 - 335.

JOURNAL OF ANKARA MEDICAL SCHOOL Vol 23, No 2, 2001 161-166

THE USE OF ULNAR ISLAND FLAP FOR COVERAGE OF A DORSAL HAND SKIN DEFECT*

M. Erol Demirseren** ❖ Serdar Gökrem** ❖ O. Murat Özdemir** ❖ Zeki Can**

SUMMARY

Ulnar island flap is a modification of the standard dorsal ulnar artery flap that has been used successfully in the reconstruction of medium-sized wrist defects. In this report, we present the use of ulnar island flap with a greater arc of rotation for the coverage of a large-sized dorsal hand skin defect.

Key Words: *Ulnar Island Flap, Dorsal Hand Skin Defect*

ÖZET

ULNAR ADA FLEBİ

Ulnar ada flebi standart dorsal ulnar arter flebinin bir modifikasyonudur. Orta büyüklükteki el bileği defektlerinin onarımında başarılı olarak kullanılmıştır. Bu yayında bu flebin daha büyük bir rotasyon arkı ile geniş bir el dorsumu defektinin onarımı için kullanımı sunulmuştur.

Anahtar Kelimeler: *Ulnar Ada Flebi, El Dorsumu Defekti*

There are many methods available for the reconstruction of dorsal hand skin defects. If the paratenon is intact, skin graft coverage is the most suitable method. However, in the case of tendon and bone exposure, flaps must be used. To minimize morbidity, single-staged flap reconstructions such as posterior interosseous flap, reverse radial forearm flap and free flaps are preferred (1). A relatively seldom-used ulnar flap was first described by Becker and Gilbert (2). This flap is supplied by the dorsal branch of the ulnar artery and associated veins. It is a technically simple but reliable flap that provides good-quality coverage for medium-sized skin defects of the wrist (2). In this report, island modification of this flap to cover a large-sized dorsal hand skin defect is presented.

Surgical Anatomy

The pedicle of the ulnar island flap is the ascending branch of the dorsal branch of the ulnar artery. This artery originates between 2-5 cm proximal to the psiforme and branches in two as it passes medially beneath the flexor carpi ulnaris tendon in an oblique line from volar surface to the dorsoulnar surface of the distal forearm. The proximal branch enters the flexor carpi ulnaris muscle and the distal branch enters the psiforme and anastomoses with the dorsal carpal arc. When it reaches the deep fascia, it gives off ascending and descending branches (3). After passing between the ulnar crest and the posterior border of the flexor carpi ulnaris muscle, the ascending branch divides into multiple ramifications, nourishing a large area of skin on the ulnar side of the forearm (Figure 1) (4).

**This report appeared as a poster at the XXI. National Plastic, Reconstructive and Esthetic Surgery Congress*

***Ankara University Medical School, Department of Plastic and Reconstructive Surgery Ankara, Turkey*

Received: Aug 11,2000 Accepted: Oct 26,2000

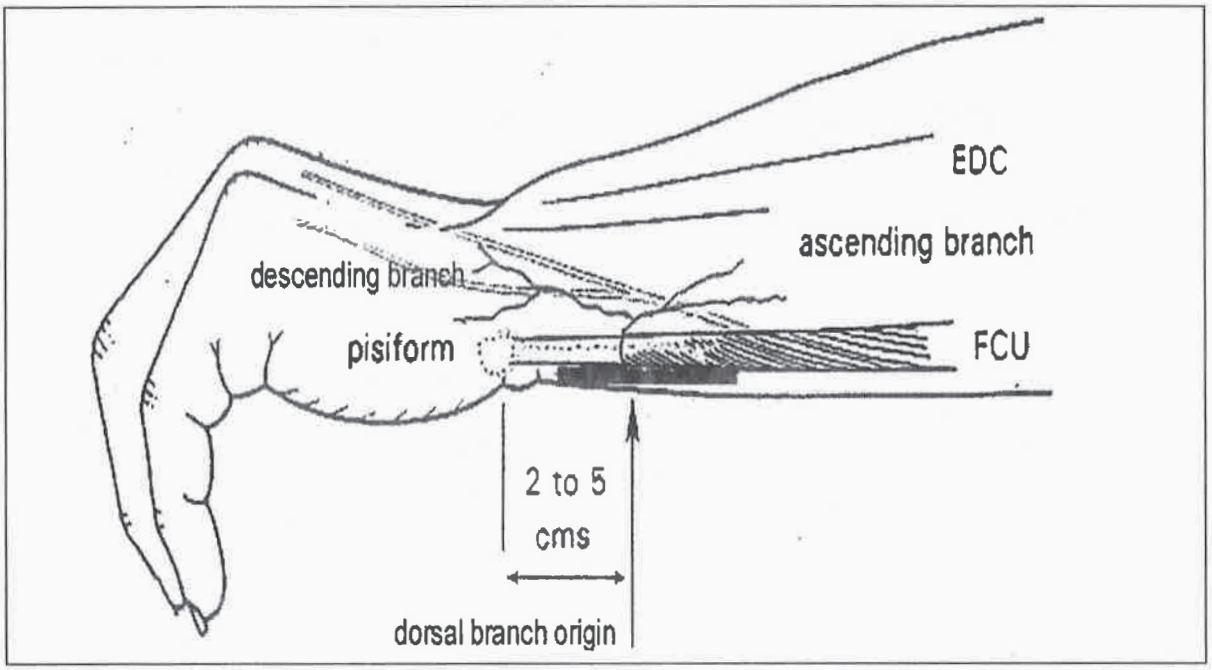

Figure 1: Schematic illustration of dorsal ulnar artery and its terminal branches (Modified by Cormarck GC, Lamberty BGH: The Arterial Anatomy of Skin Flaps. 2nd edition, Edinburgh, Churchill Livingstone, 1994).

Case Report

A 75-year-old man presented with a 3x3 cm squamous cell carcinoma on the dorsum of the hand (Figure 2). A surgical excision with a 1.5 cm margin including skin and paratenon was made (Figure 3). An island ulnar flap measuring 6.5x6.5 cm was designed on the skin territory of the ascending branch (Figure 4). The dorsal branch of the ulnar artery was localized as it emerged under the flexor carpi ulnaris tendon 4 cm proximally to the psiforme bone. The flap was incised through skin and subcutaneous tissue down the

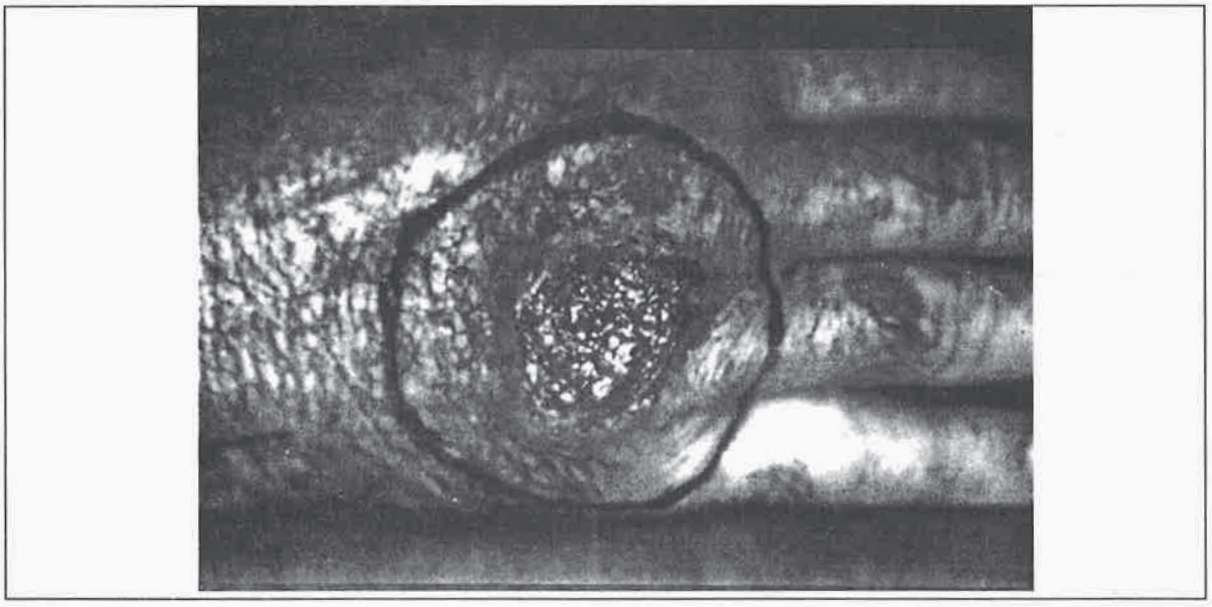

Figure 2: A 3x3 cm squamous cell carcinoma on the dorsum of the hand.

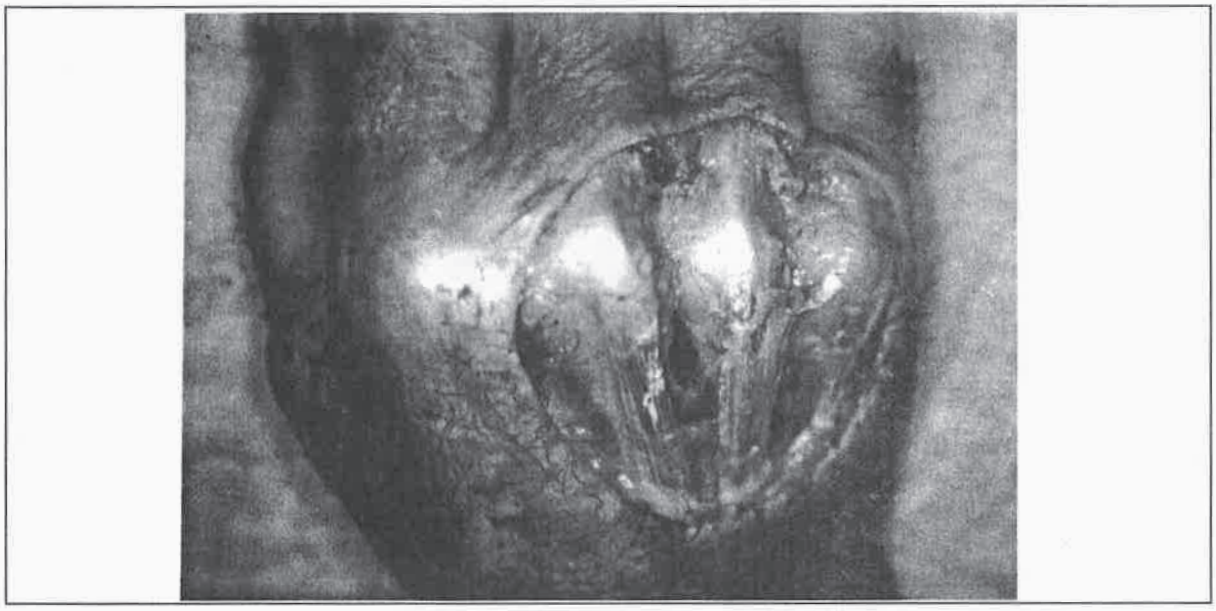

Figure 3: A 6.5x6.5 cm ulnar island flap was designed.

deep fascia along its proximal and ulnar margins and through skin only along its distal margin and then raised from proximal to distal without including the deep fascia. The subcutaneous pedicle was liberated up to the dorsal branch of the ulnar artery, preserving the ascending branch and its associated veins (Figure 5). A meticulous dissection was made to increase the mobility of the flap, which was transferred between the donor area and the recipient area without sacrificing healthy skin (Figure 6). The donor site defect was repaired with a full thickness skin graft (Figure 7). There were no postoperative complications. The flap was completely viable, with full motion of the fingers observed (Fig 8a, 8b). Cosmetic results of recipient and donor sites were also acceptable (Figure 9a, 9b).

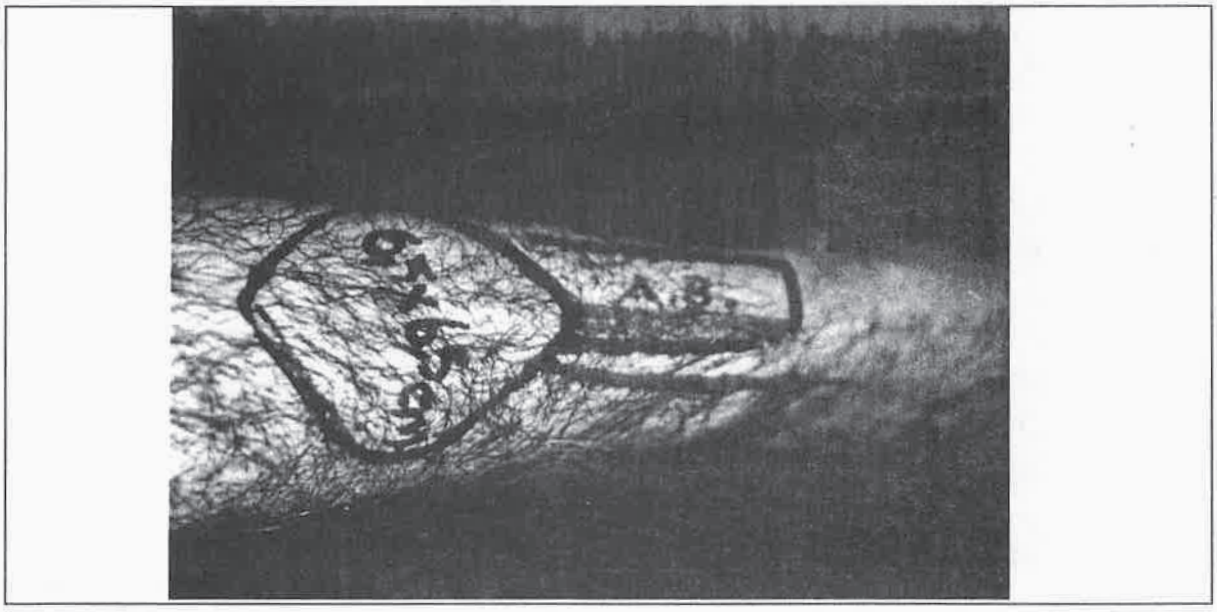

Figure 4: A wide excision was made.

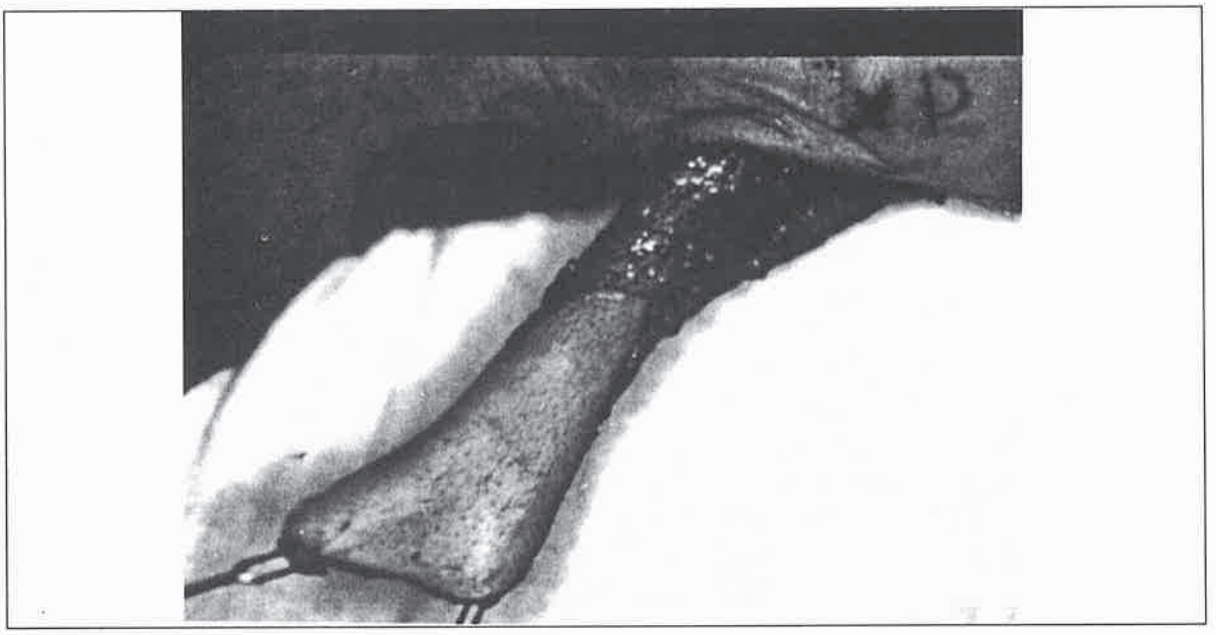

Figure 5: The flap was raised, based on the vessels and surrounding subcutaneous tissue.

DISCUSSION

Reverse radial forearm flap, posterior interosseous flap and free flaps are three types of flap currently used for the coverage of dorsal hand skin defects (1). Each type requires certain considerations. The use of reverse radial forearm flap necessitates the preoperative evaluation of the vascular supply of the hand to confirm that circulation through the ulnar artery will be sufficient after the division of the radial artery (1). The use of reverse posterior interosseous flap may result in ulnar bone exposure if direct closure of the donor site cannot be achieved (1). Free flap coverage is technically difficult, requiring a spe-

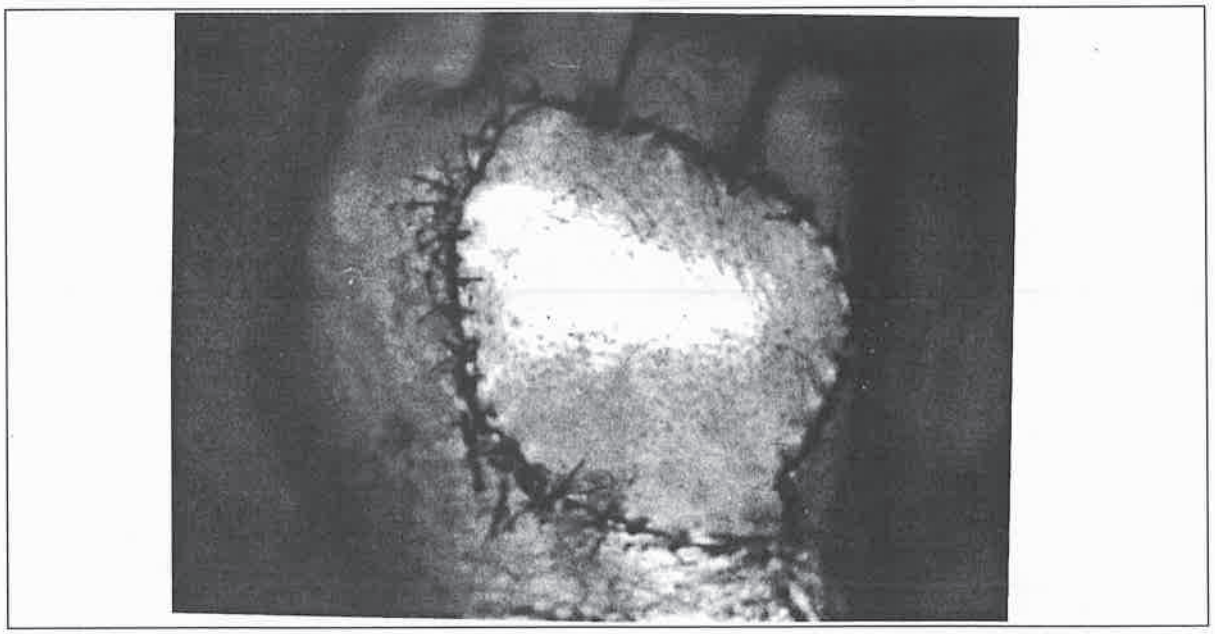

Figure 6: The flap was transferred.

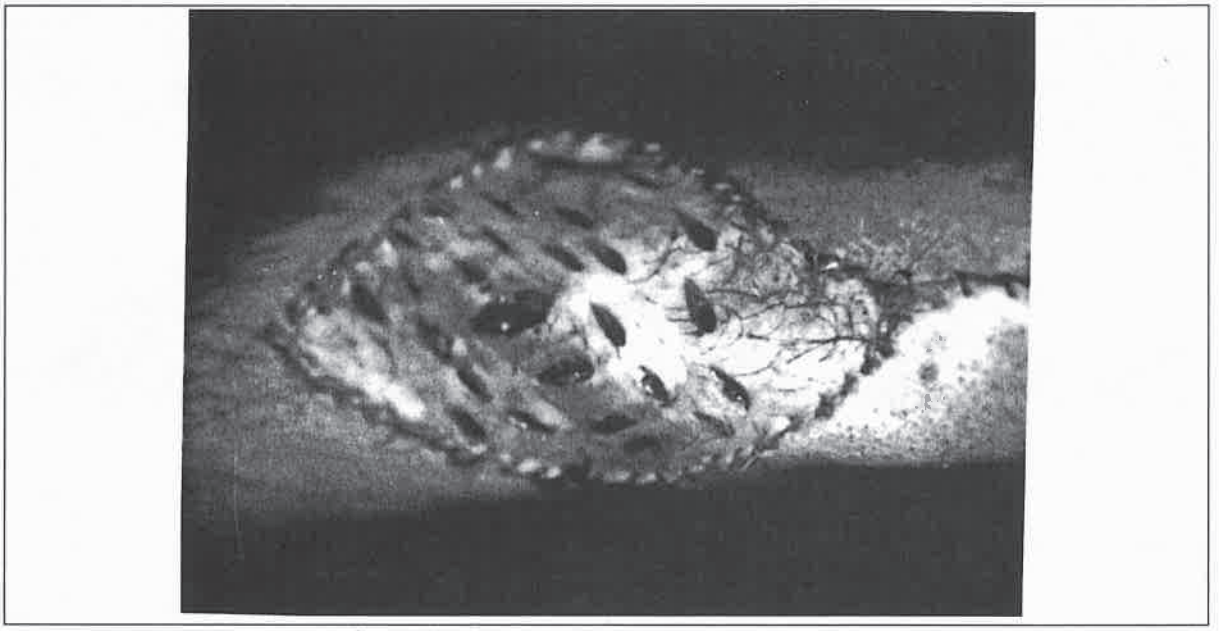

Figure 7: The flap was totally viable postoperatively, and the cosmetic result of the donor site was acceptable.

cialized team and equipment.

The standard ulnar flap first described by Becker and Gilbert is a technically simple and reliable flap that provides good-quality coverage for medium-sized skin defects of the hand (2). However, this flap has a very short arc of rotation, limiting its use for large-sized dorsal hand skin defects. Use of this flap also sacrifices the healthy skin between donor and recipient areas. Moreover, future contour deformities are frequently encountered (4). In order to overcome these disadvantages, an island modification of this standard flap was proposed. The pedicle of the ulnar island flap was formed by the ascending branch of the dorsal branch of the ulnar artery and associated vein. This modification provided a greater arc of rotation to cover large dorsal hand skin defects (4). It also avoided the need to sacrifice the healthy skin between donor and recipient areas, and no contour deformity was observed. As a result, we conclude that ulnar island flap may be a good choice for reconstruction of dorsal hand skin defects.

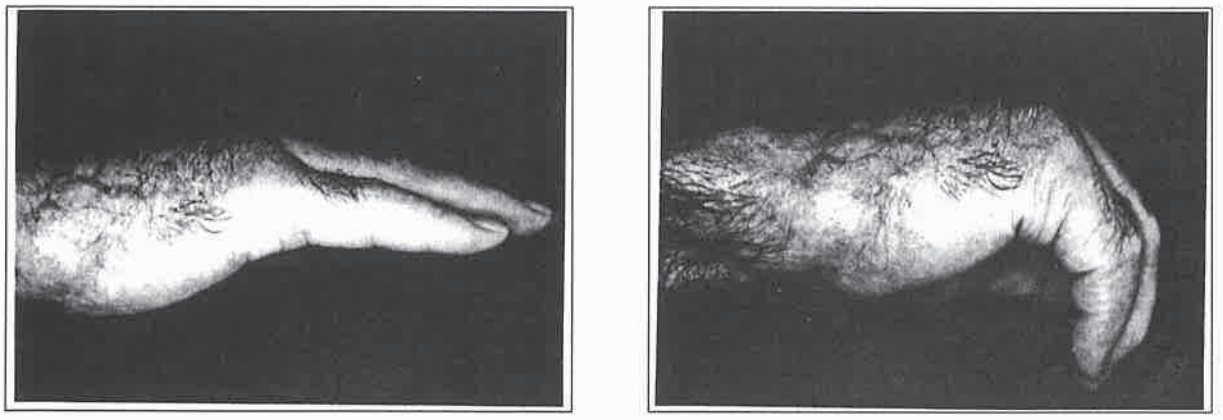

Figure 8 a,b: Full extension and flexion of the fingers was observed at 6-month follow-up.

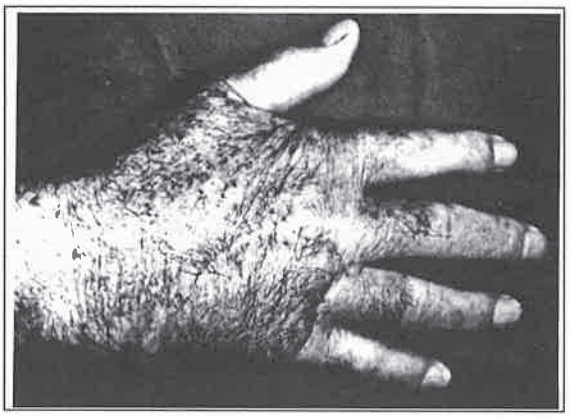

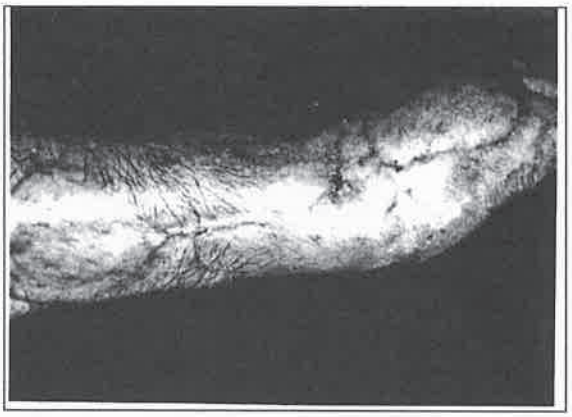

Figure 9 a,b: Cosmetic results of recipient and donor sites.

REFERENCES

1. Mathes SJ, Nahai F: Reconstructive Surgery. Principles, Anatomy and Technique. New York, Churchill Livingstone, 1997.
2. Becker C, Gilbert A: The ulnar flap-description and applications. Eur J Plast Surg 1988 11: 79-82.
3. Cormack GC, Lamberty BGH: The Arterial Anatomy of Skin Flaps. 2nd edition, Edinburgh, Churchill Livingstone 1994 : 490-493.
4. Karacalar A, Özcan M: Use of a subcutaneous pedicle ulnar flap to cover skin defects around the wrist. J Hand Surg 1998 23(A): 551-555.

DÜZELTME

Journal Of Ankara Medical School Cilt 23, Sayı 1, 2001'de yayınlanan "Vavular, Myocardial And Pericardial Involvement In Patients With Rheumatoid Arthritis" başlıklı makalede bulunan Şekil 4 yanlışlıkla, Şekil 5'in yerine basılmıştır.

Orjinali aşağıda verilmiştir. Özür dileriz.

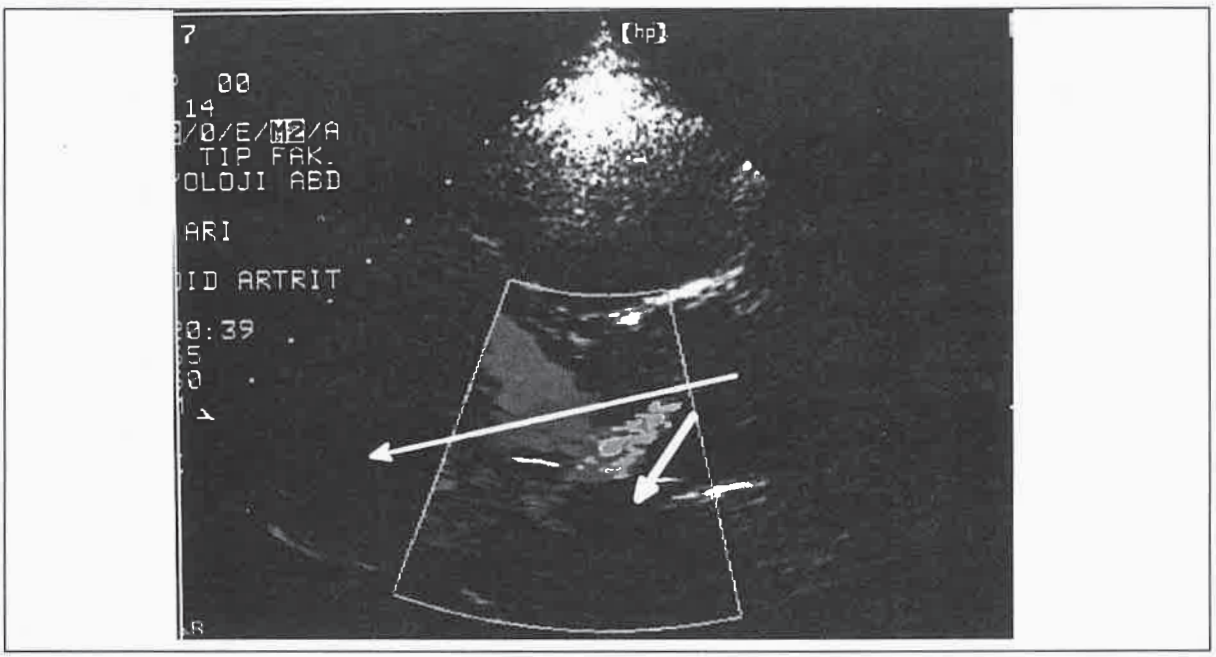

Figure 5. The eccentric (anterior) location of the nodule in Figure 4 caused an eccentric (posteriorly directed) regurgitation jet (small arrow). In a typical case of regurgitation due to aortic annulus dilatation, the regurgitant jet is generally expected to be in the middle of the left-ventricular outflow tract (long arrow).